

# Results from measurements on a roof integrated PV system with preheating of fresh air

Lauritz Sørensens Gård



# **Results from measurements on a roof integrated PV system with preheating of fresh air**

**Lauritz Sørensens Gård**

**Søren Østergaard Jensen**

**Solar Energy Centre Denmark  
Danish Technological Institute**

**April 2003**

## Preface

This report concludes Solar Energy Centre Denmark's measuring work in the project "Roof integration of solar cells with roofing-felt as under roofing and preheating of ventilation air by the solar cells" financed by the Danish Ministry of Environment and Energy - journal no. 51181/01-0013.

The project group:

Cenergia Energy Consultants  
Frederiksberg's hosing association, Privatbo  
Solarvent  
Icopal  
Gaia Solar  
Pålssons architects  
Witraz architects  
Solar Energy Centre Denmark, Danish Technological Institute

The following persons has participated in the measuring project:

Søren Østergaard Jensen, M.Sc. Solar Energy Centre Denmark  
William Otto, laboratory technician, Solar Energy Centre Denmark  
Ole Larsen, laboratory technician  
Lars Molnit, student (B.sc.), Solar Energy Centre Denmark

Results from measurements on a roof integrated PV system  
with preheating of fresh air – Lauritz Sørensens Gård  
1<sup>st</sup> printing, 1<sup>st</sup> edition, 2003  
© Danish Technological Institute  
Energy division

ISBN: 87-7756-704-8  
ISSN: 1600-3780

## List of contents

1.	Introduction .....	3
1.1.	Laurtiz Sørensens Gård .....	3
2.	The PV ventilation systems .....	6
2.1.	Ventilation system .....	11
3.	Measuring systems .....	18
3.1.	Weather measurements .....	18
3.2.	Temperatures on the PV/solar air collector .....	18
3.3.	Power measurements on the PV array .....	19
3.4.	Sensors in the ventilation system .....	19
3.5.	Data collection .....	24
3.6.	Treatment of measured data .....	24
3.7.	Difficulties .....	25
4.	Measurements .....	26
4.1.	Detection of malfunctioning of the systems.....	26
4.1.1.	Wrong connection of the ducting to one of the small heat exchangers .....	26
4.1.2.	Always open bypass in the large heat exchanger .....	29
4.2.	Description and characterization of sub-systems .....	31
4.2.1.	The PV-array .....	31
4.2.1.1.	Electricity production .....	31
4.2.1.2.	PV-panel temperatures .....	34
4.2.2.	The solar air collector .....	40
4.2.2.1.	Efficiency of the solar air collector .....	44
4.2.2.2.	Heating of the air during the night .....	50
4.2.3.	The large heat exchanger .....	54
4.3.	Conclusions .....	60
5.	Annual performance of the systems .....	61
5.1.	Power from the solar air collector .....	61
5.2.	Annual performance of the system .....	63
5.2.1.	PV-panels .....	63
5.2.2.	Solar air collector .....	64
5.2.3.	Heat exchanger .....	64
5.2.4.	Demands .....	64
5.2.5.	Annual performance .....	64
5.2.5.1.	The system above Lauritz Sørensensvej 24 .....	64
5.2.5.2.	The system above Lauritz Sørensensvej 28 .....	65
5.3.	Conclusions .....	66
6.	Conclusion .....	67
7.	References .....	68
	Appendix A The PV-panels .....	69

## 1. Introduction

The aim of the demonstration project was to develop good standard solutions of roof integration of PV in existing buildings with special focus on cheap and good architectural solutions. The aim was further to investigate roofing systems under the PV-panels which is feasible for combined PV and ventilation where the PV cells is cooled by the ventilation air.

The idea is that fresh air to the building is taken in from behind the PV-panels so that the air is preheated at the same time as the PV cells are cooled. The cooling will increase the performance of the PV cells.

The ventilation concept allows for:

- heat recovery during the winter
- cooling of the PV cells
- energy savings, low electricity demand, heat recovery
- utilization of solar energy
- improved indoor climate
- improved possibilities for integration
- possible to use different solutions for the under roofing

It was originally the idea to use the principles in the BPS guidelines for integration of solar collectors into the roof there rainproof solutions are obtained by using roofing-felt as under roofing. However, in practise it has been difficult to convince the architects about this solutions among other things because no existing hand on examples on how to do is available.

Roof integrated PV is in cooperation with Frederiksberg's housing association for the present installed on to building complexes – Lauritz Sørens Gård and Havremarken, Frederiksberg. It was originally the intention that all 170 dwellings at Lauritz Sørensens Gård should have the ventilation concept, however, by the start of the project the building owner decided only to install the ventilation concept on a minor part of the building. So in order still to achieve the aim of the project in testing different solutions for roof integration of PV part of the project was transferred Havremarken, Frederiksberg. However, only the project at Lauritz Sørensens Gård will be dealt with here.

The project is also a part of the EU project SynPack concerning overall assessment of renovation projects with total economical analysis of the energy saving measures.

### 1.1. Lauritz Sørensens Gård

Lauritz Sørensens Gård is a housing block with originally 170 dwellings situated in the area of Copenhagen called Frederiksberg. The five story-housing block was erected in 1930 and is typical for that period with its red external tile walls and roof. The building had anyway to be renovated with new bathrooms, renovation of the kitchens, new heating system and ventilation systems. Further 16 apartment with external lift towers were during the renovation established in the attic. The renovation was carried out in 2001-2002. Figure 1.1 shows a site plan of the housing block while figure 1.2 show the external facades.

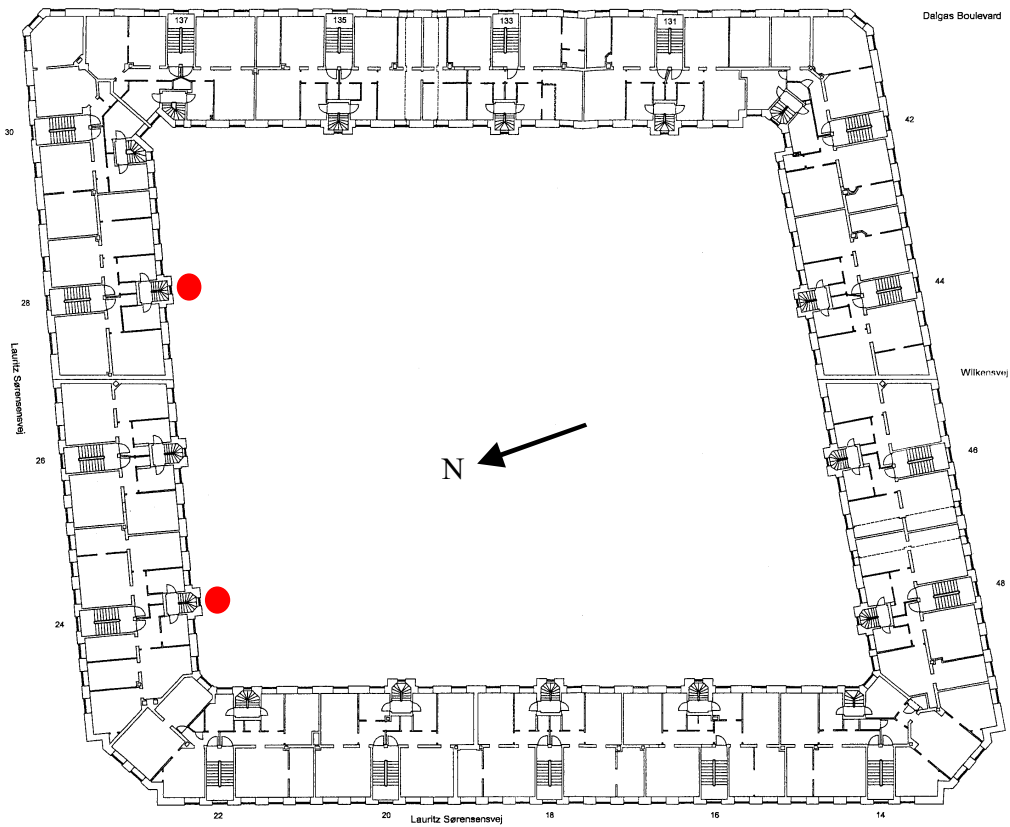


Figure 1.1 Site plan of the housing block Lauritz Sørensen's Gård with an indication of the two staircases where two PV ventilation systems has been installed – Lauritz Sørensenvej 24 and 28.



Figure 1.2. The facades of the housing block.

Figure 1.3 shows the courtyard with the two PV/solar air collectors on the roof, while figure 1.4 shows a close up of one of the systems.



Figure 1.3. The two PV/solar air collectors mounted on the roof above two staircases.



Figure 1.4. Close up of one of the PV/solar air collectors.

## 2. The PV ventilation systems

Figures 2.1-2 show drawing of the two PV/solar air collectors.

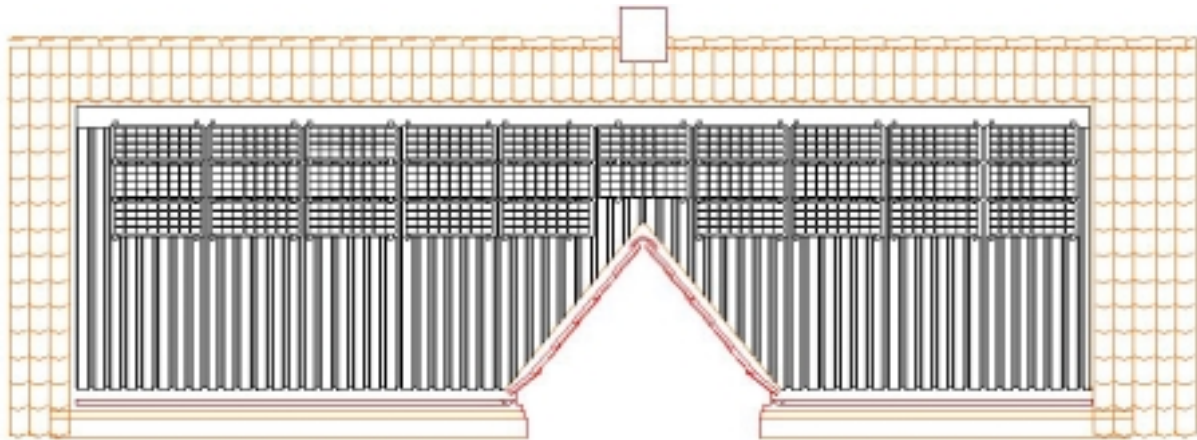


Figure 2.1. The PV/solar air collector above Lauritz Sørensenvej 24.

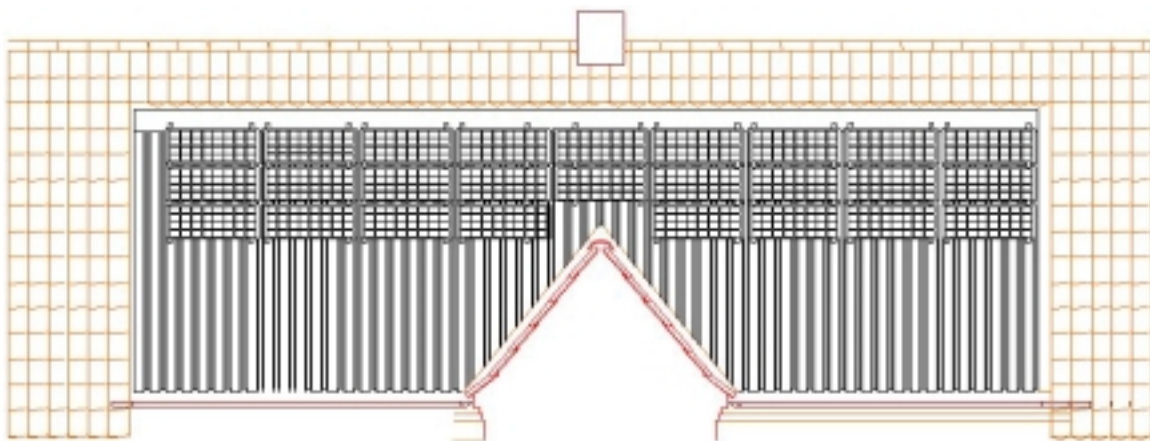


Figure 2.2. The PV/solar air collector above Lauritz Sørensenvej 28.

The area of the two PV/solar air collectors are slightly different:

- the PV/solar air collector area above Lauritz Sørensenvej 24 consists of 28 PV panels (29 are shown in figure 2.1, however, one is a dummy panel) of in total 12.4 m<sup>2</sup> with a peak performance of approx. 1123 W<sub>p</sub> and a total solar air collector area of 35.3 m<sup>2</sup> (incl. the area of the PV-panels).
- the PV/solar air collector area above Lauritz Sørensenvej 28 consist of 26 PV panels of in total 11.5 m<sup>2</sup> with a peak performance of approx. 1043 W<sub>p</sub> and a total solar air collector area of 31.7 m<sup>2</sup> (incl. the area of the PV-panels).

Figure 2.3 shows a cross section of the roof with the PV/solar air collector.

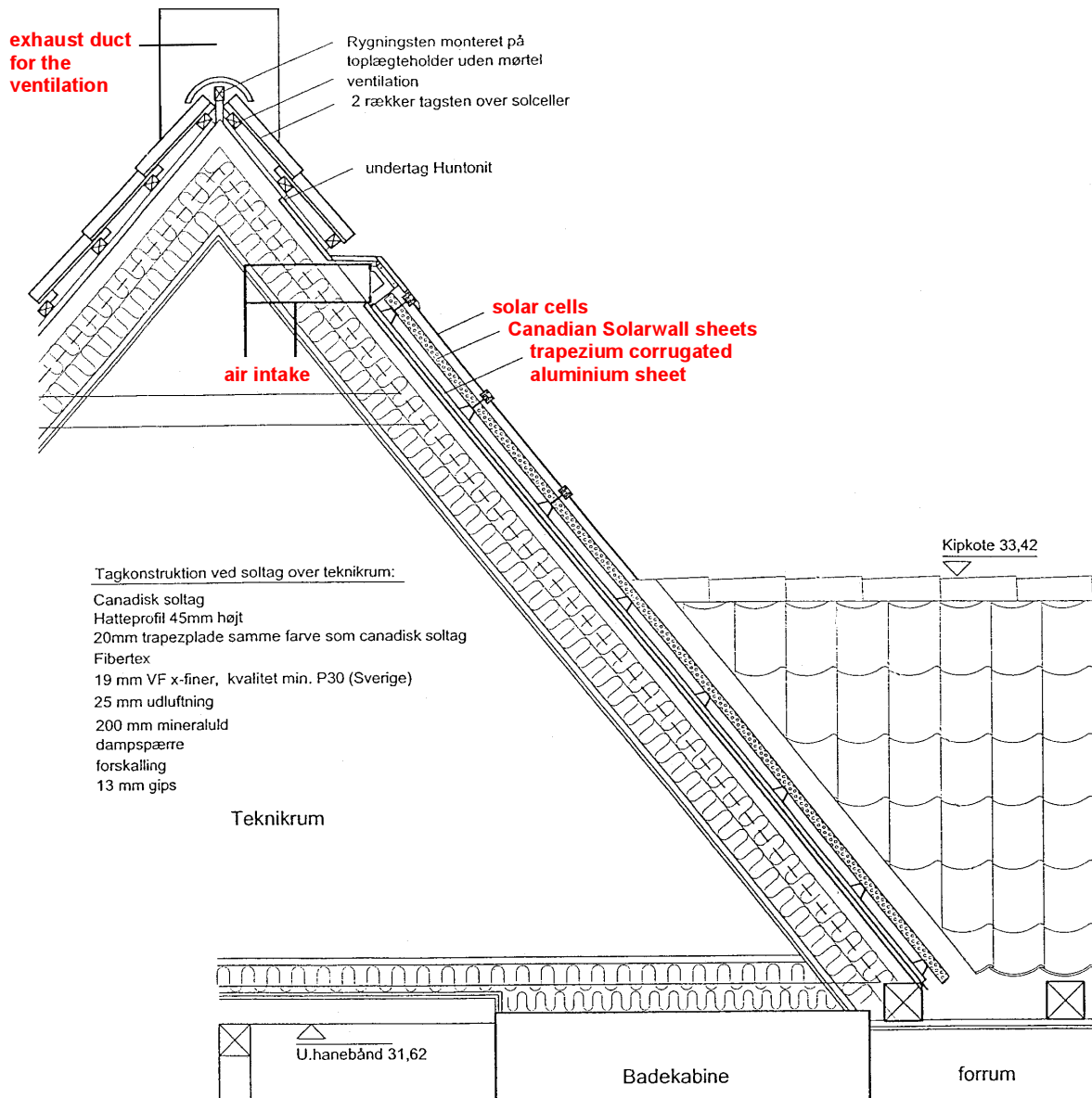


Figure 2.3. Cross section of the roof with the PV/solar air collector

Figure 2.4 shows the under roofing made of trapezium corrugated aluminium sheets and the Canadian solarwall sheet. The Solarwall sheets are made of trapezium corrugated aluminium sheets with small holes as seen in figure 2.4 but more clearly in figure 2.5.

The PV-panels is mounted 37 mm above the top of the Solarwall sheets as seen in figure 2.6. The distance between the PV-panels is shown in figure 2.7. The PV-panels are a mixture of mono-crystalline panels from Gaia Solar type GS37MIX, GS39MIX, GS40MIX and GS42MIX ( $W_p$ : 37, 39, 40 and 42) – a data sheet for the PV-panels is included in appendix A. The mean peak power for the panels in  $40.1 W_p$ .



Figure 2.4. The under roofing and the Solarwall sheet.

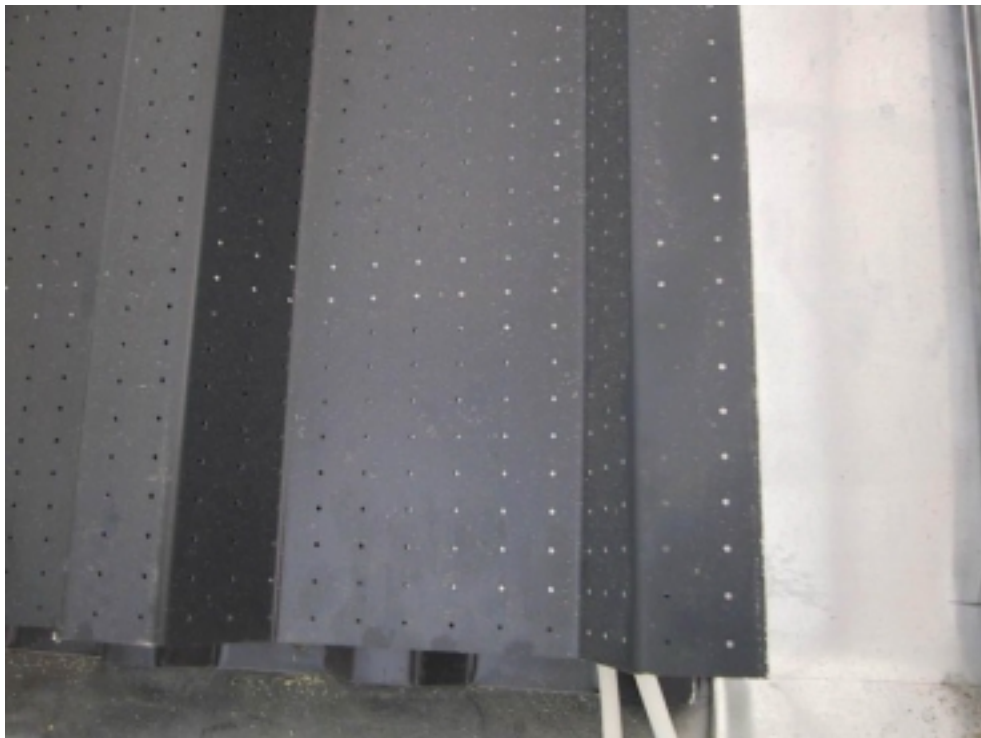


Figure 2.5. The perforation of the SolarWall sheets.

The PV/solar air collector arrays have a tilt of  $51^\circ$  and are orientated nearly south – approx.  $15^\circ$  from south towards west.



Figure 2.6. The PV-panels mounted on top of the Solarwall sheets.

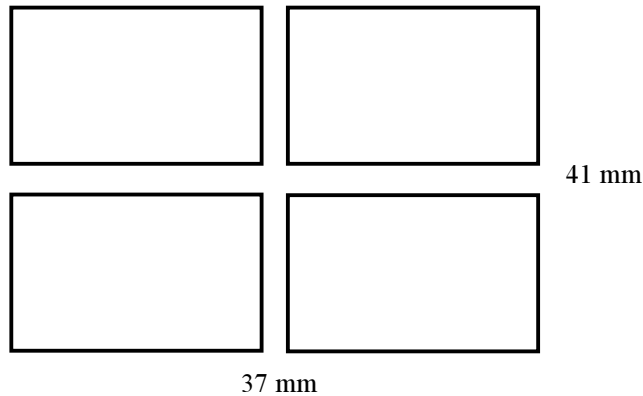


Figure 2.7. The distance between the PV panels.

The purpose of the Solarwall sheets is twofold: to preheat fresh air and to create a well distributed air flow behind the PV-panels in order to cool these.

For the uncovered Solarwall sheets the air is mainly heated while passing the holes of the sheets. However, high volume flow rates of air are required in order to obtain a high efficiency of this type of uncovered solar air collector as seen in figure 2.8 where the efficiency of the Solarwall air collector is compared with the efficiency of covered solar air collectors.

Figure 2.9 shows the intended cooling of the PV-panels during the winter with fresh air intake through the PV/solar air collector while figure 2.10 shows the intended cooling of the PV-panels during the summer without fresh air intake through the PV/solar air collector but with buoyancy driven air flow behind the PV-panels.

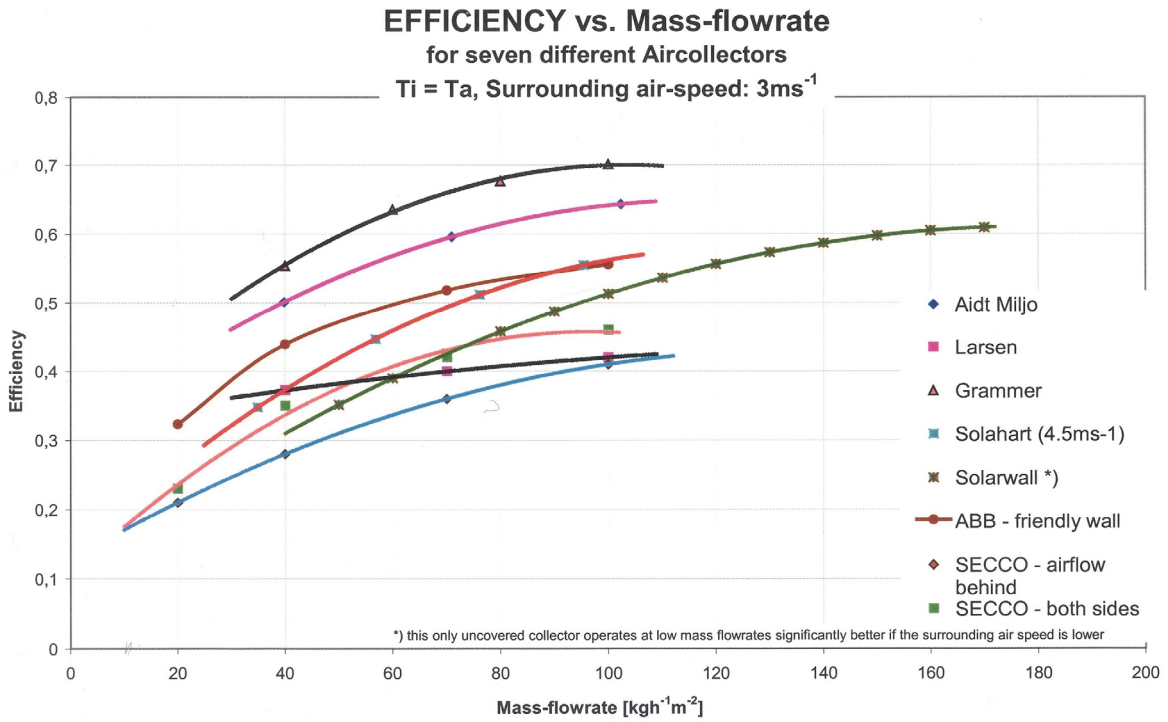


Figure 2.8. The efficiency of 8 commercial solar air collectors (Fechner, 1999).

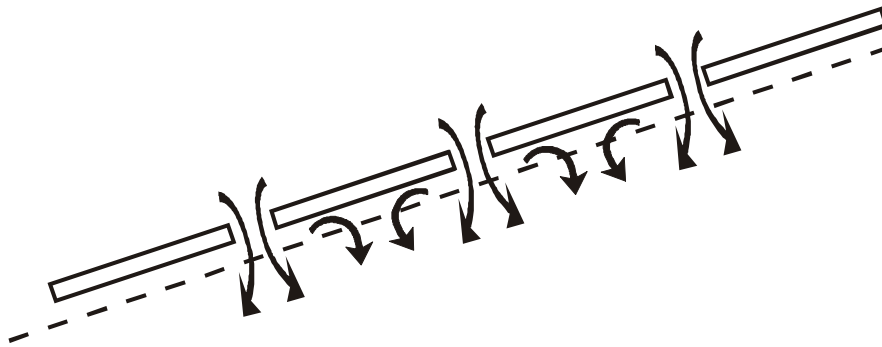


Figure 2.9. The intended cooling of the PV-panels during the winter with fresh air intake through the PV/solar air collector.

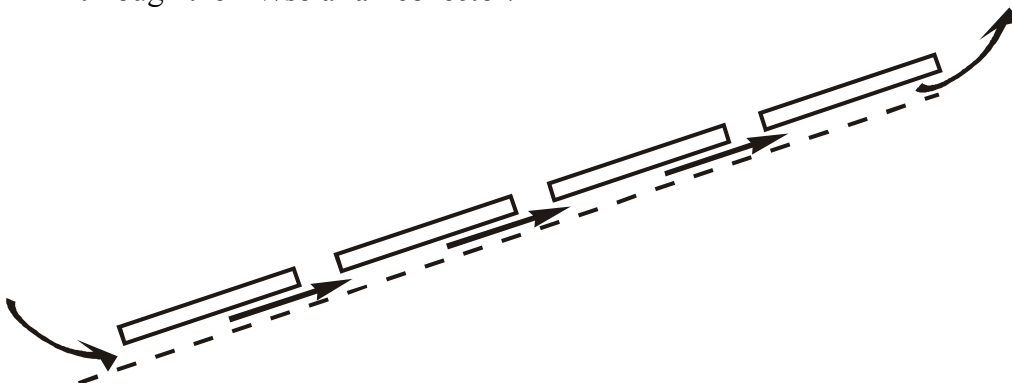


Figure 2.10. The intended cooling of the PV-panels during the summer without fresh air intake through the PV/solar but with buoyancy driven air flow behind the PV-panels.

The PV-panels is interconnected and connected to a Sunrise inverter for each PV array. Both inverters are situated in the technician room in the attic behind the PV/solar air collector above Lauritz Sørensensvej 24 as seen in figure 2.11. The inverters convert the DC PV power to 230 V AC which is feat into the public grid via an energy meter.



Figure 2.11. The two Sunrise inverters – one inverter for each of the two PV array.

## 2.1. Ventilation system

Figure 2.12 shows the principle of the ventilation system.

The solar heated fresh air is let to a manifold at the top of the PV/solar air collector array. From here the air is sucked into the technician room in the attic behind the PV/solar air collector through four 600 x 150 mm ducts which are connected to a  $\varnothing 400$  mm duct as indicated in figure 2.13 and seen in figure 2.14.

From the manifold duct the preheated fresh air is let to three air to air heat exchangers where the fresh air is heated further if necessary by the exhaust air: a large heat exchanger for the original 10 apartments per stair case and a small heat exchanger for each of the new apartments. One large heat exchanger had been sufficient, however it was wished also to try separate heat exchangers for each apartment. The large heat exchanger is for stair case 24 a cross

flow heat exchanger from Exhausto type VEX140 with an efficiency of 61 % (Exhausto, 2003), while the large heat exchanger of stair case 28 is from AirVex type JoVex1000 with an efficiency of about 80 % (Jensen, 2001). The two smaller heat exchangers are a cross flow heat exchanger from Exhausto type Vex90 (efficiency about 83 % (Olsen et al. 2003)) and a counter flow heat exchanger from AirVex type S450-190DC (approx. 80 % (Jensen, 2001)).

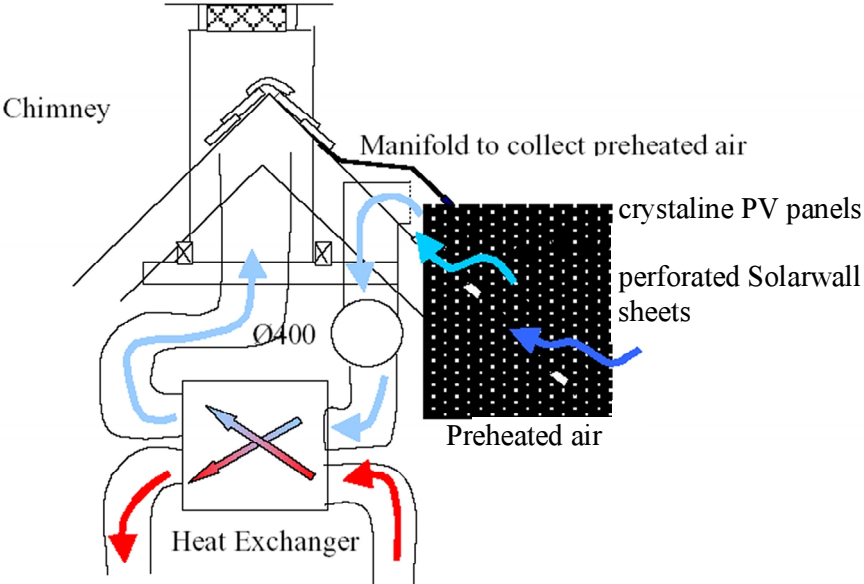


Figure 2.12. Principle of the ventilation system.

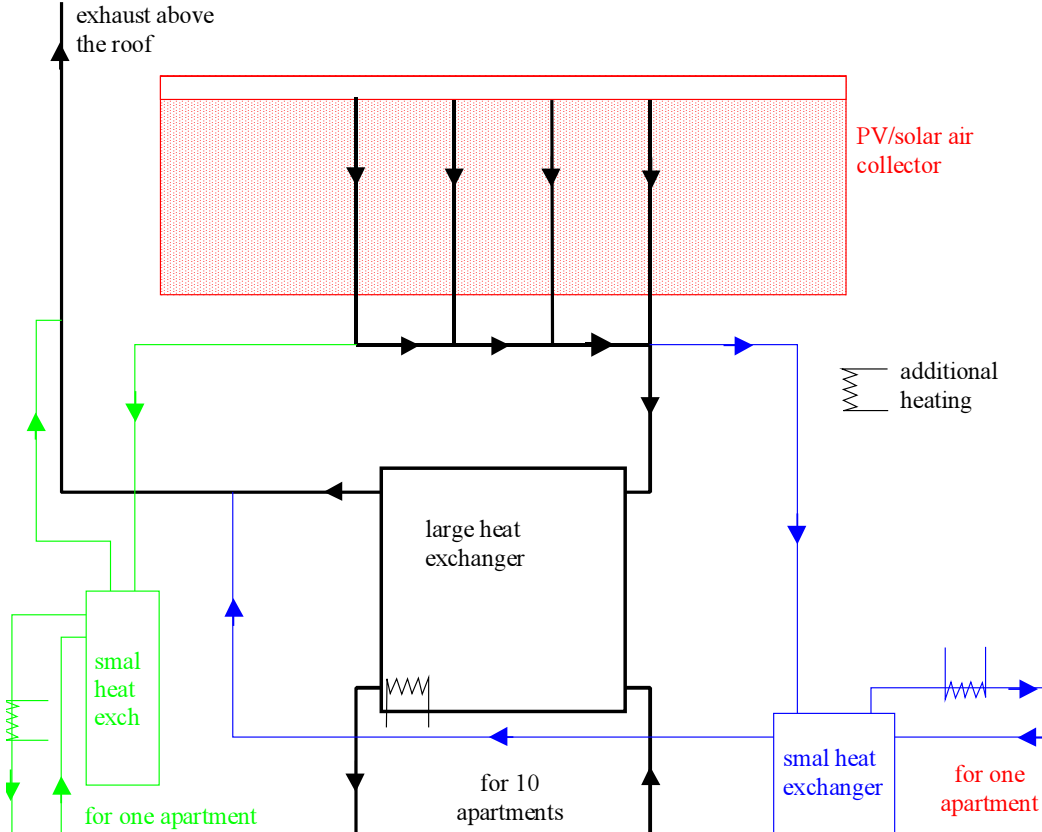


Figure 2.13. More detailed principle of the ventilation system.

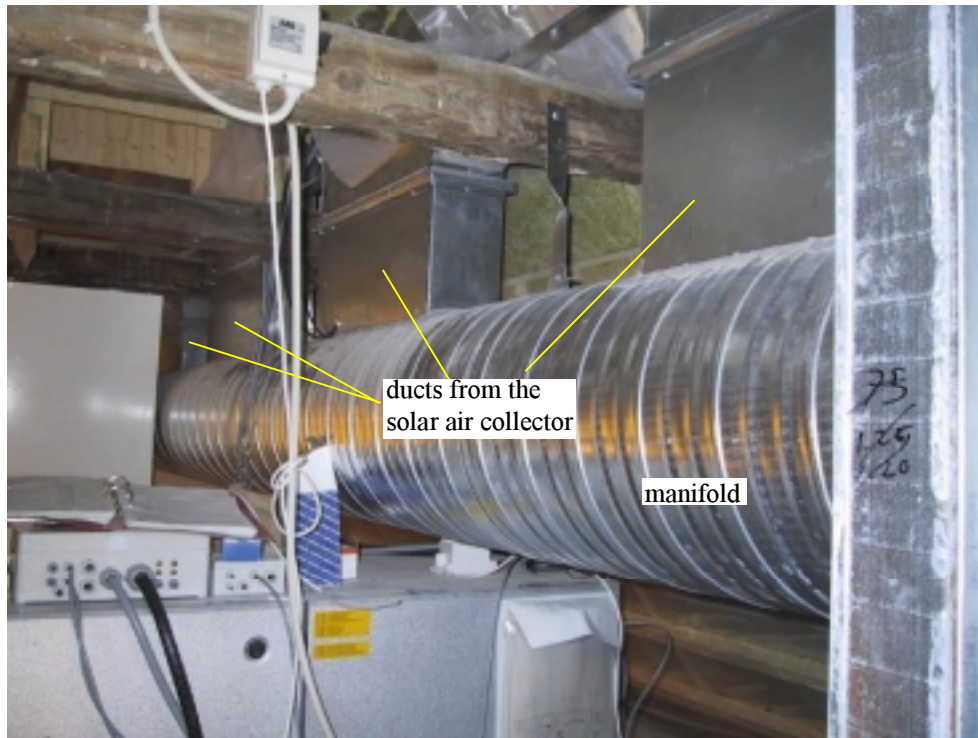


Figure 2.14. The four inlet ducts from the solar air collector and the manifold in the attic before insulation.

Figures 2.15-17 show the three heat exchangers above Lauritz Sørensenvej 24.



Figure 2.15. The large heat exchanger from Exhausto for 10 apartments.



Figure 2.16. The small heat exchanger from Exhausto for the top apartments to the right.



Figure 2.17. The small heat exchanger from AirVex for the top apartments to the left.

Especially figure 2.13 leaves the impression that the ventilation system is very complex – and it is, however, the system is really more complicated than indicated in figure 2.13 and is com-

pressed into a very little space in the technician room in the attic. This is illustrated in the below collage.



Figure 2.18. Collage with pictures from the technician room above Lauritz Sørensenvej 24 before insulation.

In order to increase comfort a heater is situated in the fresh air stream after the heat exchangers as shown in figure 2.19. The heater in connection with the large heat exchanger above Lauritz Sørensensvej 24 is located inside the cabinet of the heat exchanger (see figure 4.7).



Figure 2.19. The heater after one of the small heat exchangers.

The heaters are controlled by thermostats as seen in figure 2.20 with at temperature sensor in the air stream of fresh air after the heaters as seen in figure 2.19.



Figure 2.20. Thermostat for controlling one of the heaters in the ventilation systems.



### 3. Measuring system

The ventilation systems in Lauritz Sørensens Gård are as described in the previous chapter rather complex, which makes it difficult to perform measurements. The focus of the present project was on the PV/solar air heating system. A measuring system with special emphasis on this has, therefore, been developed. As the two PV/solar air heating systems in principle are identical except for a slight difference in array area and different large heat exchangers it was decided to limit the measurements to the system at Lauritz Sørensensvej 24, and further focus on the performance of the PV/solar air collector and the large heat exchanger.

#### 3.1. Weather measurements

The global solar radiation on the PV/solar air collector has been measured using a calibrated pyranometer from SolData type 80SP. The ambient temperature was measured using a PT100 class A temperature sensor located in a shield consisting of two concentric tubes in order to screen it from the sun. The two sensors are shown in figure 3.1.



Figure 3.1. The pyranometer and ambient temperature sensor

#### 3.2. Temperatures on the PV/solar air collector

One of the main features of the systems were the ability to cool the PV-panels. Figure 2.13 indicates that the inlets from the PV/solar air collector to the ventilation system through four ducts don't cover the whole width of the PV/solar air collector. The width of the inlets is actually only 3.65 m while the width of the PV/solar air collector is 10.5 m. There may, thus, both be a vertical and horizontal temperature stratification of the PV-panels. Temperature sensors

were, therefore, located at the back of four PV-panels and further two air temperature sensors in the air gap behind two of these PV-panels as shown in figure 3.2.

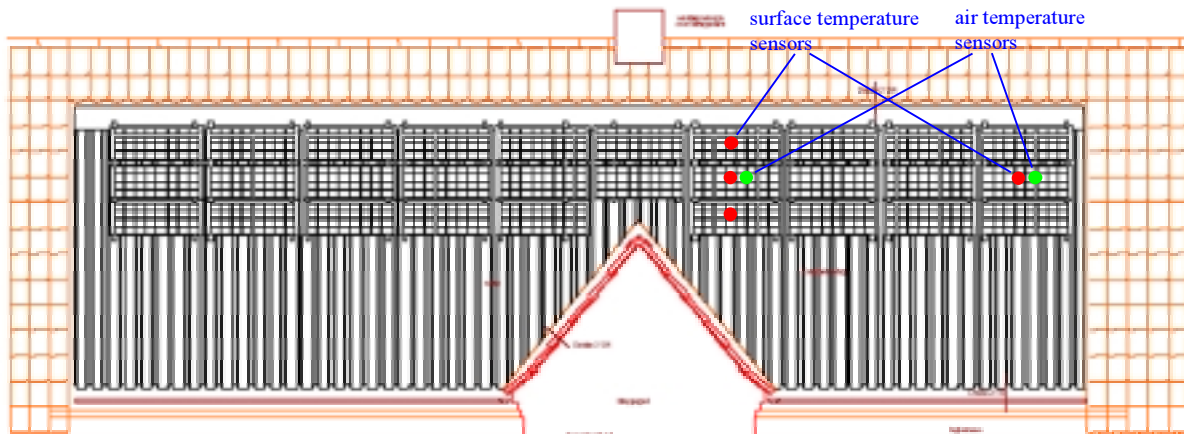


Figure 3.2. Temperature sensors on the PV/solar air collector.

All temperature sensors were PT100 class A temperature sensors. The temperature sensors at the back of the four PV-panels were mounted by means of aluminium tape. Thermo pasta was located between the PV-panels and the sensors in order to obtain a good thermal connection between the sensor and the panel.

### 3.3. Power measurements on the PV array

The power from the PV array was measured using a standard energy meter from Revalco type RCEM230i. The power from the PV array was transferred to the measuring system by counting the pulses given out by the energy meter. Figure 3.3 shows the energy meter mounted between the two inverters.

### 3.4. Sensors in the ventilation system

Figure 3.4. shows the location of the sensors in the ventilation system.

The air temperature sensors were all PT100 class A sensors. A temperature sensor was located in each of the inlets from the PV/solar air collector and further one temperature sensor in the start of the duct to the large heat exchanger. The sensors were located in the middle of the air streams.

Further four air temperature sensors also PT100 class A sensors were situated in the in- and outlets of the large heat exchangers. It was later discovered that one more temperature sensor was needed. The intention was to measure the air temperature out of the heat exchanger, but as indicated in figure 2.13 the post heating of the fresh air is done inside the cabinet of the heat exchanger and not after the heat exchanger as for the small heat exchangers as seen in figure 2.19. A sensor was, therefore, located in the large heat exchanger before the heating unit as indicated in figure 3.4 and shown in figure 3.5.



Figure 3.3. The energy meter on the PV array.

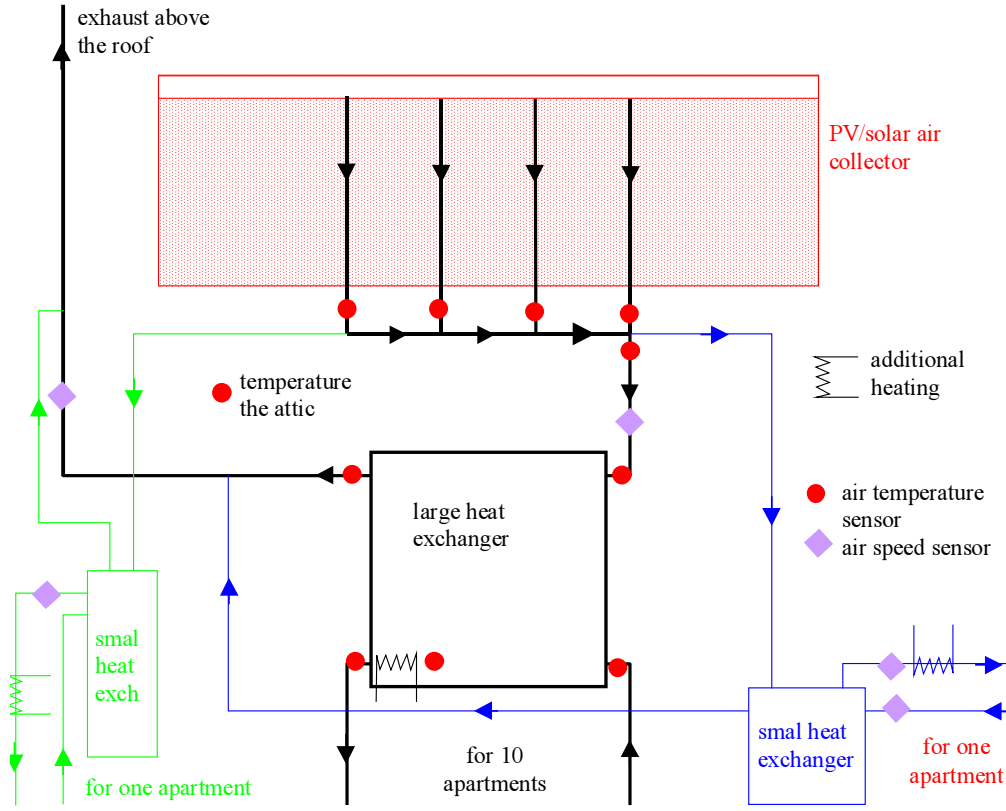


Figure 3.4. The air temperature and air speed sensors in the ventilation system

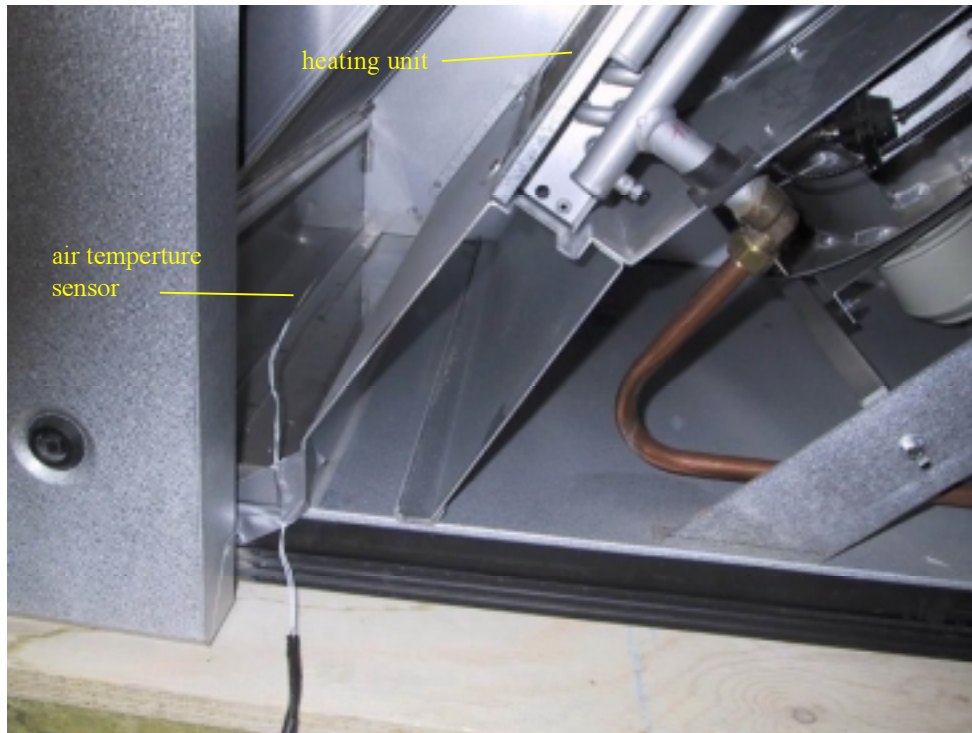


Figure 3.5. The air temperature sensor in the fresh air stream in the large heat exchanger before the post heating.

The system is as indicated in figure 2.18 rather complex and is further squeezed into a rather small room. It has, therefore, been rather difficult to find locations in the ductworks with well developed air flow where the air speeds could be measured precisely. Figure 3.6 shows an example. The top photo shows the inlet duct for fresh air to the large heat exchanger, while the bottom photo shows the location of the air speed sensor.

All applied air speed sensors were previous to mounting calibrated in laboratory. Due to the special difficult conditions the air speed sensors were later calibrated on location, which, however, was very difficult especially because it was difficult to control the air flow rates of the systems during the calibration as the air flow rates were determined by the individual apartments. At first the air speed sensors were, therefore, not calibrated on location. However, check measurements revealed that this was necessary so the air speed sensors were calibrated on location as late as in December 2002 when the last faults on the systems were corrected as described in section 4.1.

The applied air speed sensors were except for the air speed sensor in the exhaust duct Vent-Captors – one of the applied VentCaptor is shown in figure 3.7. The air speed sensor in the exhaust was an Envic type AFT-10 sensor – the sensor is shown in figure 3.8.

The focus has been on obtaining the air flow through the PV/solar air collector and through the large heat exchanger. It was, therefore, also necessary to measure the air flow of fresh air to the small heat exchangers and the exhaust air flow from one on the small heat exchangers in order to obtain the two desired flow rates – as seen in figure 3.4.

The room air temperature in the technician room was as the other temperatures measured using a PT100 class A sensor mounted freely hanging in the air as shown in figure 3.9.



Figure 3.6. Top picture: the inlet duct of fresh air to the large heat exchanger before insulation. Bottom picture: the location of the air speed sensor.



Figure 3.7. One of the applied VentCaptor air speed sensors.



Figure 3.8. The applied Envic type AFT-10 air speed sensor in the exhaust duct.



Figure 3.9. The temperature sensor measuring the air temperature in the technician room.

### 3.5. Data collection

All sensors were connected to a data logger system with modules from Analog Devices. The sensors were scanned each 5<sup>th</sup> second and averaged into ten minutes mean values and stored on the hard disk of a PC.

The PC controlled via the software Labview 5.0 the data logger system. Spot values of the sensor readings together with curves showing several hours of measurements for some values were continuously shown on the screen of the PC as seen in figure 3.10.

### 3.6. Treatment of measured data

Using the data logger system/PC the measured values were either directly translated into physical understandable values like temperatures and solar radiation while the air flow rates later were calculated using the equations found as a result of the calibration of the air speed sensors. The electrical/thermal performance of the PV/solar air collector and ventilation system

was later evaluated in the form of energy output and efficiency of the PV/solar air collector and the large heat exchanger.

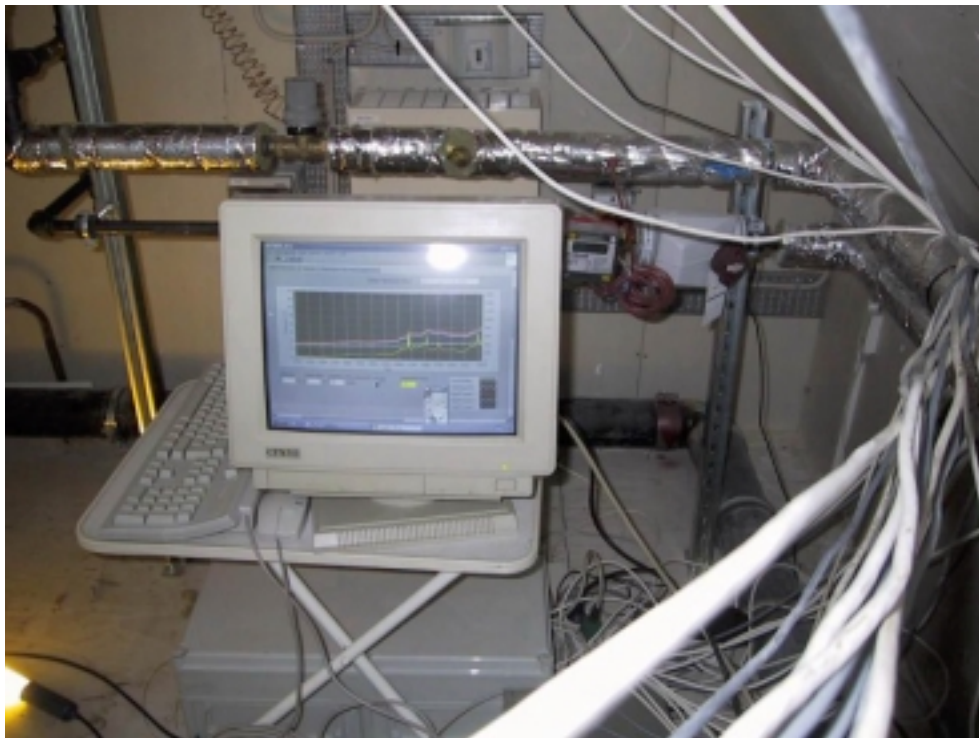


Figure 3.10. The data logger system.

### 3.7. Difficulties

The air speed sensors were as explained earlier calibrated on location much later than the installation. This should of course not create problems, as the calibration equations are valid for the measurements before and after the calibration. However, this is not true for the air flow rates for the small heat exchangers. Someone had "forgotten" to put in noise reduction in the two small systems. These two systems, therefore, became too noisy. Noise reductions were put in the systems just before the calibration of the air speed sensors. The change of the systems resulted in relocation of the air speed sensors, which means that the calibration equations obtained on location aren't valid for the measured data from before the calibration.

The "loss" of data regarding the air flow rates of the small systems is, however, not a big problem as the last faults on the systems were corrected just before the calibration of the air speed sensors. The air flow rates of the small systems are, however, in the next section used from periods before the calibration where the uncertainty of these air flow rates, therefore, are rather high. The air flow rates are although mainly used indicative where the pattern of the air flows rather than the absolute values are of interest.

## 4. Measurements

Measurements have been carried out at Lauritz Sørenssens Gård for more than one year starting by the beginning of April 2002 to April 2003. One sensor, however, has been in operation during a shorter period – the sensor inside the large heat exchanger (figure 3.5). This sensor was installed by the middle of August 2002. The late installation of this sensor didn't lead to loss of important data, as the large heat exchanger was malfunctioning (as seen later) until the beginning of December 2002. The data logger system has been running stable with out many losses of data except for two weeks stop – one in August 2002 and one in March 2003 – and few occasions where the PC was turned off and restarted because the communication program for data transfer was hanging.

The chapter is divided into two main sections: the first section describes how the measurements have been used to detect major malfunctions in the ventilation systems, in the second section the function of the different sub-systems is described by showing measured data from selected weeks and characterized by calculations based on the measurements from larger parts of the measurements.

### 4.1. Detection of malfunctioning of the systems

As the systems are extensively monitored it is possible to evaluate the performance of the systems over time and thereby detect problems which may not be caught by spot measurements.

Two major malfunctions of the systems were found in this way during the measuring campaign: wrong connection of the ducting to one of the small heat exchangers and always open bypass in the large heat exchanger.

#### 4.1.1. Wrong connection of the ducting to one of the small heat exchangers

The measurements on the AirVex type S450-190DC heat exchanger to the top apartment to the left (see figure 2.17) early indicated that there was something wrong with the installation of this heat exchanger. Figure 4.1 shows the air flow of fresh air through this heat exchanger during week 19, 2002 while figure 4.2 shows the temperature of the fresh air from the solar air collector. Figure 4.3 shows the location of the air temperature sensors giving the measurements in figure 4.2.

The five temperatures out of the solar air collector should be rather identical – and they are after the AirVex heat exchanger is switched off on day 129 (May 9). Before that especially the temperature at the inlet from the solar air collectors where the heat exchanger from AirVex gets the fresh air (the pink line in figure 4.2 - labelled "from collector 1") is very different from the other temperatures. No other changes have been measured on day 129, which could lead to the shift in pattern shown in figure 4.2.

After careful thinking it was concluded that the observed pattern could be due to the fact that the heat exchanger instead of getting air from the solar air collector in fact was blowing exhaust air out through the solar air collector. This showed to be the case. The ducting to and from the heat exchanger was correct on November 25, which as figures 4.4-5 show solved the problem.

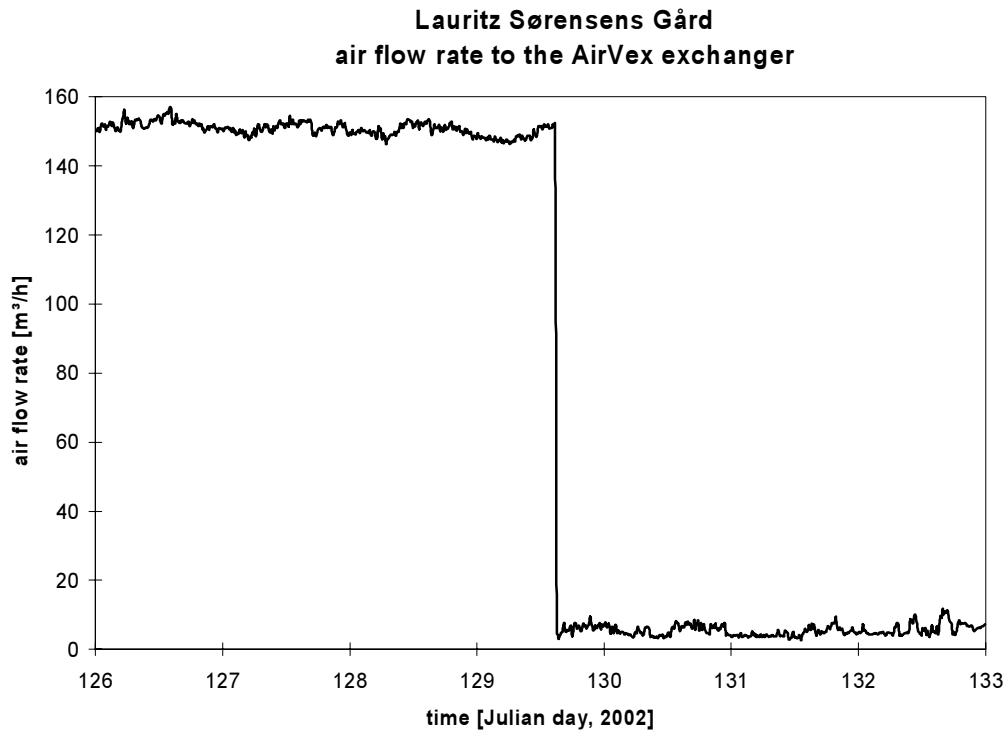


Figure 4.1. The air flow rate of fresh air through the small high heat exchanger from AirVex during week 19, 2002 (May 6-12).

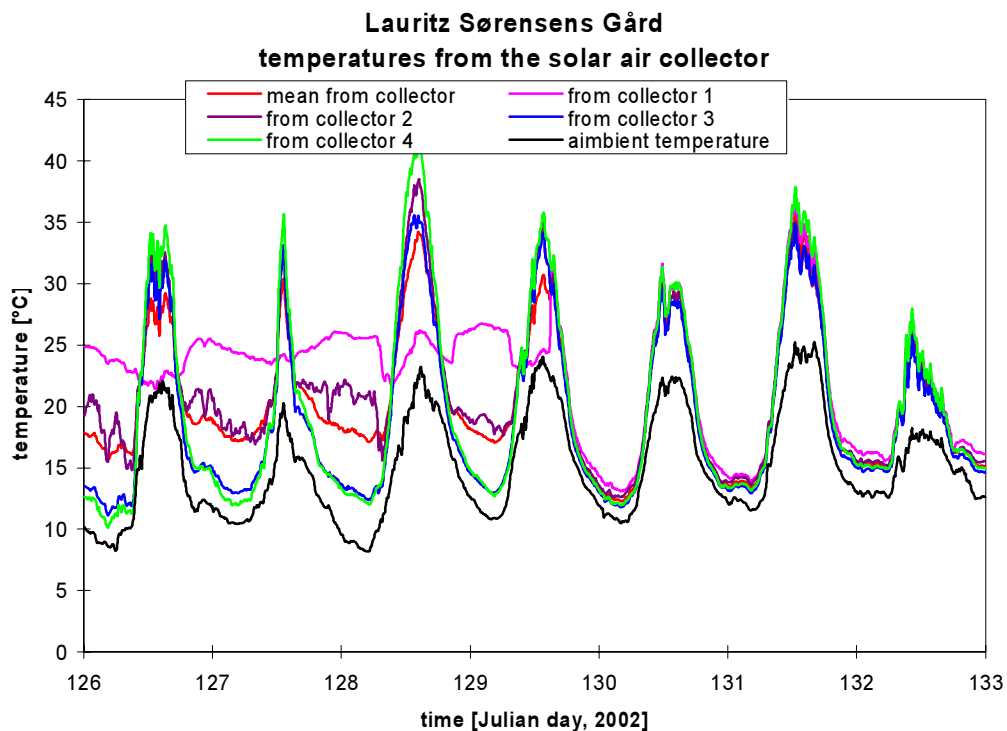


Figure 4.2. The measured air temperatures from the solar air collector during week 19, 2002 (May 6-12).

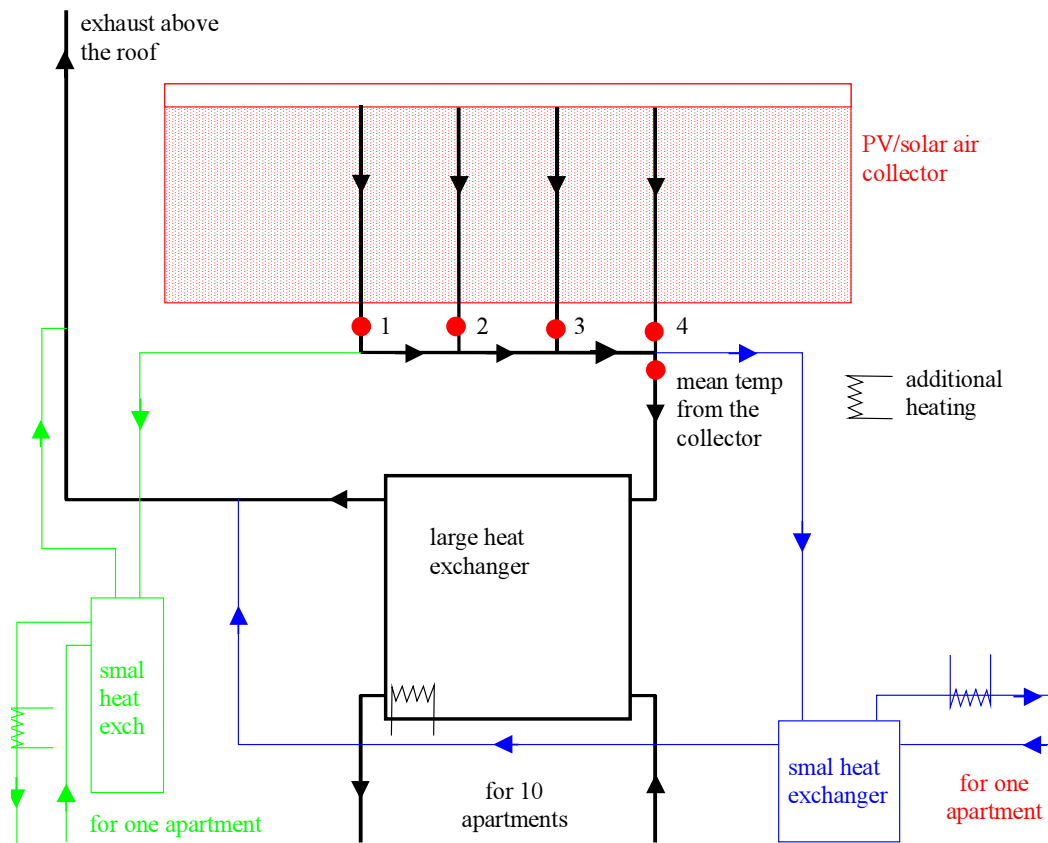


Figure 4.3. The location of the air temperatures sensors in the outlets from the solar air collector.

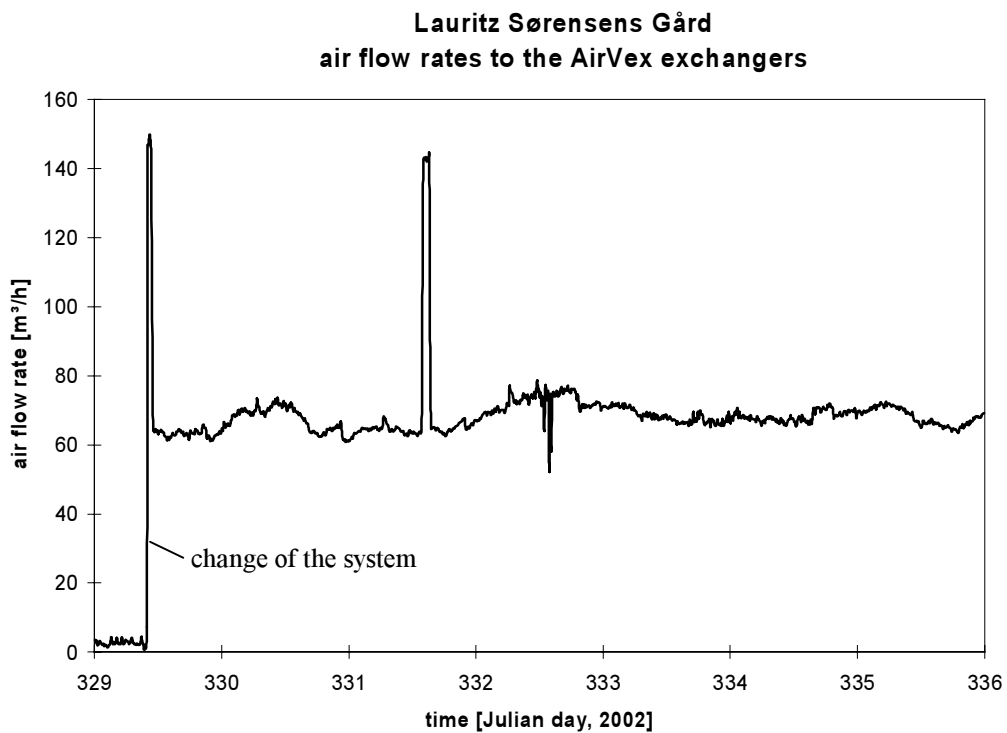


Figure 4.4. The air flow rate of fresh air through the small high heat exchanger from AirVex during week 48, 2002 (November 25-December 1).

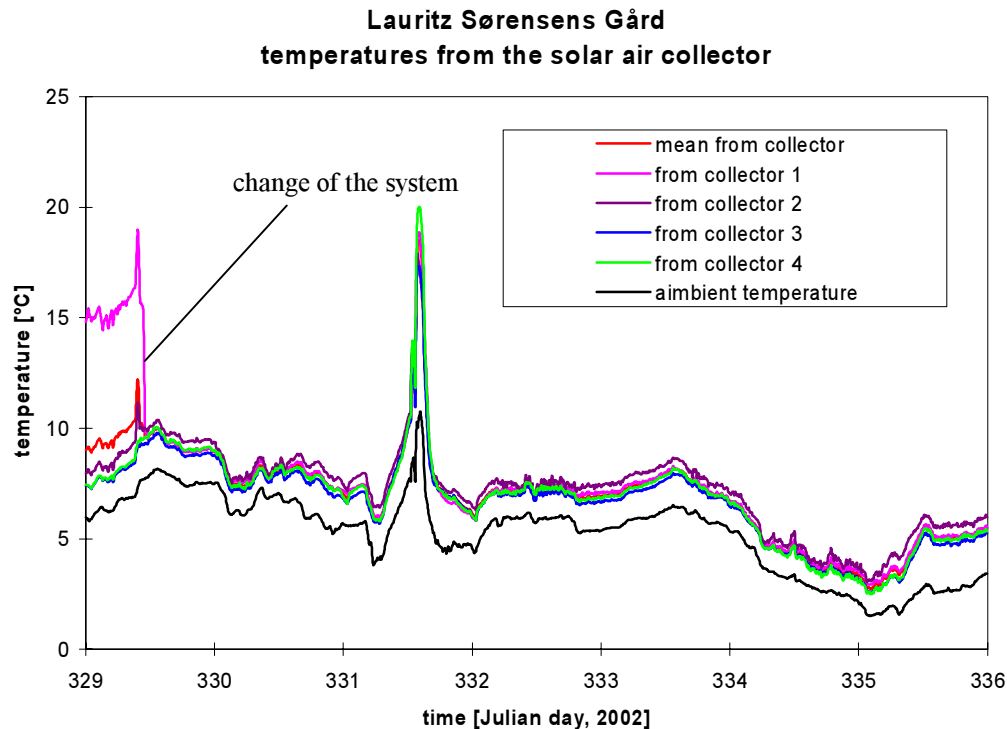


Figure 4.5. The measured air temperatures from the solar air collector during week 48, 2002 (November 25-December 1).

#### 4.1.2. Always open bypass in the large heat exchanger

If the temperature of the fresh air is above the temperature of the air from the building, the fresh air will be cooled by the exhaust air. The large heat exchanger is, therefore, equipped with a bypass so that the fresh air may bypass the heat exchanger. However this bypass did not work as intended – in fact the bypass was always open. This is seen in figure 4.6 showing the temperatures around the heat exchanger. The figure shows that the exhaust temperature from the heat exchanger (dark blue) is higher than the exhaust temperature from the apartments (light blue). At first it was believed that this was because the two sensors accidentally had been switched when being installed. However, later calculations of the efficiency of the heat exchanger when the temperature sensor inside the heat exchanger (before the heater) was installed showed an efficiency of about 10%. An inspection of the measuring system revealed that the temperature sensors were correctly mounted and that the bypass was open when it actually should be closed – see figure 4.7.

The reason for the problem is also seen in figure 4.6. The temperature of the fresh air after the heater is most of the time above 21°C, which was the set point for opening the bypass of the heat exchanger. The temperature of the fresh air is between 30 and 35°C when no heat is delivered from the solar air collector. The reason for this high fresh air temperature is seen in figure 2.20, where the thermostat is set to 4.5. The range on the thermostat is a bit difficult to see, but it is 10-38°C. 4.5 on the thermostat will then lead to the observed approx. 35°C. The heater seems to be switched off when warm fresh air is starting to be delivered to the heat exchanger even though the fresh air temperature is only just above 20°C – why cannot be explained based on the measurements.

It was further discovered, that the pressure control of the system wasn't active. This was put into operation and the air flow rates were adjusted.

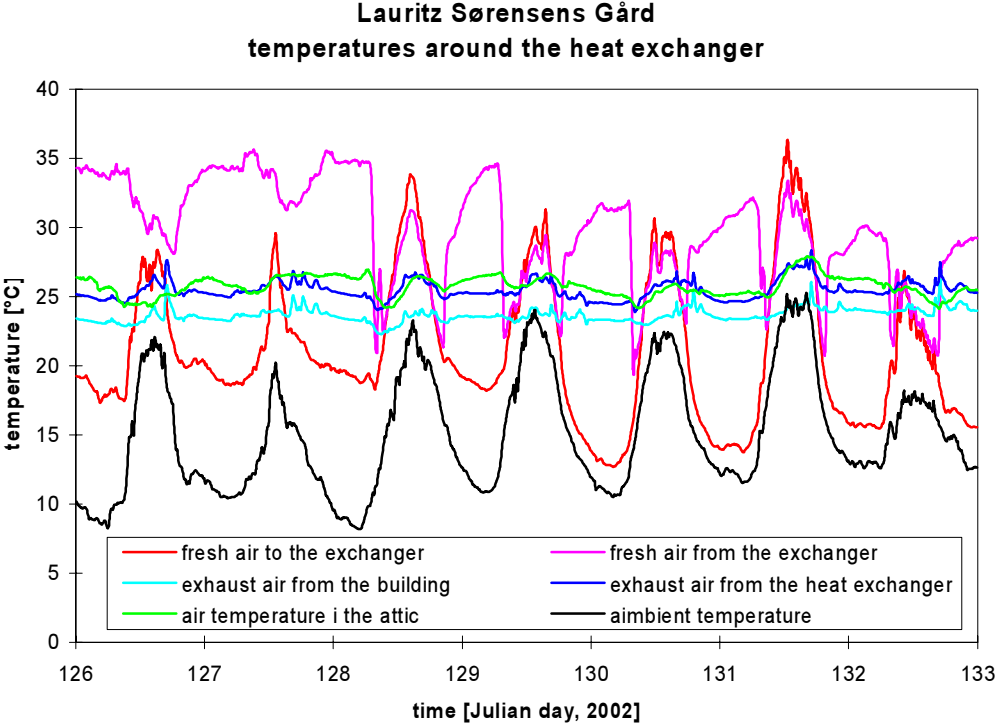


Figure 4.6. The air temperatures around the large heat exchanger during week 19, 2002 (May 6-12).

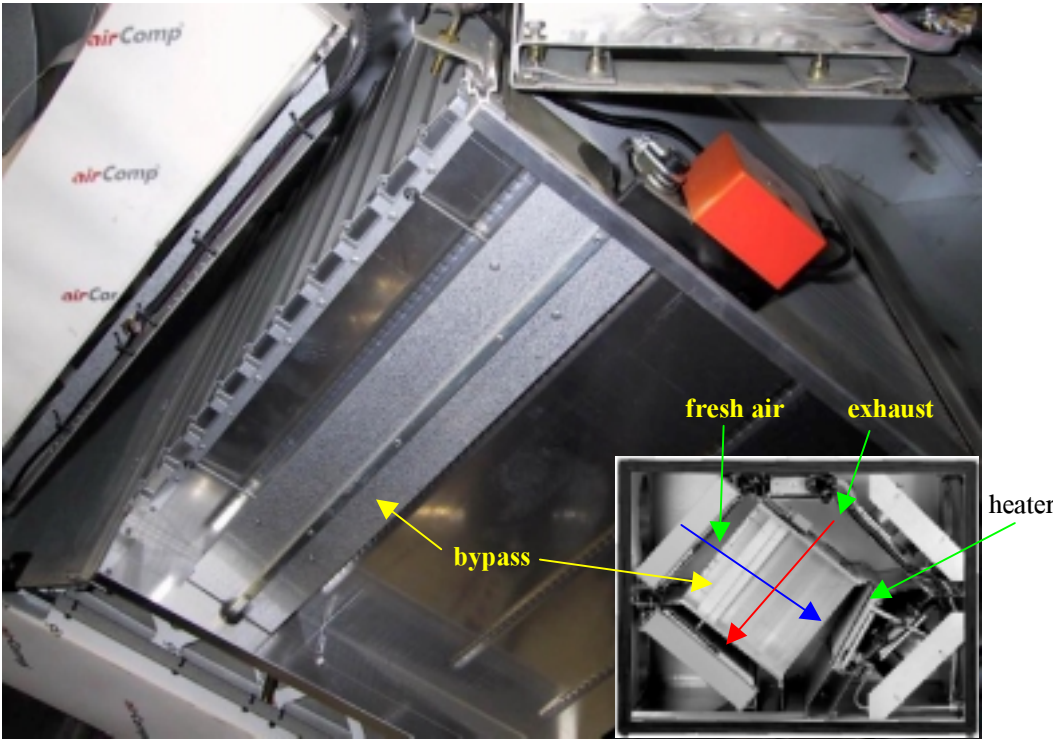


Figure 4.7. The bypass in the large heat exchanger.

The manufacture of the heat exchanger replaced the thermostat shown in figure 2.20 with a new and changed the set point of the bypass on December 4. The result is clearly seen in figure 4.8. Before noon on December 4 the outlet temperature of the exhaust air from the heat exchanger get below the inlet temperature of exhaust air to the heat exchanger. The temperature of the fresh air after the heater is now stable and around 24°C.

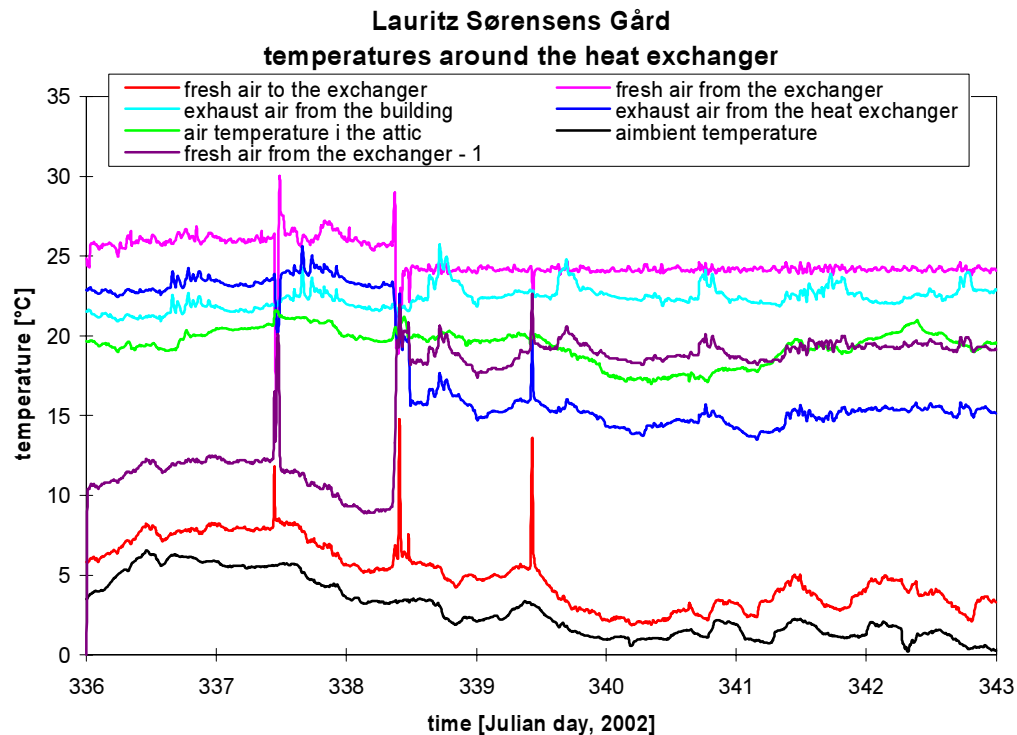


Figure 4.8. The air temperatures around the large heat exchanger during week 49, 2002 (December 2-8).

The reason why the temperature of the exhaust air increased over the heat exchanger before December 4, 2002 is believe to be due to the heat produced by the fan and the heater.

## 4.2. Description and characterization of the sub-systems

The function of the three major sub-systems: the PV-array, the solar air collector and the large heat recovery unit will be investigated in the following.

### 4.2.1. The PV-array

Based on the measurements two items will be investigated for the PV-array: the electricity production and the benefit on the performance of having an air flow behind the PV-panels.

#### 4.2.1.1. Electricity productions

Figure 4.9 shows the weather conditions during week 33, 2002 (August 12-18), which was a very good summer week with high ambient temperatures and rather much sunshine but also a

day with overcast and one day with overcast before noon. Figure 4.10 shows the electricity production during the same week.

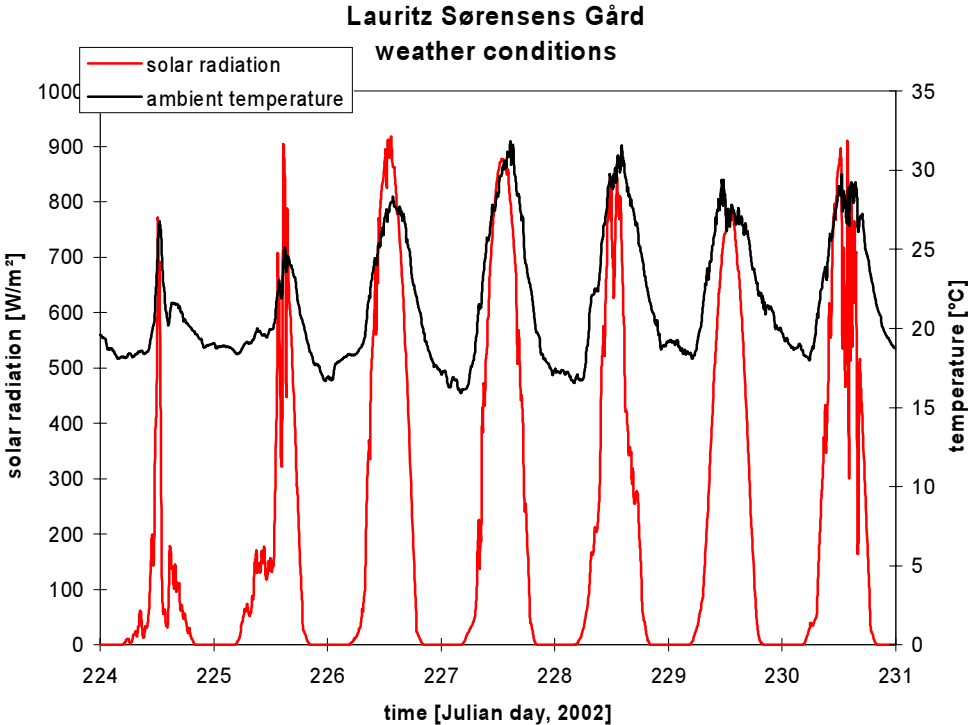


Figure 4.9. The weather conditions during week 33, 2002 (August 12-18).

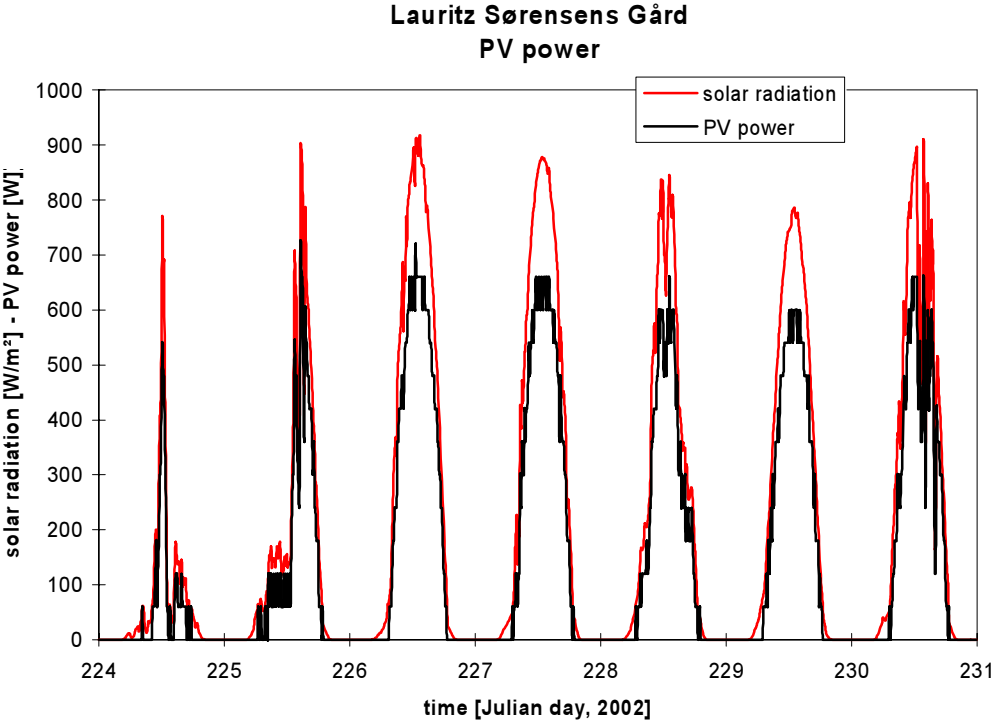


Figure 4.10. The electricity production and total solar radiation during week 33, 2002 (August 12-18).

Figure 4.11 shows the produced electricity dependent on the total solar radiation on the PV-panels for week 33, 2002.

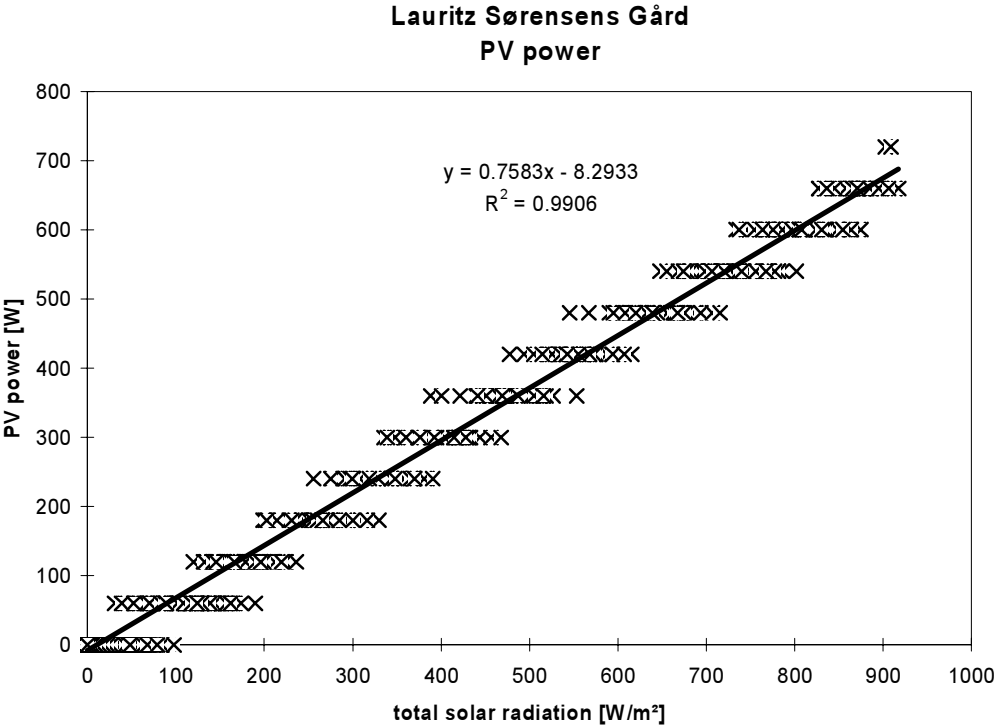


Figure 4.11. The electricity production dependent on the total solar radiation during week 33, 2002 (August 12-18).

The discrete levels of data in figure 4.11 are because the electricity produced is measured by counting pulses from the energy meter. A regression line and equation of the data is also shown in figure 4.11. Based on figure 4.11 the performance of the PV-panels at a solar radiation of 1000 W/m<sup>2</sup> will thus be 750 kWh, which is considerably less than the 1123 W<sub>p</sub> given on page 6. However, the 1123 W<sub>p</sub> is the performance of the PV-panels at a cell temperature of 25°C and with no losses in wiring and inverter.

Figure 4.12 shows the temperature on the back side of the PV-panel measured with the sensor PV2 (see figure 4.13). At a total solar radiation of 1000 W/m<sup>2</sup> the PV-panels will be in the order of 72.5°C. The performance of the PV-panels decreases with 0.45% for each degree increase in cell temperature – see appendix A. At a PV-panel temperature of 72.5°C the decrease is  $(72.5-25) \cdot 0.45 = 21.4\%$ . The peak performance of 1123 W<sub>p</sub> is, therefore; reduced to 883 W in this situation. The losses in the wiring between the PV-panels and the inverter should not exceed 3%. The power reaching the inverter is thus around 856 W. The efficiency of the inverter is 91-93%, which means that the power to the grid should be 779-796 W, which is only 4-6% higher than the measured power. This is inside the uncertainty on the measurements. For the whole year April 21, 2002-April 20, 2003 the measured energy from the PV-array (after the inverter) was 777 kWh this is less than 5 % lower than expected based on the measured solar radiation. So again a rather good agreement.

The overall efficiency (after the inverter) of the PV-panels was 6%.

It may, therefore, be concluded that the PV-array performs as expected under the given conditions.

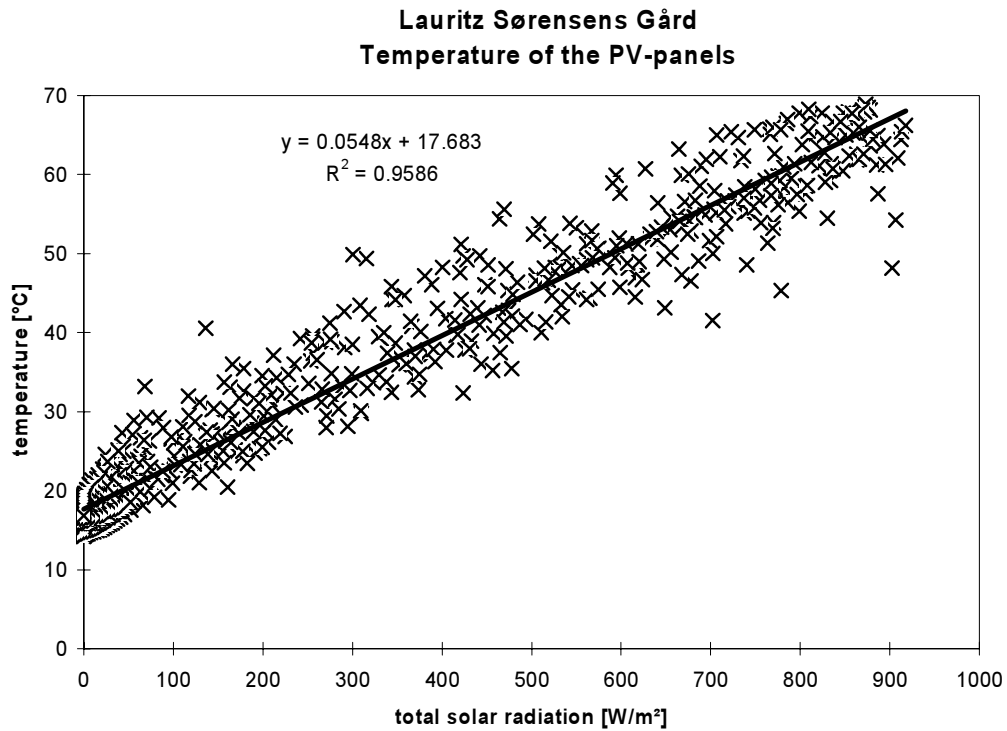


Figure 4.12. The PV-panel temperature (PV2 on figure 4.13) dependent on the total solar radiation during week 33, 2002 (August 12-18).

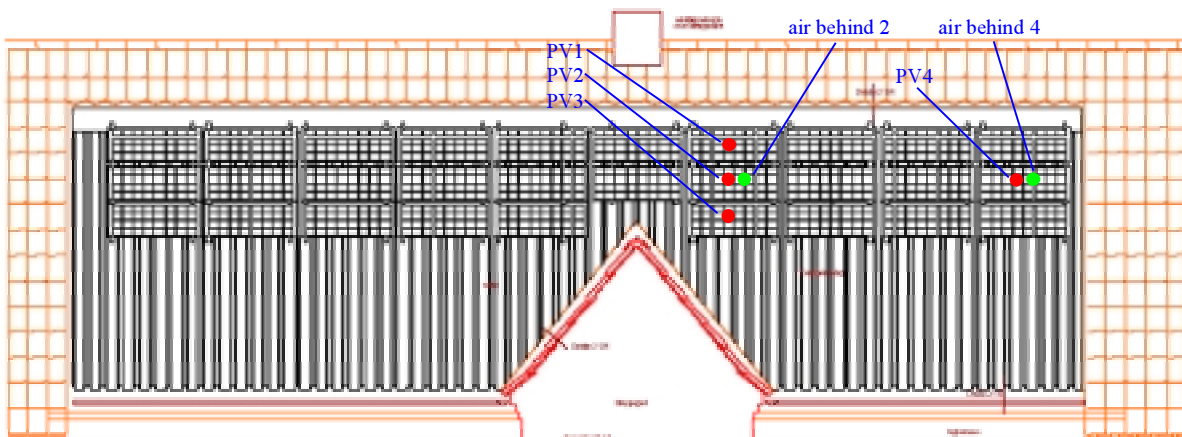


Figure 4.13. The labels of the temperature sensors in connection with the PV-array – compare with figure 3.2.

#### 4.2.1.2. PV-panel temperatures

Figure 4.13 shows the location and labels of the 6 temperature sensors located on or behind four of the PV-panels.

Figure 4.14 shows the temperatures on and behind the PV-panels during week 33, 2002.

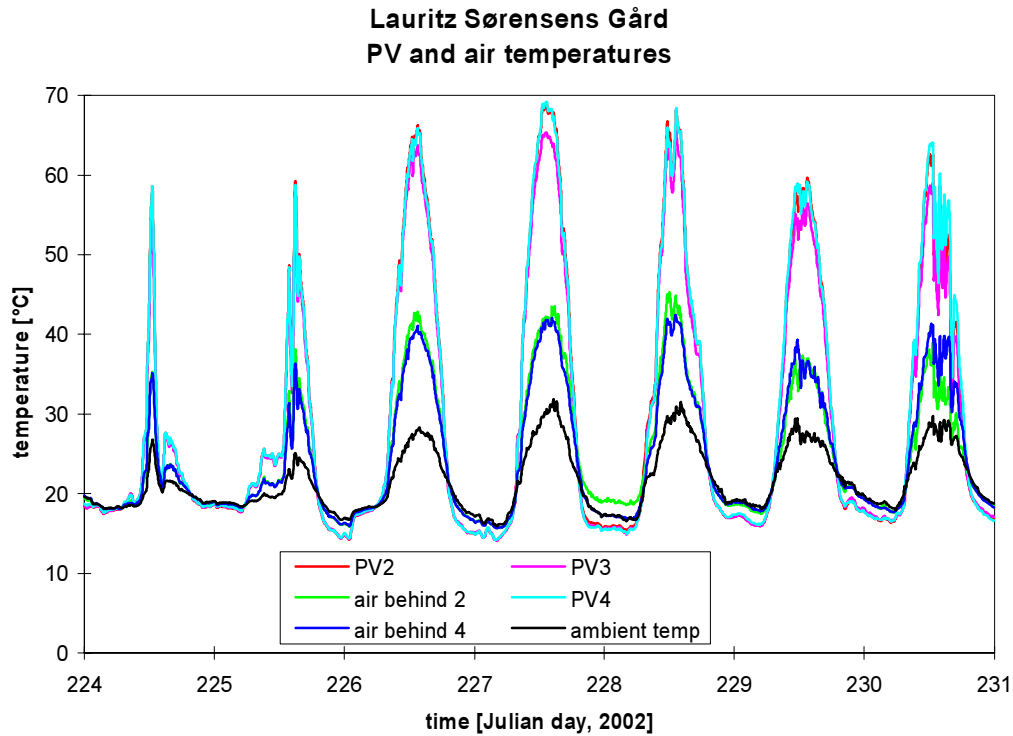


Figure 4.14. The temperature on and behind the PV-panel and the ambient temperature during week 33, 2002 (August 12-18).

PV1 is unfortunately not shown on figure 4.14. Although checked when mounted it turned out that there was a improper soldering between the sensor and the wiring to the data logger. The sensor, therefore, gave false readings.

Figure 4.14 shows a general picture of the temperatures on and behind the PV-panels for the whole measuring period.

Figure 4.14 shows that the temperature on PV-panel PV2 and PV4 is almost identical while PV3 is below the two other temperatures. On August 15 at noon (day 227) PV3 is approx. 3.5 K below the two other PV-panel temperatures. PV2 and PV4 is as seen in figure 4.13 on the same level, while PV3 is located one level lower. This indicates that the temperature of the PV-panel increases when going up vertically. Unfortunately PV1 is not able to more clearly show this.

As PV2 and PV4 + the temperatures of the air behind these PV-panels are almost identical this indicates that the air flow behind these PV-panels are very similar.

Figure 4.15 shows the air flow rate to the heat exchangers during week 33, 2001. Figure 4.15 shows that the air flow to the large heat exchanger was switched off on day 227 and on again on day 228. The air flow through the small heat exchangers was on during this period, but the air flow through the solar air collector was low. In figure 4.16 the temperatures on and behind the PV-panels are compared with the air flow through the large heat exchanger and the solar radiation during day 227-228. The small drop in the temperatures at noon day 228 is due to a short decrease in the solar radiation.

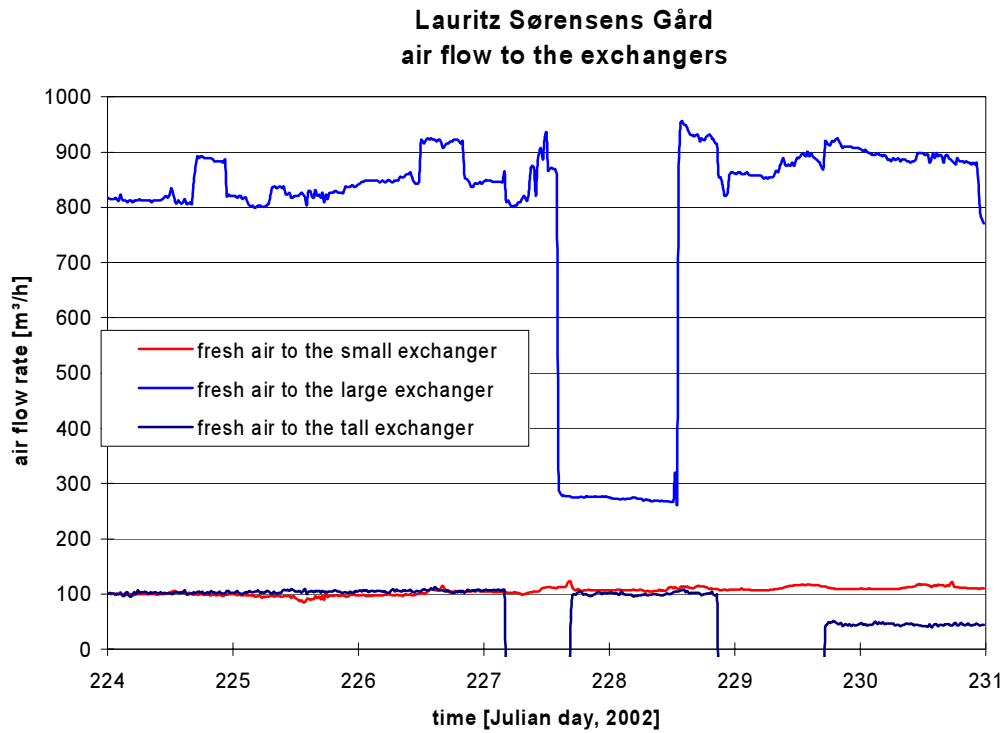


Figure 4.15. The air flow rate to the heat exchangers from the solar air collector during week 33, 2002 (August 12-18).

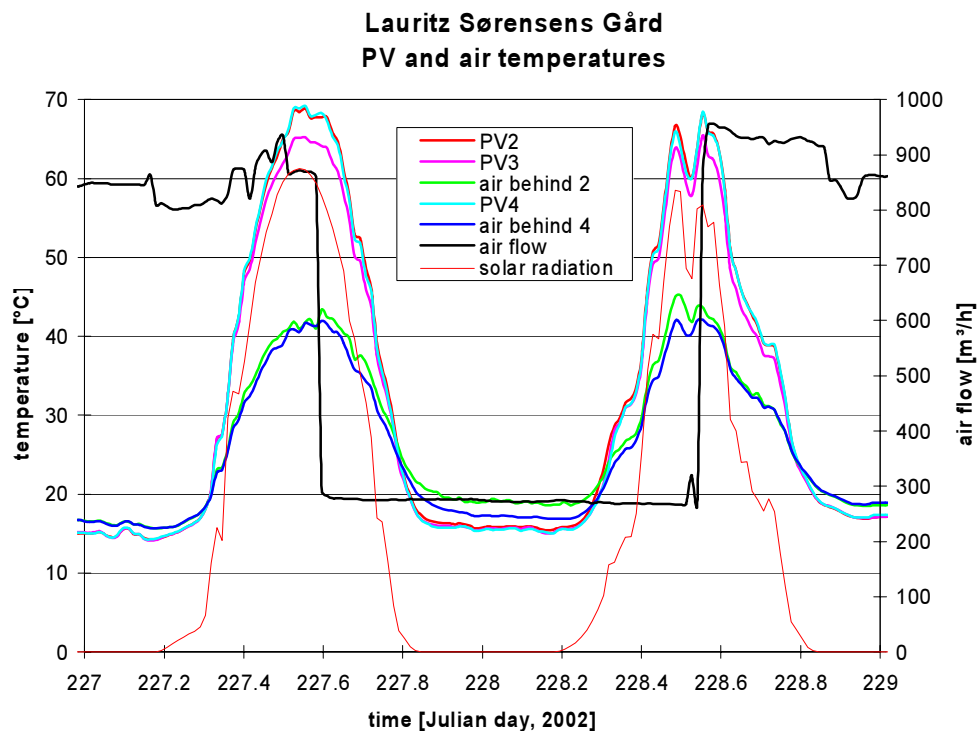


Figure 4.16. The temperatures on and behind the PV-panels, the air flow through the large heat exchanger and the total solar radiation during day 227-228 (August 15-16).

Figure 4.16 shows no change in the temperature on and behind the PV-panels due to the change in air flow rate through the large exchanger – only due to the solar radiation. This indicates that the temperatures on and behind the PV-panels is not effected by the air flow rate to the building through the solar air collector. The reason for this is the rather low air flow rate through the solar air collector – below  $30 \text{ m}^2/\text{hm}^2$ . It is, therefore, supposed that the air flow behind the PV-panels mainly is buoyancy driven – i.e. as shown in figure 2.10.

Figure 4.17 shows the air flow to the heat exchangers from the solar air collector during the last two days in week 37 and five first days in week 38, 2002 (September 14-20), where the "fresh" air intake to the small high heat exchanger was switched off – i.e. not blowing air into the solar air collector as in figure 4.15 – se section 4.1.1 for further explanation. The air flow rate through the large heat exchanger was further rather low. The weather conditions during this "week" are shown in figure 4.18.

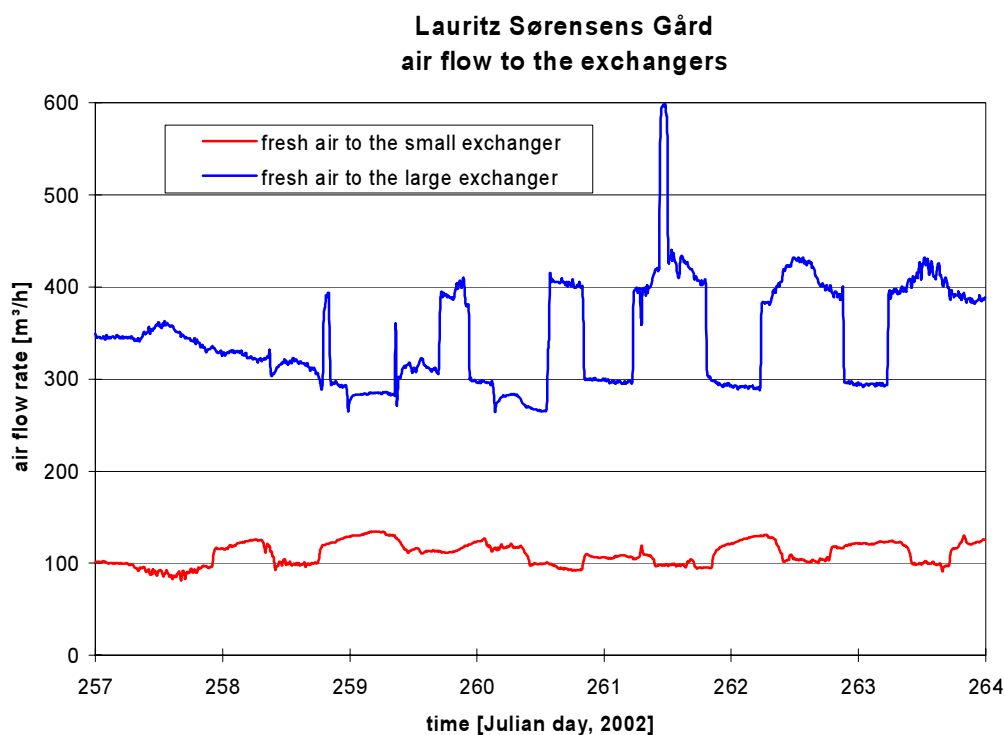


Figure 4.17. The air flow rate to the heat exchangers from the solar air collector during week 37-38, 2002 (September 14-20).

For days with large solar radiation - day 226-229 in figure 4.9 and 257, 258 and 262 in figure 4.18 – the following has been investigated: the temperature increases of PV2 and air behind 2 (i.e.  $PV2-T_{\text{ambient}}$  and  $\text{air behind } 2-T_{\text{ambient}}$ ) has been plotted against the total radiation as seen in figure 4.19 including regression lines and regression equations. Based on the regression equations for the above-mentioned days the temperature increase of PV2 and the air behind 2 at a solar radiation of  $1000 \text{ W}/\text{m}^2$  (in order to be able to compare) has been found – these are listed in table 4.1 and shown graphically in figure 4.20. No firm conclusion may be obtained of the dependency of the temperature increase of the PV-panels on the air flow rate through the solar air collector, while there is a clear tendency of decreasing air temperature behind the PV-panels with increasing air flow rate through the solar air collector. The variation is mainly supposed to be due to the wind along the PV-panels. Based on this it is concluded that the air flow through

the solar air collector has no or minor influence on the temperature of the PV-panels and thereby the performance of the PV-panels – at least not for the rather low air flow rates measured at Lauritz Sørensens Gård – i.e. below 50 m<sup>3</sup>/hm<sup>2</sup>.

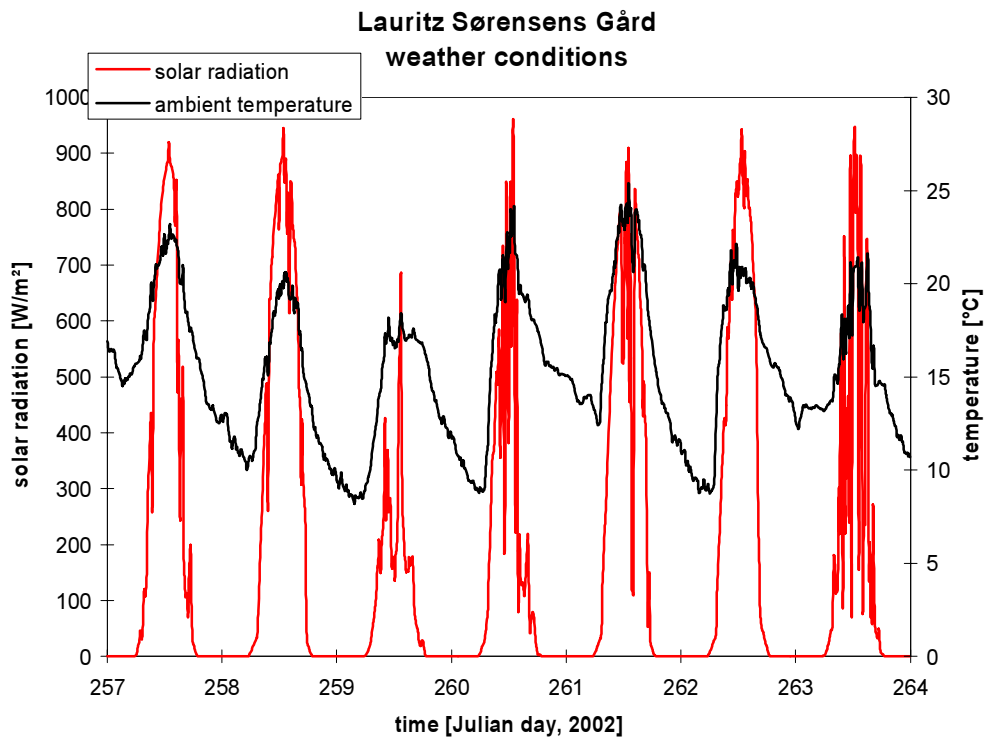


Figure 4.18. The weather conditions during week 37-38, 2002 (September 14-20).

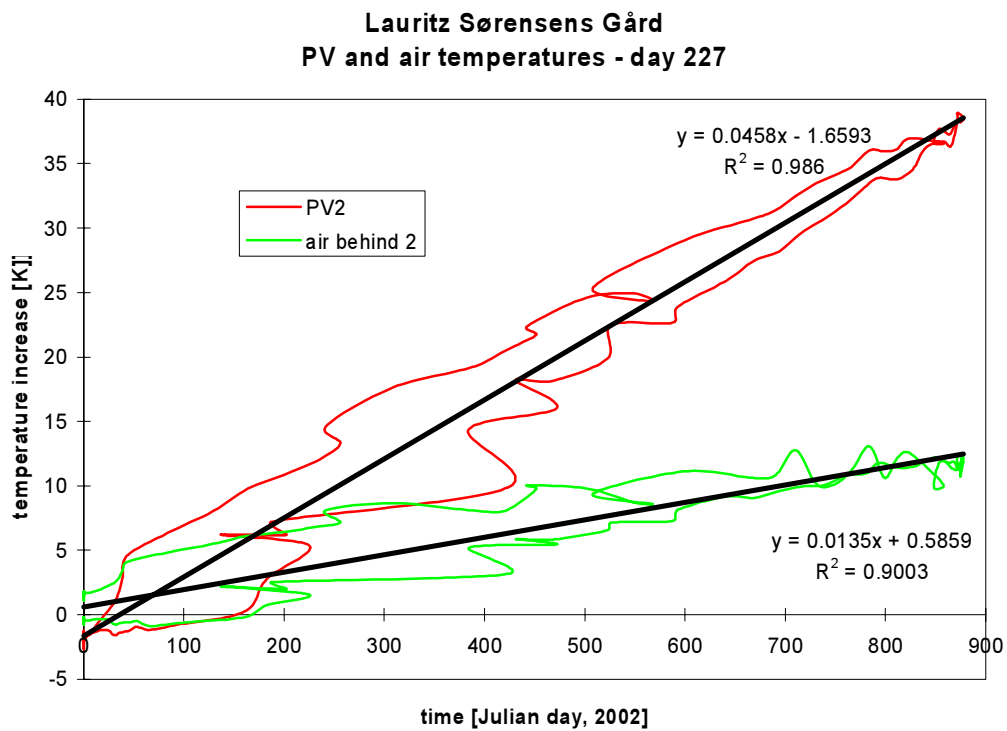


Figure 4.19. Temperature increase of PV2 and the air behind PV2 during day 229, 2002 (August 17).

Day number 2002/2003	Temperature increase for PV2 [K]	Temperature increase for air behind 2 [K]	Approx. air flow rate [m <sup>3</sup> /h]
226	40.8	15.6	1000
227	44.1	12.9	1000
228	46.1	15.5	400
229	41.0	8.7	1000
257	43.4	17.7	450
258	44.2	12.0	420
262	40.2	17.9	530
84	41.9	12.6	1400
85	42.1	9.9	1400
86	44	8.4	1600
87	44.2	10.7	1600
90	39.1	13.6	1100
94	37	12.8	1100

Table 4.1. The temperature increase at a total radiation of 1000 W/m<sup>2</sup> for PV2 and air behind 2.

The air flow rate in both table 4.1 and figure 4.20 is only tentative as the uncertainty on the air flow of fresh air to the small exchanger due to the calibration procedure (section 3.7) is very high and that the the system with the small tall heat exchanger actually blowed air to the solar air collector instead of sucking air from it on the days 226-229. The latter is although regarded as a minor problem as the small tall heat exchanger is connected to the solar air collector away from the location of the temperature sensors on and behind PV2.

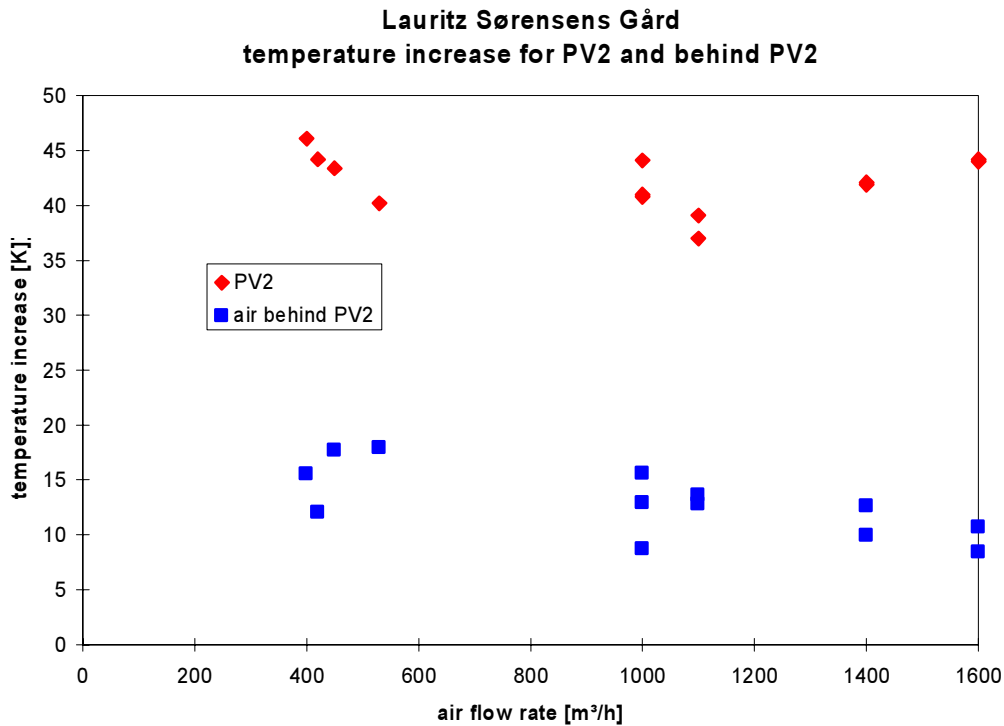


Figure 4.20. The dependency of the temperature increase of PV2 and the air behind PV2 (from table 4.1) on the air flow rate through the solar air collector.

### 4.2.2. The solar air collector

The fresh air to the building is preheated in the solar air collector, which consists of the total area of perforated Solarwall sheets both with and without PV-panels on top. The functionality of the two areas of the solar air collector is different. For the area without PV-panels the air is heated when passing the holes in the Solarwall sheets while for the other area the air is heated when passing behind the PV-panels. The efficiency of the two areas as solar air collector is, therefore, different. Further while only minor reflection occurs on the Solarwall sheets reflection occurs on the PV-panels due to the glass - especially at high incidence angles.

Figures 4.21-24 show the measured parameters related to the solar air collector for week 23, 2002 (June 3-9). Figure 4.21 shows the weather conditions for that week. The week was characterized with much solar radiation and high ambient temperatures. Figure 4.22 shows the air flow rates from the solar air collector (the air flow of "fresh air" to the small tall heat exchanger was zero, which is why this week was chosen, as this air flow as earlier explained was opposite as intended – blowing instead of sucking). Figure 4.23 shows the total mass flow rate per m<sup>2</sup> collector area, while figure 4.24 shows the temperatures of the air out of the solar air collector (the numbering is shown in figure 4.3). The temperature increase over the solar air collector is up to about 10 K. There is a temperature difference between the four inlet temperatures of up to 4 K. This is seen more clearly in figure 4.25, which only shows June 5. Figure 4.25 shows that the inlet temperatures of inlet 1 and 4 is higher than inlet 2 and 3, which is due to the fact that the manifold was not as long at the solar air collector and further centred with regard to the solar collector as seen in figure 4.3. This means that inlet 1 and 4 serves a much larger area than inlet 2 and 3. If the air flow rates in the four inlets are similar (which is assumed) the temperature increase of the air to inlet 1 and 4 will be higher than to inlet 2 and 3 due to a lower air speed through the collector areas served by inlet 1 and 4. Figures 4.24-25 further show that the measured mean air temperature out of the manifold in fact is the mean temperature of the four inlet temperatures. The fluctuations observed in figure 4.25 is partly due to the shown fluctuations in the ambient temperature (most possible wind induced) partly due to fluctuations in the mass flow rate.

Figure 4.26 shows the power transferred to the air in the solar air collector. The power is during week 23, 2002 up to 3.000 W, which as seen later is rather low compared to the large collector area. The air is as seen in figure 4.26 also heated during the night without solar radiation due to the heat loss from the building through the roof. This is dealt with later.

Figure 4.22 and 4.24 show a problem with the ventilation systems. The fresh air to the building is pre-heated although the ambient temperature often is above 25°C. The system will thus lead to overheating of the building. There should have been a possibility to bypass the solar air collector when no pre-heating of the air is necessary. The tenants can, however, turn off the fresh air supply individually.

Figure 4.27 shows the temperatures around the large heat exchanger. Although the bypass of the heat exchanger was open the fresh air is cooled a bit in the heat exchanger. If the bypass had not been open the fresh air could have been cooled even more. Due to the wrong setting of the thermostat of the heater in the heat exchanger – see section 4.1.2 - the air was heated to around 27°C during the night.

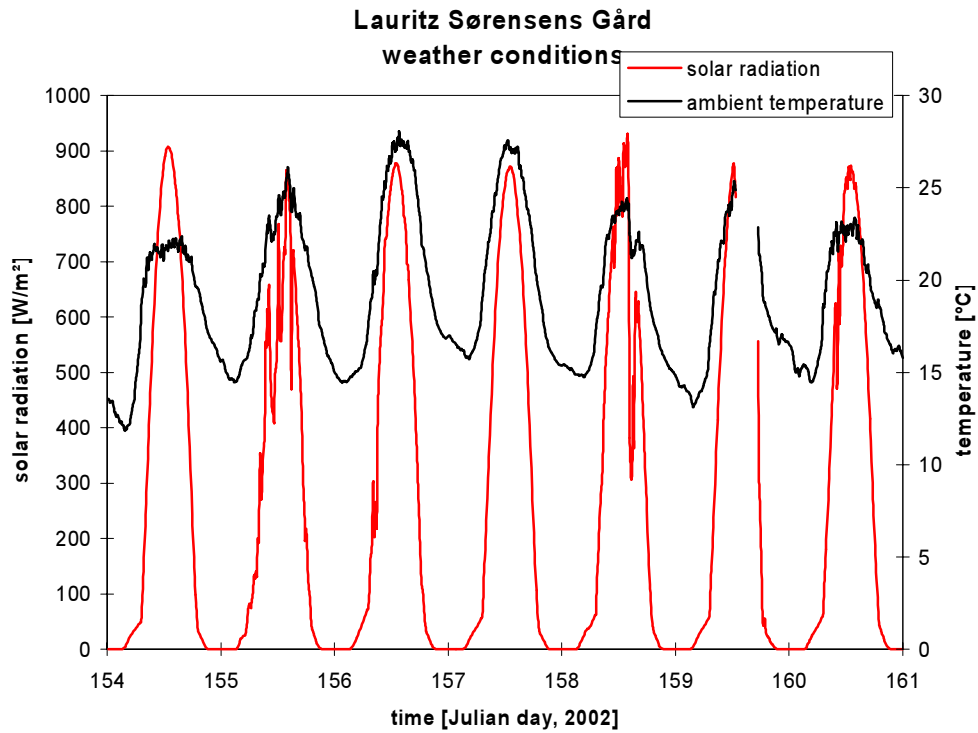


Figure 4.21. The weather conditions during week 23, 2002 (June 3-9).

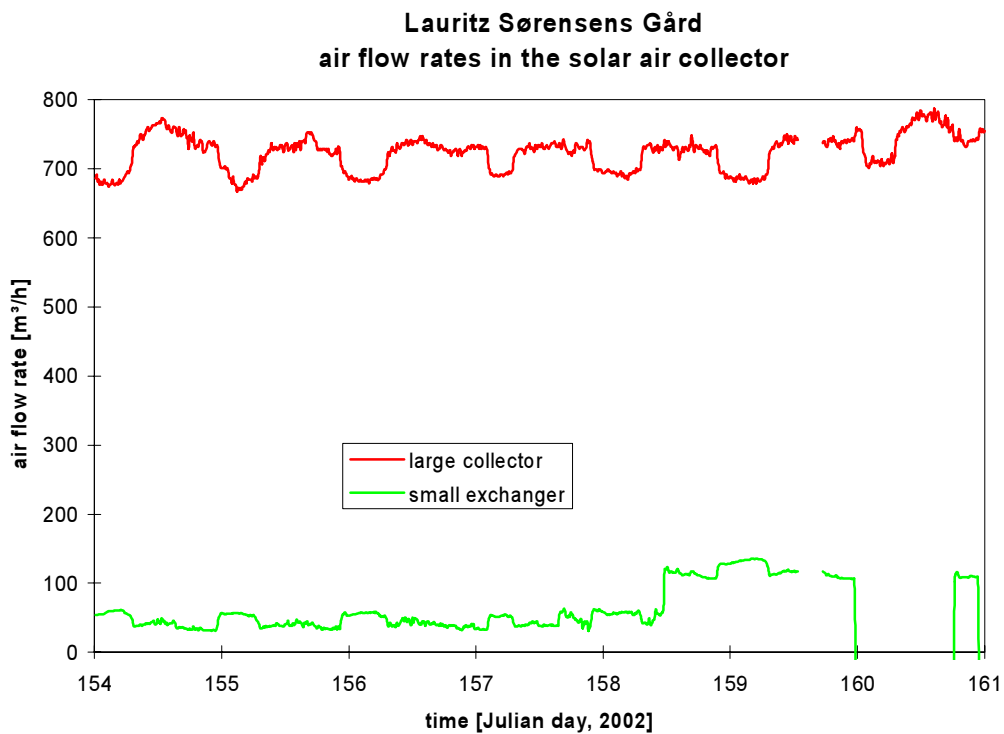


Figure 4.22. The air flow rates through the solar air collector during week 23, 2002 (June 3-9).

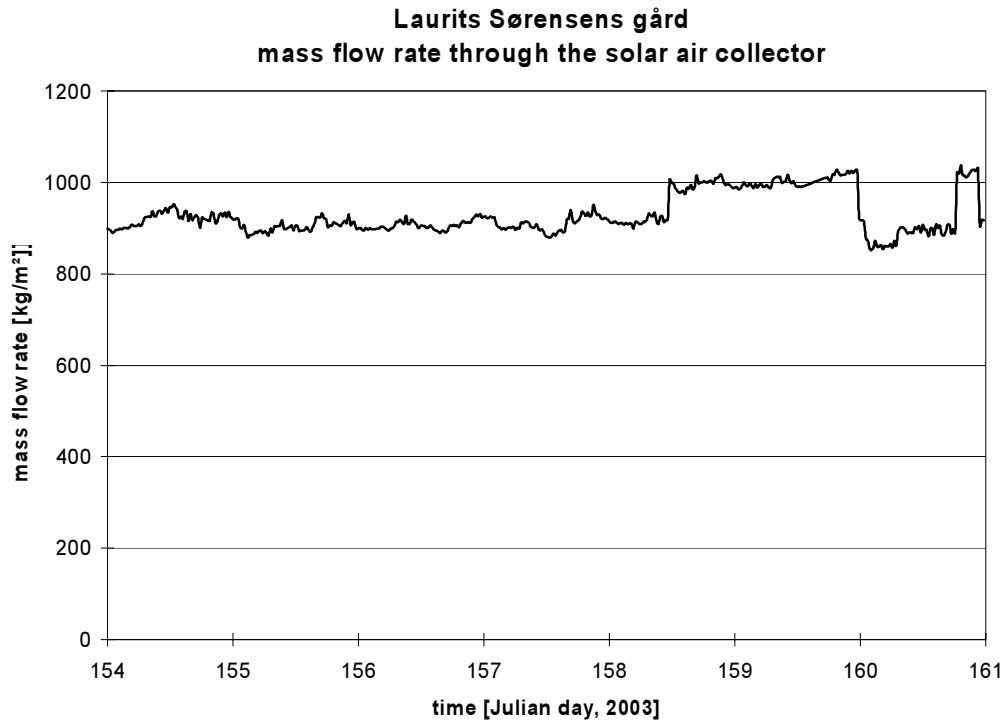


Figure 4.23. The mass rates through the solar air collector during week 23, 2002 (June 3-9).

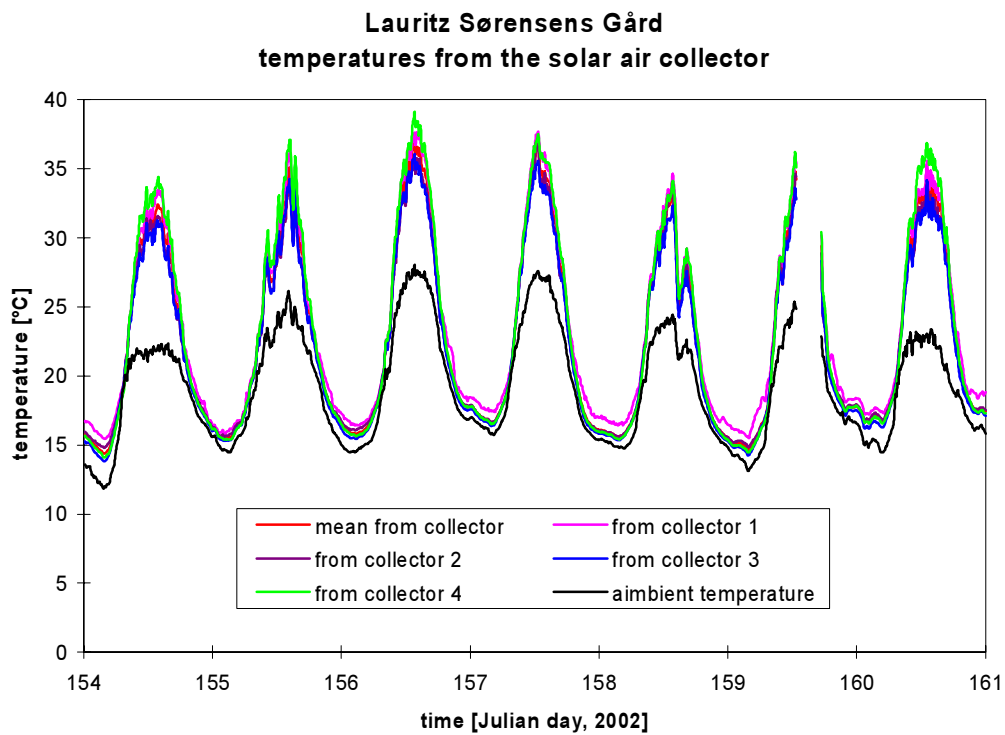


Figure 4.24. The air temperatures out of the solar air collector during week 23, 2002 (June 3-9).

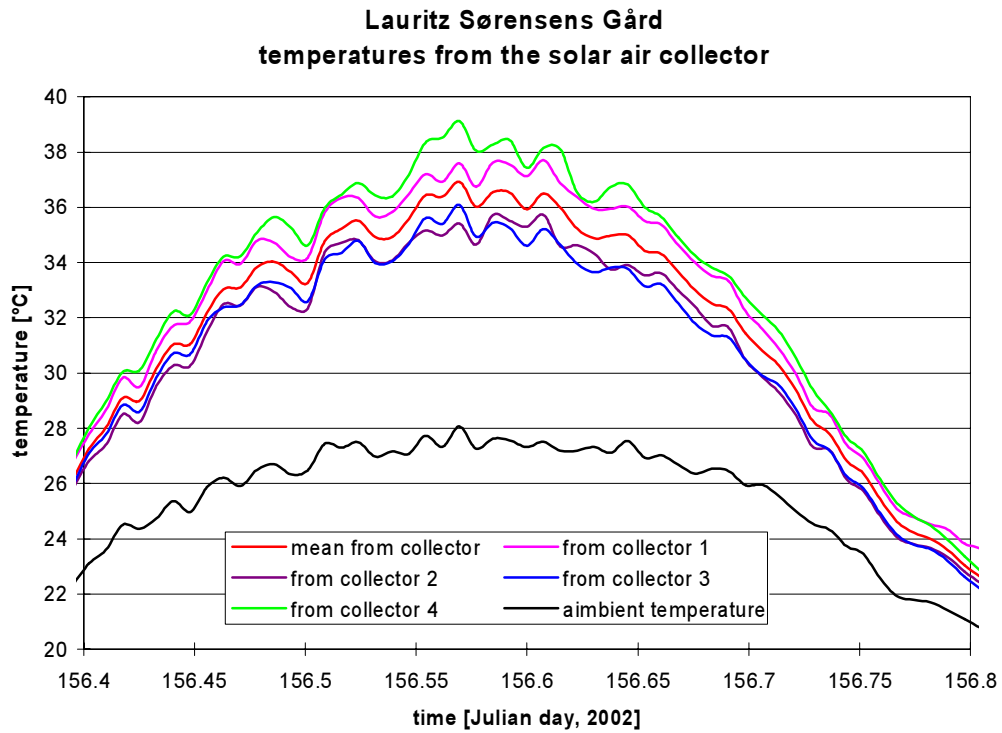


Figure 4.25. The air temperatures out of the solar air collector during June 5, 2002.

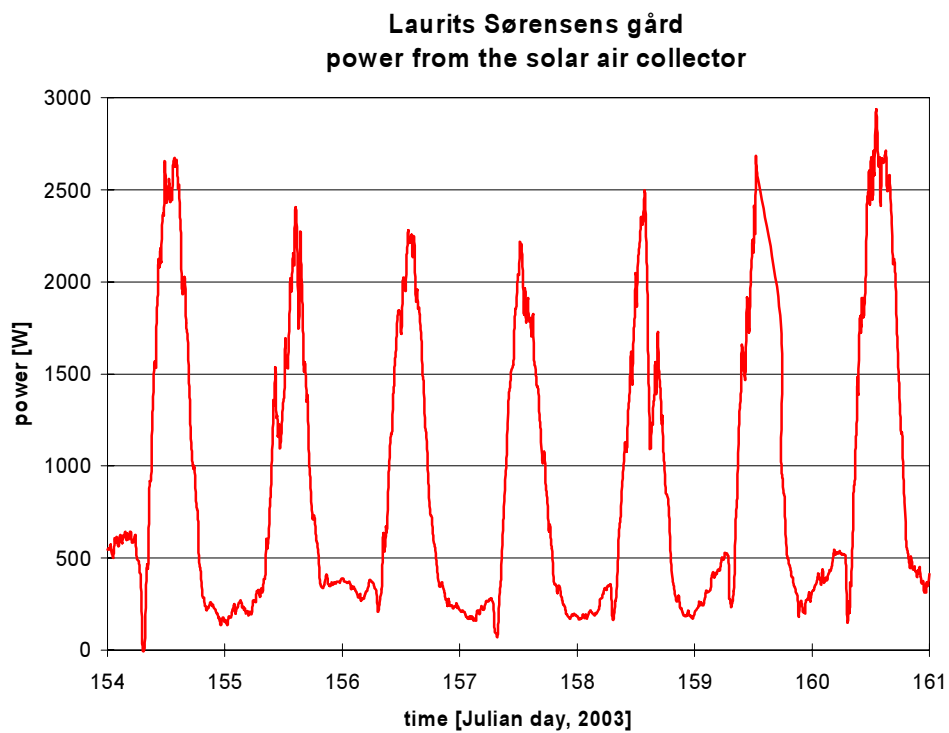


Figure 4.26. The power transferred to the air in the solar air collector during week 23, 2002 (June 3-9).

#### 4.2.2.1. Efficiency of the solar air collector

Based on figure 4.26 it is possible to calculate the efficiency of the solar air collector. The efficiency of the solar air collectors was calculated in the following way:

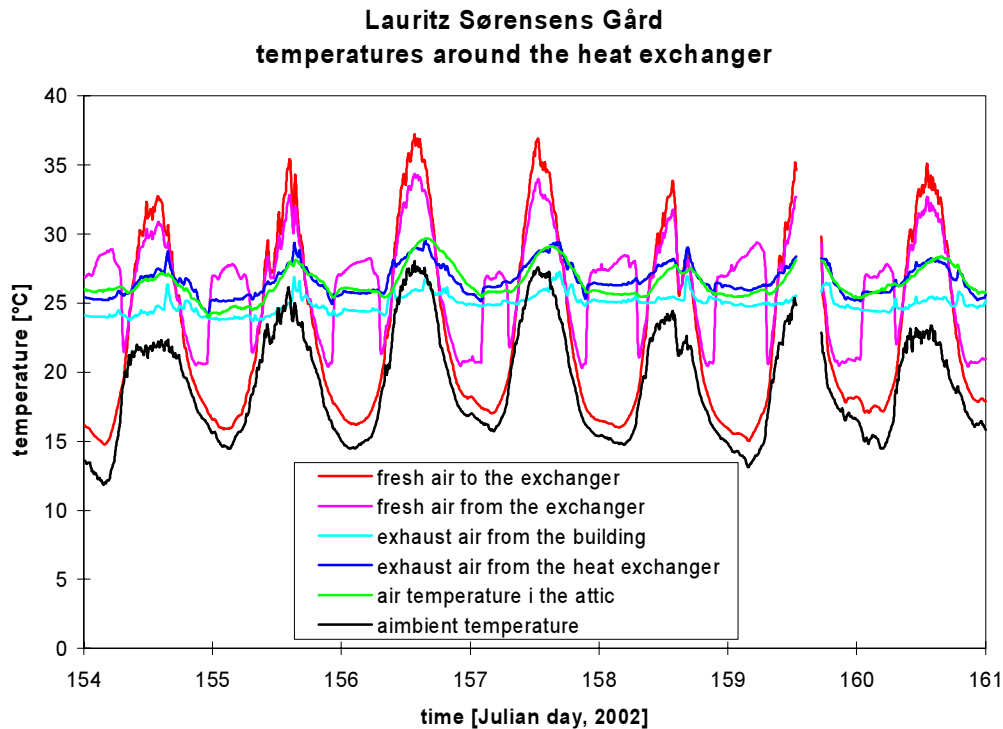


Figure 4.27. The air temperatures around the large heat exchanger during week 23, 2002 (June 3-9).

$$\eta = q_{\text{coll}} / (E_{\text{usefull}} \cdot A_{\text{coll}}) \quad [4.1]$$

where  $q_{\text{coll}}$  is the power transferred to the air [W],  
 $E_{\text{usefull}}$  is the useful solar radiation [ $\text{W}/\text{m}^2$ ] – i.e. total solar radiation corrected for reflection losses in the cover of the PV-panels,  
 $A_{\text{coll}}$  is the area of the total solar air collectors.

The total radiation on the solar air collectors was transformed into useful radiation by taking into account the reflection of the solar radiation in the glazing of the part of the solar air collector covered with PV-panels at periods with a non zero incidence angle for the solar radiation. No correction for the Solarwall sheets was required. In order to correct for the reflections at the PV-panels it is necessary to calculate the split between direct and diffuse radiation based on the measured total radiation. This was done using the equations in (Duffie and Beckman, 1991). The calculated split introduces a small uncertainty compared to a case where both total and diffuse radiation is measured. The following equation has been applied to account for the reflection in the cover – the factor should be multiplied with the direct and diffuse irradiation:

$$k = 1 - \tan^a(\theta/2) \quad [4.2]$$

where  $\theta$  is the incidence angle for the radiation: the actual incidence angle for the direct radiation and  $60^\circ$  for the diffuse radiation.  $a$  is 3.2 (Nielsen, 1995).

The efficiency and normalized mass flow rate (per  $m^2$  collector area) is shown in figure 4.28. Figure 4.28 shows a rather scattered picture. The very high peaks of the efficiency is as seen in figure 4.26 due to the small heating of the air during the night, which divided with the very low solar radiation at sunup and sundown gives the high efficiencies. Figure 4.29, therefore, shows a close up for June 5, 2002 where also the measured total radiation on the solar air collector is shown. For radiation levels above  $200 \text{ W/m}^2$  the efficiency of the solar air collector is slowly increasing over the day. This is due to dynamic character of the solar air collector – i.e. the heating up and cooling down of the solar air collectors. During increasing solar radiation part of the heat from the sun is used to heat the materials of the solar air collectors and thereby leading to a lower efficiency, while during decreasing solar radiation the heat stored in the materials is transferred to the air leading to a higher efficiency. Figures 4.28-29 give, thus, not a clear picture of the steady state efficiency of the solar air collector. An even more scattered picture of the efficiency may be obtained if looking at a day with drifting clouds – i.e. very scattered solar radiation.

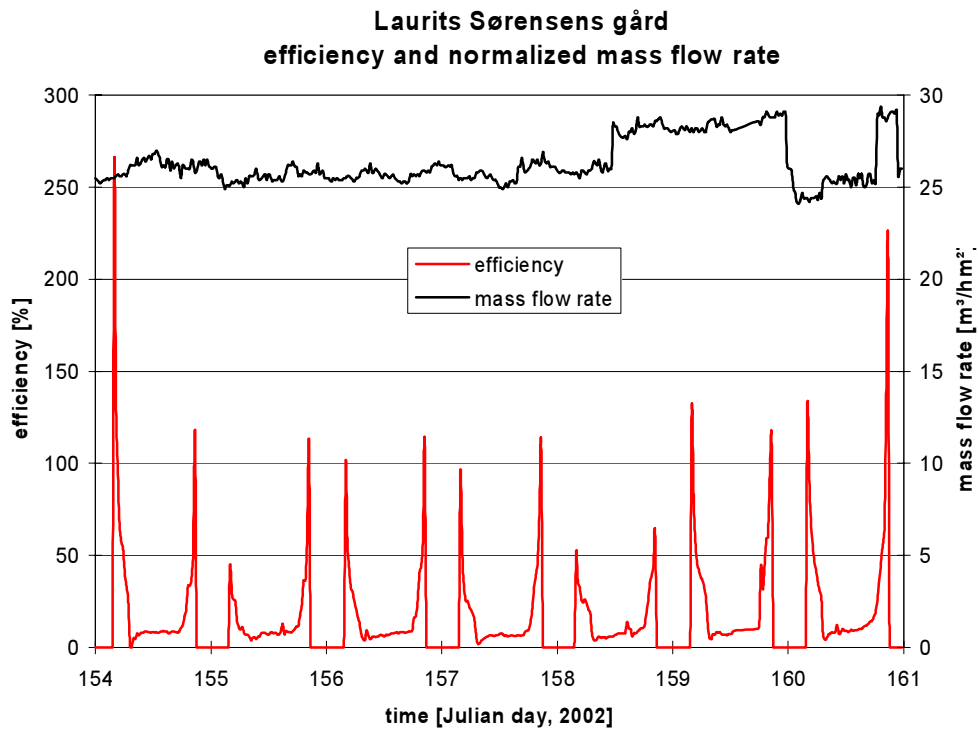


Figure 4.28. The efficiency of the solar air collector and the normalized mass flow rate through the solar air collector during week 23, 2002 (June 3-9).

A method for determination of the steady state efficiency of solar air collectors were developed in (Jensen, 1999) and validated in (Jensen and Bosanac, 2002). The essence of the method is to show the efficiency and mass flow rate as a function of the useful solar radiation on the solar air collector. The efficiency of the solar air collector is too low during periods with increasing solar radiation and too high during periods with decreasing solar radiation due to the heating and cooling of the materials in the solar air collector. Therefore, the steady state radiation must be found just around the time, when the radiation level on a sunny day is at its maximum. The

thermal capacity does, however, that the right time is somewhat after the maximum solar radiation occurs dependent on the amount of thermal mass. But on a day with clear sky conditions there is an almost vertical plateau on the curve showing the solar radiation, which allows for the determination of the steady state efficiency of the solar collector with a rather good precision as shown in (Jensen and Bosanac, 2002).

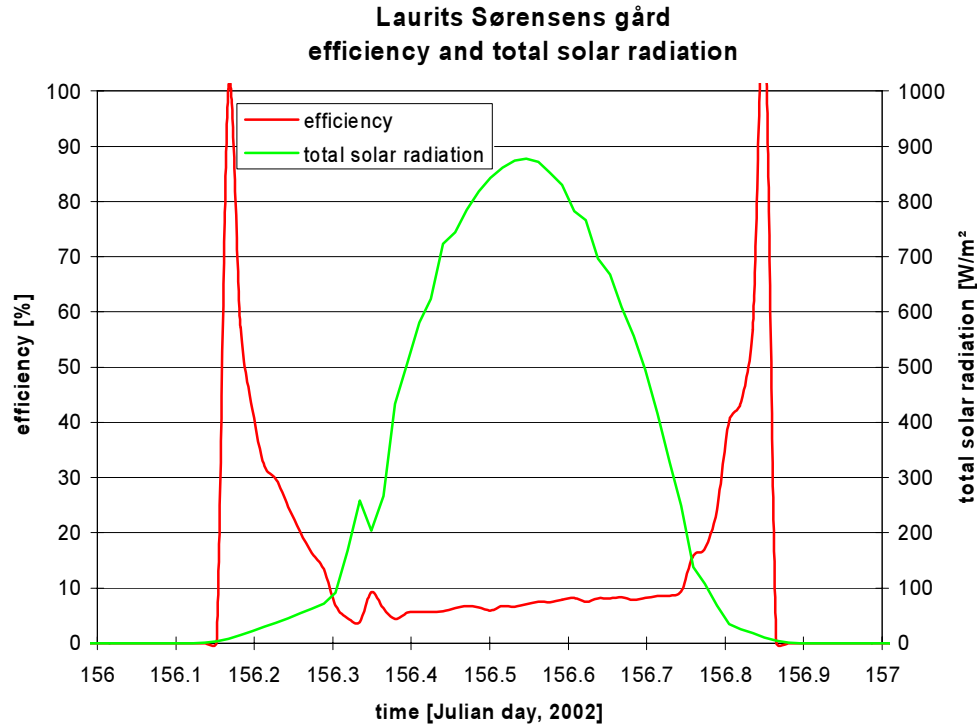


Figure 4.29. The efficiency of the solar air collector and measured total solar radiation on the solar air collector during June 5.

Figure 4.30 shows the efficiency and normalized mass flow for June 3, 2002 as function of the useful solar radiation. Figure 4.30 shows an efficiency of about 8 % at a normalized mass flow rate of 27 kg/hm<sup>2</sup>. Figure 4.31 shows the results using the above method on days in both 2002 and 2003 with clear sky conditions and stable air flow through the solar air collector - and for 2002 where the small, tall heat exchanger was turned off. This because the fresh air flow of the small tall heat exchanger was reverse during most of 2002 (blowing instead of sucking from the solar air collectors) so only days without "fresh" air flow of the small tall heat exchanger may be used for determination of the efficiency of the solar air collector. It should further be remembered, that the mass flow rate for 2002 is more uncertain than for 2003 as the calibration equation for the fresh air of the small heat exchanger as earlier explained really isn't valid for this period. However, as this mass flow is only a minor part of the overall mass flow rate through the solar air collector, the uncertainty of the total mass flow rate is less effected. Figure 4.31 further shows a regression line and equation for the measured efficiencies.

Figure 4.31 further show the efficiency of the Solarwall from figure 2.8. Figure 4.31 still show some scattering of the efficiency. This is due to wind as the efficiency of both the Solarwall sheets and the PV-panels as solar air collector is very sensitive to the wind speed. Figure 4.31 shows that the efficiency of the solar air collector at Laurits Sørensens Gård is as expected lower than for the Solarwall collector (PV solar air collectors has a lower efficiency than the

Solarwall collector). In figure 4.31 the efficiency is further compared with the efficiency of the PVT collectors at Lundebjerg (Jensen, 2001). The PVT collectors were so-called solar chimneys as shown in figure 4.32. The PVT collectors was totally covered with PV-panels with sealing between the PV-panels so that air was sucked in at the bottom, flowing behind the PV-panels and taken out at the top.

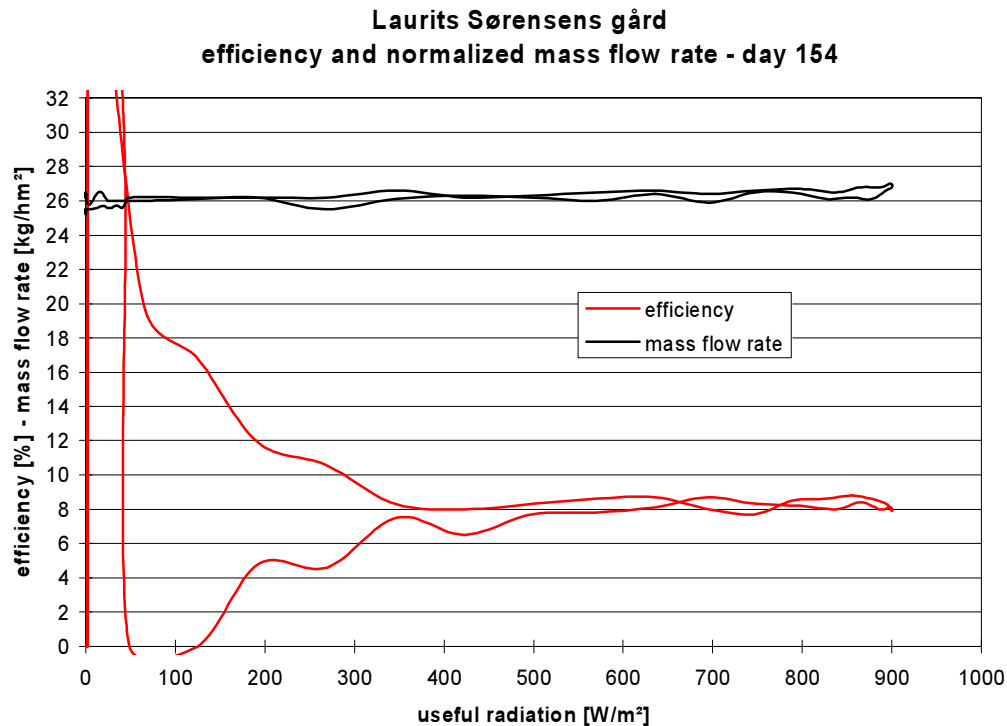


Figure 4.30. The efficiency and normalized mass flow rate dependent on the useful solar radiation for June 3, 2002.

Figure 4.31 shows that the efficiency of the solar air collector at Lauritz Sørensens Gård is higher than the efficiency at Lundebjerg (same scattering due to the influence of wind was also found for Lundebjerg) at mass flow rates above 40 kg/hm<sup>2</sup>. It was expected that the efficiency of the solar air collector at Lauritz Sørensens Gård would lay between the two curves in figure 4.31 as only about one third of the Solarwall sheets were covered with PV-panels. This indicates that the area of the solar air collector rather than being the total area of Solarwall sheets (including the part with the PV-panels) should only be the part without PV-panels – i.e. 22.9 instead of 35.3 m<sup>2</sup>. Using an area of 22.9 m<sup>2</sup> instead of 35.5 m<sup>2</sup> brings the efficiency of the solar air collector closer to the efficiency of the Solarwall collector as seen in figure 4.33, however, still lower at low flow rates. The reason for the lower efficiency at low flow rates compared to the Solarwall sheets is partly assumed to be a less good distribution of the air over the solar air collector as indicated in figure 4.25 – i.e. the higher air temperatures at inlet 1 and 4 compared to inlet 2 and 3. Partly that the part of the solar air collector covered with PV-panels doesn't contribute to the heating of the air as seen when comparing the below figure 4.34 with figure 4.24. The comparison shows that the temperature of the air behind the PV-panels is equal to or below the outlet air temperature from the solar air collector.

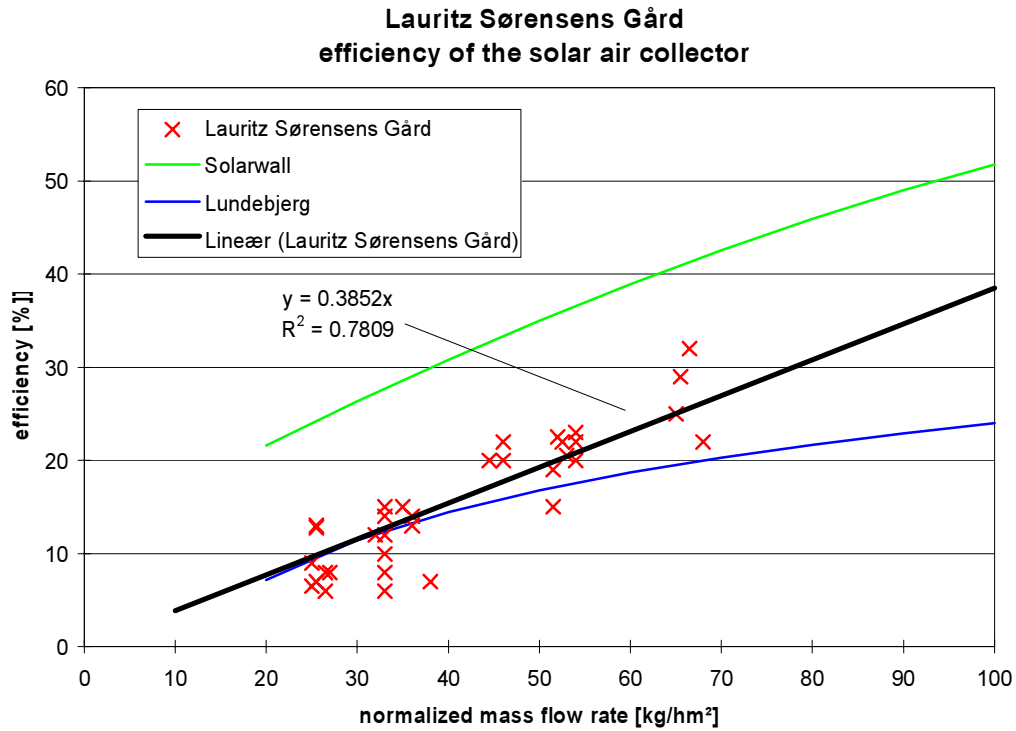


Figure 4.31. The efficiency of the solar air collector at Lauritz Sørensens Gård compared with the efficiency of the Solarwall collectors and the solar chimneys at Lundebjerg.



Figure 4.32. The solar chimneys at Lundebjerg for which the efficiency curve in figure 4.31 was found.

The efficiencies shown in figure are rather scattered leading to a rather high uncertainty on the shown regression line. It is, however, believed that the regression line gives a rather correct picture of the dependency of the efficiency of the solar air collector at Lauritz Sørensens Gård as a function of the mass flow rate through the solar air collector. It is believed that the main reason for the difference between the efficiency of the Solarwall collector and the solar air collector at Lauritz Sørensens Gård in figure 4.33 is a poor distribution of the air flow – at low flow rates - over the solar air collector at Lauritz Sørensens Gård.

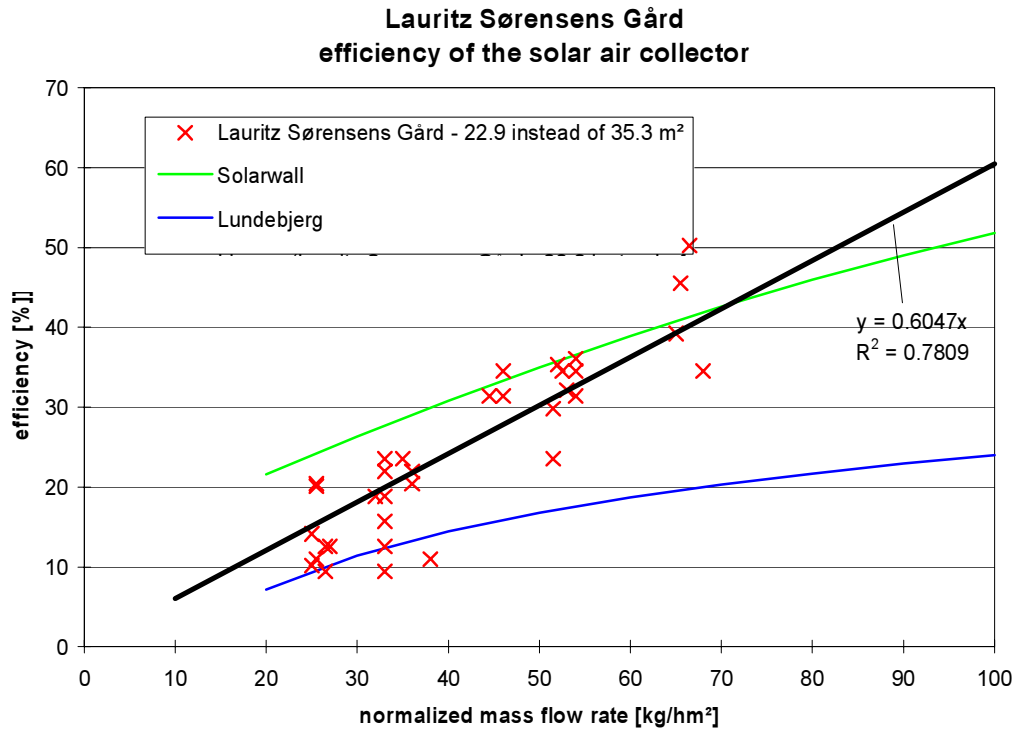


Figure 4.33. The efficiency of the solar air collector at Lauritz Sørensens Gård with an area of 22.9 m<sup>2</sup> (instead of 35.3 as in figure 4.31) compared with the efficiency of the Solarwall collectors and the solar chimneys at Lundebjerg.

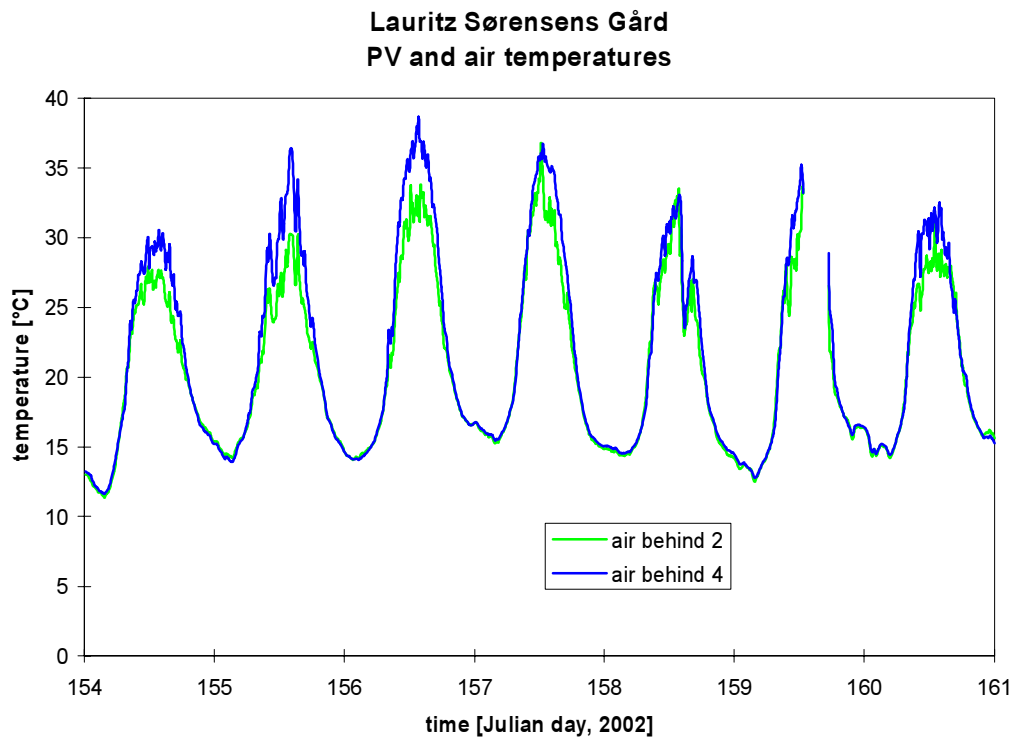


Figure 4.34. The air temperatures behind the PV-panels during week 23, 2002 (June 3-9).

#### 4.2.2.2. Heating of the air during the night

Figures 4.24 and 4.26 show that the air is heated during the night due to the heat loss from the building through the roof. This is shown more clearly in figures 4.35-36 for week 2, 2003 (January, 6-12) with low ambient temperatures and only little solar radiation (only on day 6 and 10).

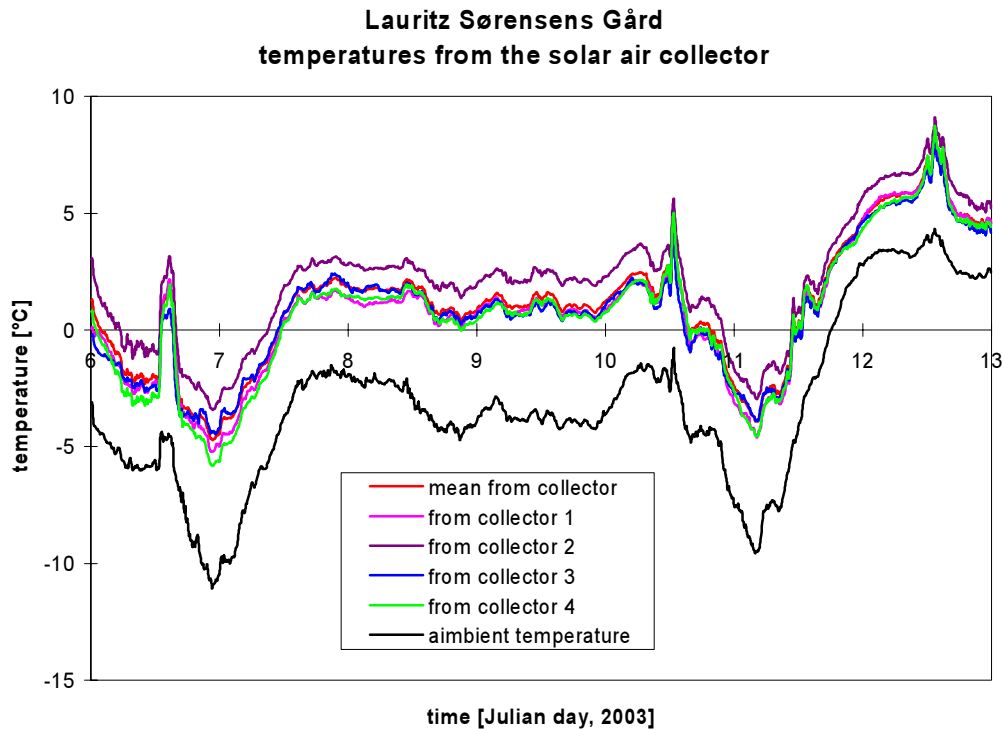


Figure 4.35. The air temperatures out of the solar air collector during week 2, 2003 (January 6-10).

Figure 4.36 shows the power transferred to the air when passing the solar air collector while figure 4.37 shows the actual mass flow rate through the solar air collector. Figure 4.36 shows that the heating of the air is in the same order of magnitude as during clear sky conditions during week 23, 2002 as seen in figure 4.26. The air is heated in the order of 5 K which is half of the heating in figure 4.26 during clear sky conditions. However, the mass flow rate is twice as high in figure 4.37 compared to figure 4.23. This is because the system was finally adjusted to a proper level of air flows by the end of December 2002, the tenants was asked to open for inlet of fresh air and because the low air temperature out of the solar air collector results in a higher density of the air.

Figure 4.38 shows the temperature increase of the air when passing the solar air collector during the night. Only values between midnight and 6:00 are shown and further max. one value per hour. Values for week 23, 2002 and December 23, 2002 - April 30, 2003 is shown in figure 4.38.

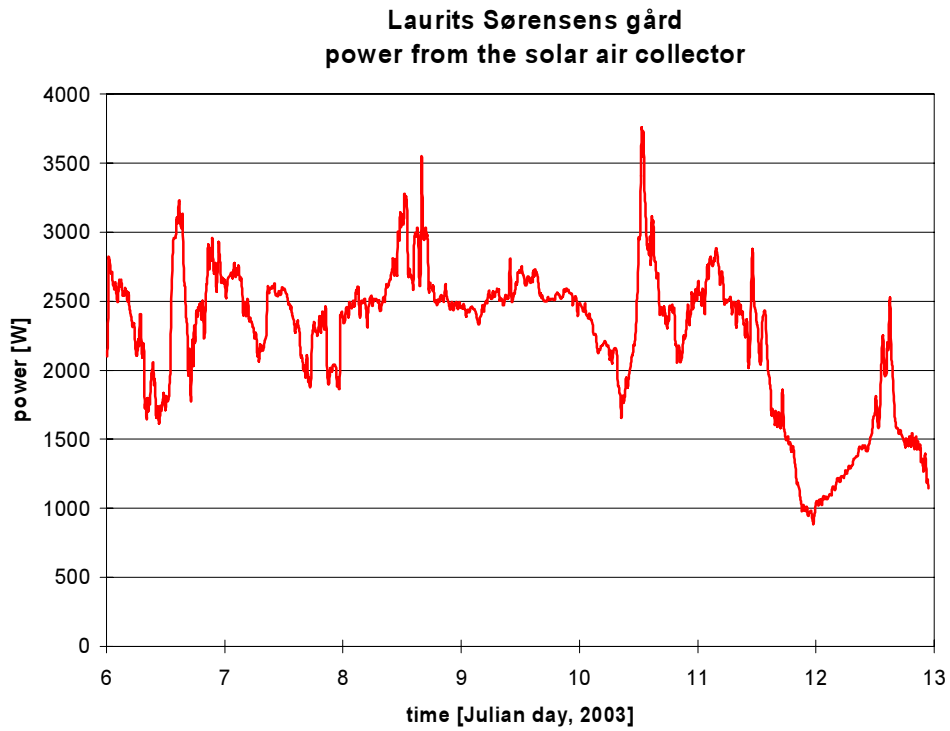


Figure 4.36. The power transferred to the air in the solar air collector during week 2, 2003 (January 6-12).

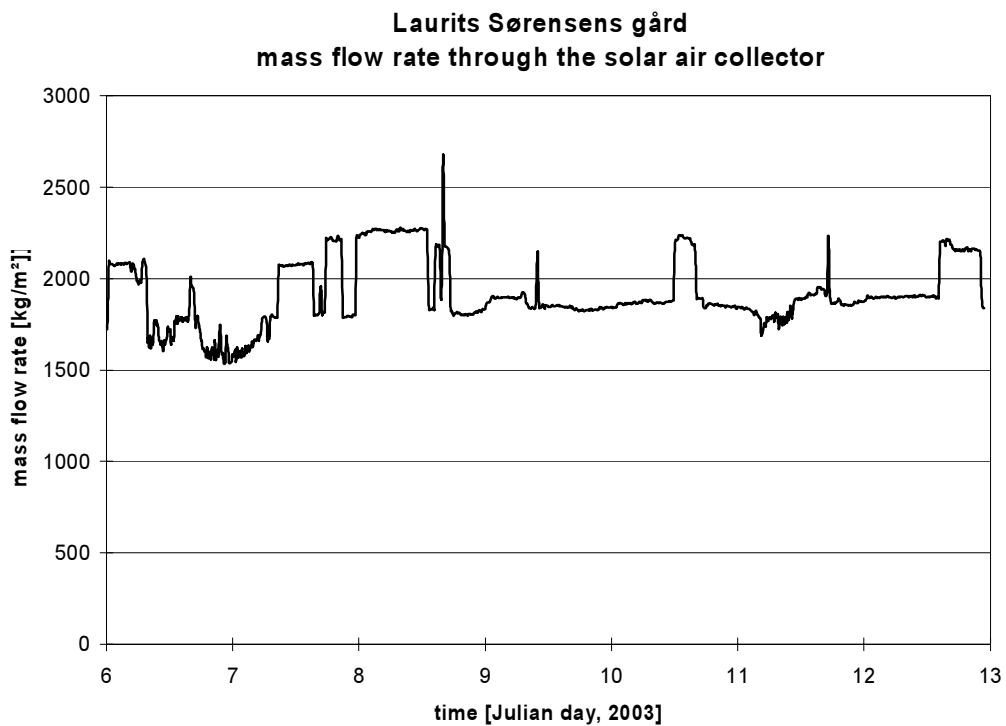


Figure 4.37. The mass flow rates of air through the solar air collector during week 2, 2003 (January 6-12).

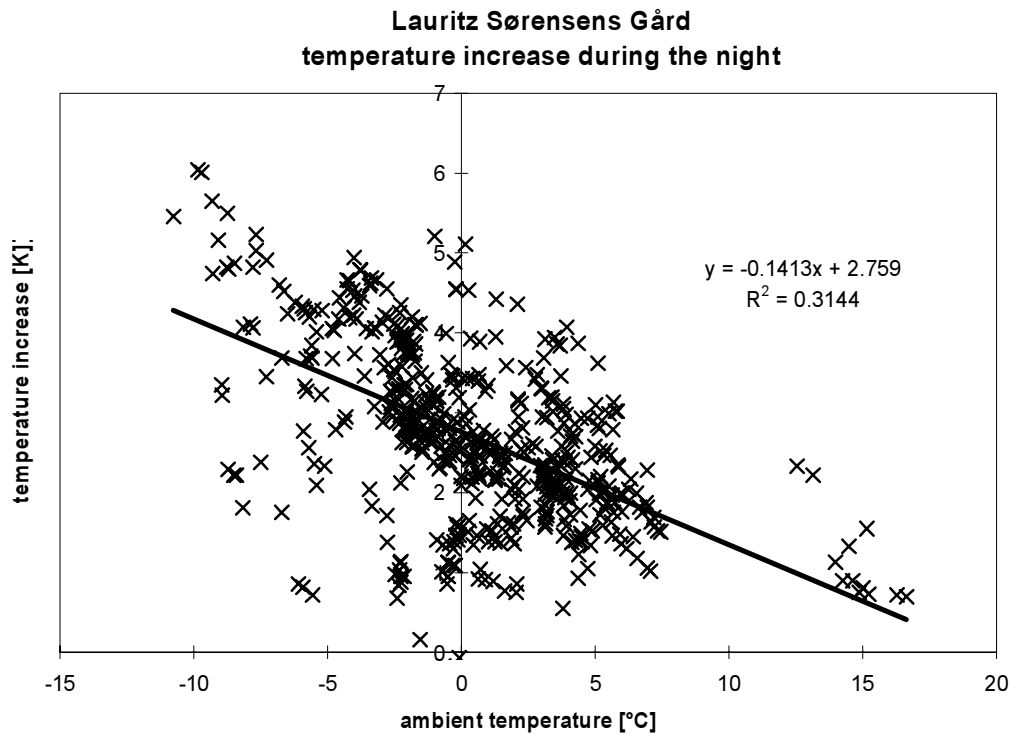


Figure 4.38. The temperature increase of the air when passing the solar air collector during the night depending on the ambient temperature.

Figure 4.38 shows a clear but scattered dependency of the temperature increase on the ambient temperature. Another parameter, which the temperature increase might be dependent on, is the flow rate of air. This is shown in figure 4.39. Figure 4.39 shows a less obvious dependency. The scattering is partly due to wind and partly due to long wave radiation exchange with the sky which is different for cloudy compared with clear sky conditions. When combining figure 4.38-39 the following dependency is obtained:

$$\Delta T = 0.0023 + 0.112 \cdot T_{\text{ambient}} + 0.0016 \cdot (\text{mass flow rate of air}) \quad (4.3)$$

Figure 4.40 shows a comparison between the measured temperature increase and the calculated temperature increases found either with the equation in figure 4.38 or equation 4.3. Figure 4.40 shows only a minor difference between the two equations meaning that the influence of the mass flow rate is negligible. Figure 4.40 shows that the equations over predict low temperature increases while under predict at higher temperature increases. However, it is expected that the equations on an annual basis give a fair impression of the temperature increase over the solar air collector and thereby the amount of recovered heat for periods without solar radiation.

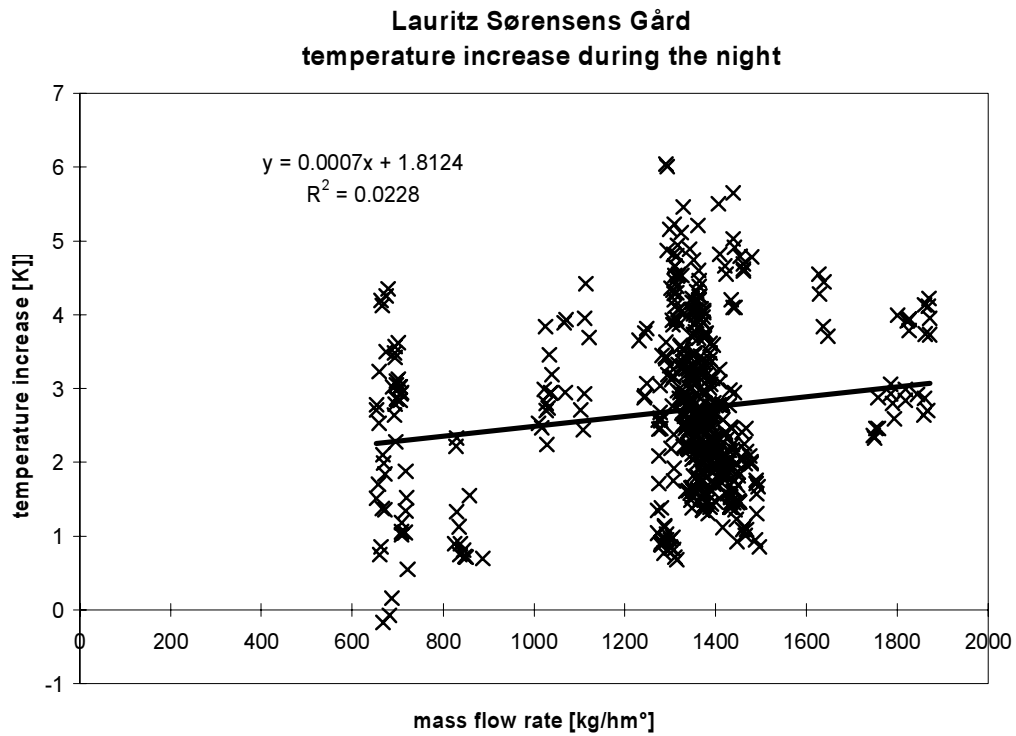


Figure 4.39. The temperature increase of the air when passing the solar air collector during the night depending on the mass flow rate through the solar air collector.

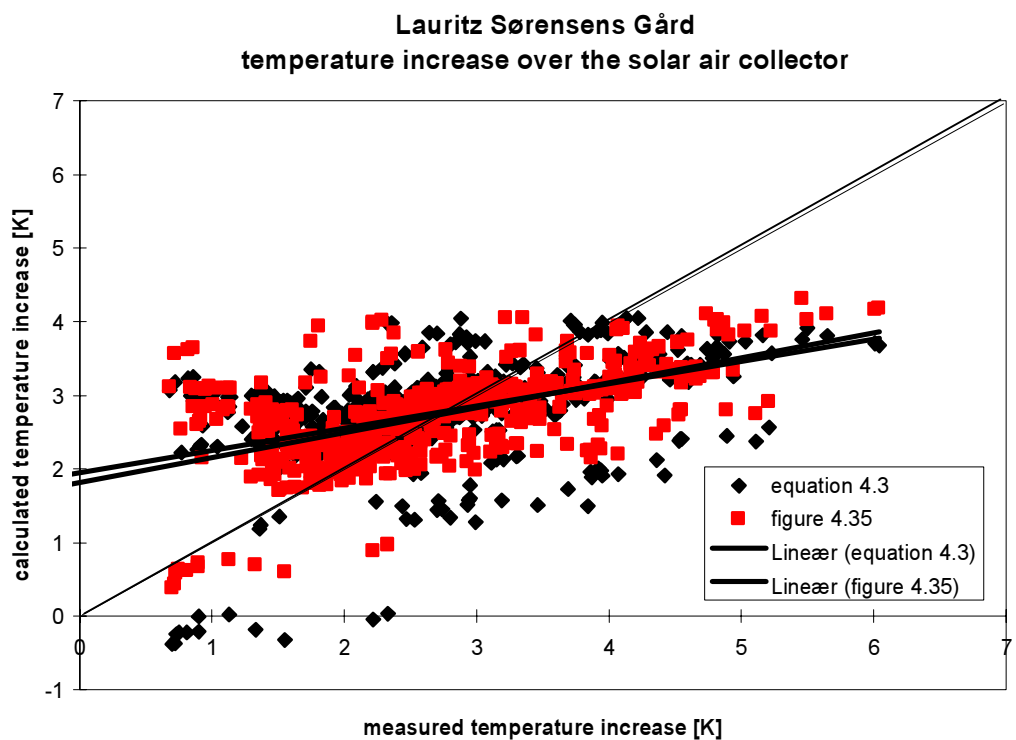


Figure 4.40. Comparison between measured and calculated temperature increase over the solar air collector during the night.

### 4.2.3. The large heat exchanger

Figures 4.41-43 shows the temperatures around the large heat exchanger and the air flow and mass flow rates through the large heat exchanger during week 2, 2003 (January 6-12). The week was characterized by only little solar radiation and low ambient temperatures (-11-+4°C) – the latter shown in figure 4.41. The exhaust air temperature from the building was in the order of 18.5-24°C while the fresh air temperature to the building after the heater laid constantly around 24°C. The air temperature of the technician room was between 22 and 25°C.

Figure 4.42 shows the air flow through the large heat exchanger. The figure shows that the balancing of the air flows are not perfect – i.e. that the air flow of fresh air is approx. 90% of the exhaust flow rate. Part of the time this is obtained – but often the flow rate of fresh air is higher than the flow rate of exhaust air. The reason for this fluctuation is that the tenants are able to control the flow rate of especially the fresh air. Figure 4.43 shows the mass flow rate through the large heat exchanger. Here the balancing is even worse due to the low air temperature to the heat exchanger leading to a high density of the air.

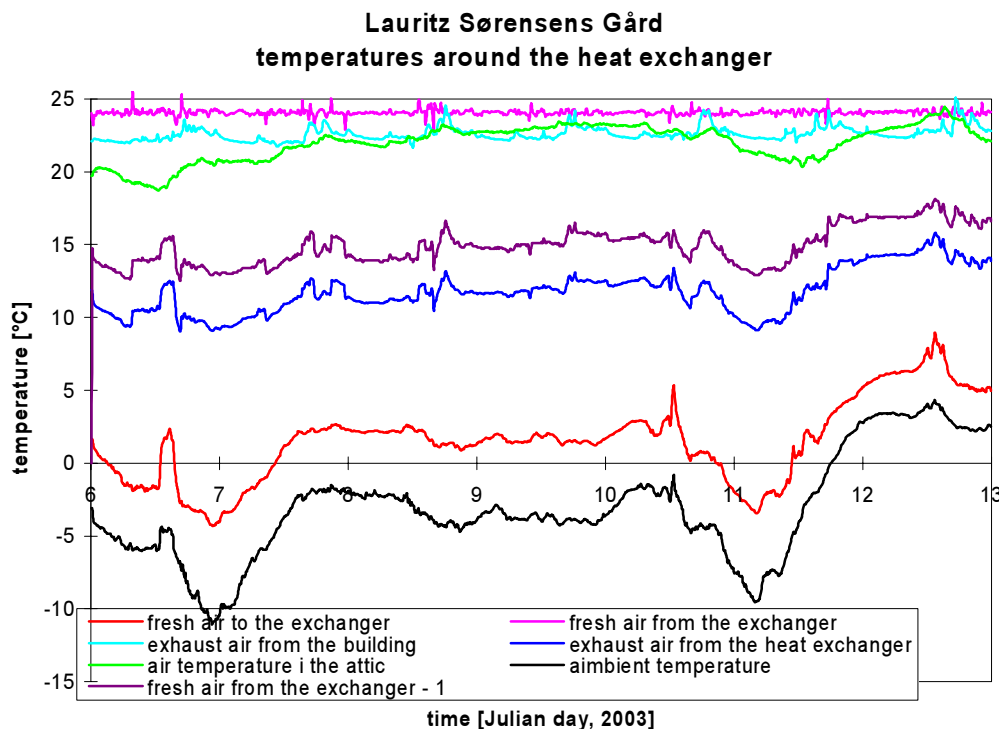


Figure 4.41. The air temperatures around the large heat exchanger during week 2, 2003 (January 6-12).

The temperature of the fresh air leaving the heat exchanger (before the heater) is only tentative as the heat exchanger is a cross flow heat exchanger where it isn't possible to measure the correct mean air temperature of fresh air leaving the heat exchanger the way it is done in figure 3.5. Relocation of the sensor will radically change the measured value. In order to obtain correct values of this temperature the heater should be switch off and the temperature sensor in the duct after the heat exchanger (and heater) should be used. However, this was not possible due to comfort reasons.

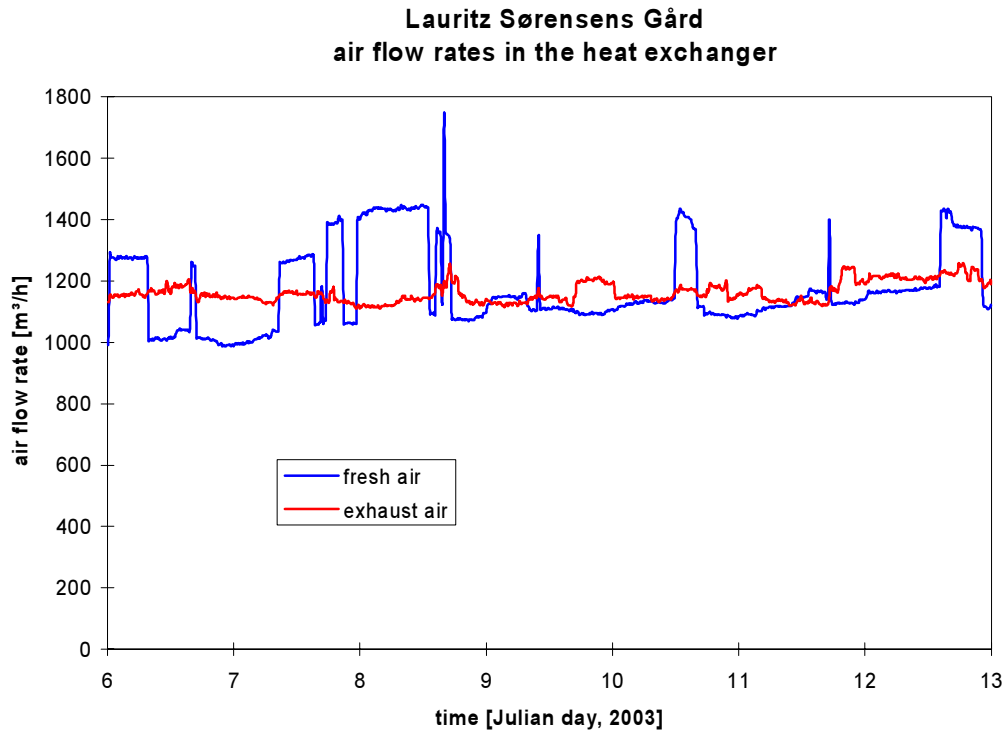


Figure 4.42. The air flow rates of fresh air and exhaust air through the large heat exchanger during week 2, 2003 (January 6-12).

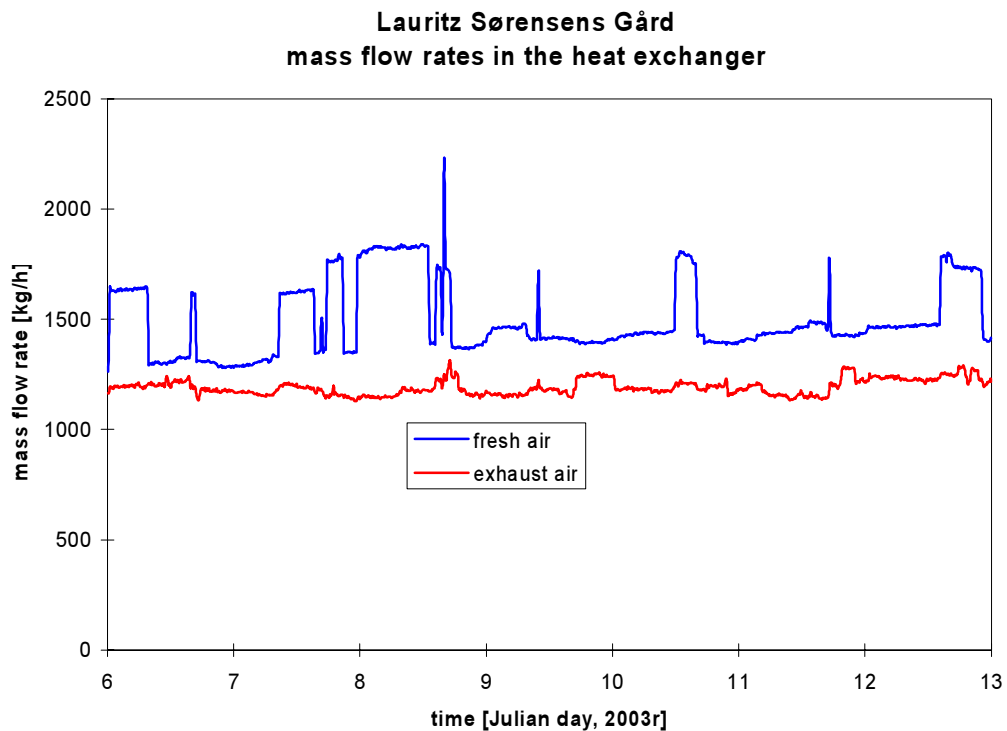


Figure 4.43. The mass flow rates of fresh air and exhaust air through the large heat exchanger during week 2, 2003 (January 6-12).

Based on figure 4.41 and 4.43 it is possible to calculate the heat transferred from the exhaust air to the fresh air and the max possible transfer of heat (if condensation is not regarded). This is done in figure 4.44. Figure 4.44 shows a max power transfer of up to 9,000 W while the actual power transfer is only half. Condensation will increase the actual heat transfer a bit, however, not much at the heat transfer coefficient on the dry side of the heat exchanger then will be determining.

Using 4.44 it is possible to determine the efficiency of the heat exchanger at the actual conditions. This is equal to the temperature difference determined based on the smallest capacity flow rate:

$$\eta_{1t} = (T_{1o} - T_{1i}) / (T_{2i} - T_{1i}) \quad (4.4)$$

where:  $\eta_{1t}$  is the temperature efficiency at the smallest capacity flow rate

$T_{1i}$  is the inlet temperature to the exchanger for the air with the smallest capacity flow rate

$T_{1o}$  is the outlet temperature from the exchanger for the air with the smallest capacity flow rate

$T_{2i}$  is the inlet temperature to the exchanger for the air with the largest capacity flow rate

The result when using equation 4.4 is shown in figure 4.45.

The efficiency of the large heat exchanger fluctuates between just below 50 and just above 55%. When comparing figure 4.45 and 4.43 it is further seen that the fluctuations in the efficiency correspond very well with the fluctuation in both mass flow rates. This is illustrated more clearly in figure 4.46 showing the efficiency dependent on the mass flow rate of fresh air divided by the mass flow rate of exhaust air.

Figure 4.46 shows a clear dependency in the considered range – ranging from 0.48-0.59. At normal recommended value of 0.9 (fresh air/exhaust air) the efficiency of the heat exchanger is 0.465. This is clearly lower than the efficiency given by the manufacture: 0.6-0.65 (Exhausto, 2003). It is, however, quite normal that the actual efficiency is lower than the one given by the manufactures. The uncertainty on the measured air flow rates is as earlier explained rather high due to the very complex installation. It is judged that the uncertainty on the above-found efficiency is in the order of  $\pm 10\%$  and maybe higher.

Figure 4.47-49 show the temperatures around the large heat exchanger, mass flow rates through the large heat exchanger and the heat transferred from the exhaust air to the fresh air and the max possible transfer of heat (if condensation is not regarded) during week 13, 2003 (March 24-30) – the measuring system did unfortunately go down the week before and first restarted on Tuesday of week 13. The week was characterized by much solar radiation and high ambient temperatures during the day – up to 19°C. This resulted in a higher inlet temperature of fresh air to the heat exchanger than the temperature of exhaust air from the building and the wished fresh air temperature from the heat exchanger of 24°C.

Figure 4.49 shows that heat is transferred from the fresh air to the exhaust air during the day. The fresh air is thus cooled a bit - however, not much as seen in figure 4.47.

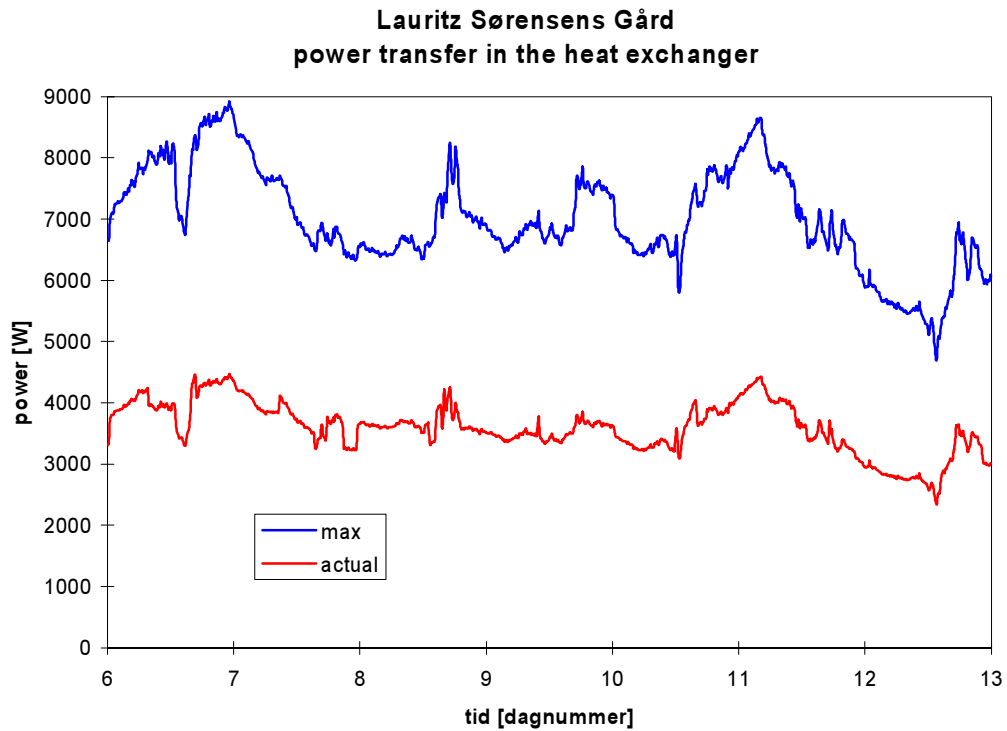


Figure 4.44. The actual and max power transfer in the heat exchanger during week 2, 2003 (January 6-12).

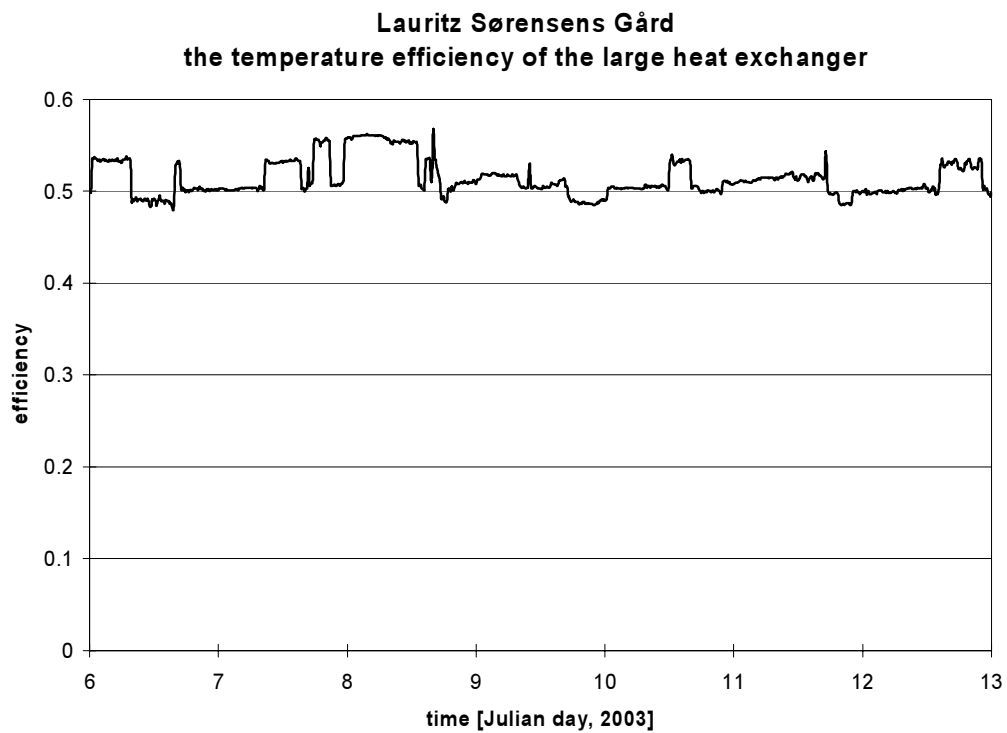


Figure 4.45. The temperature efficiency of the heat exchanger during week 2, 2003 (January 6-12).

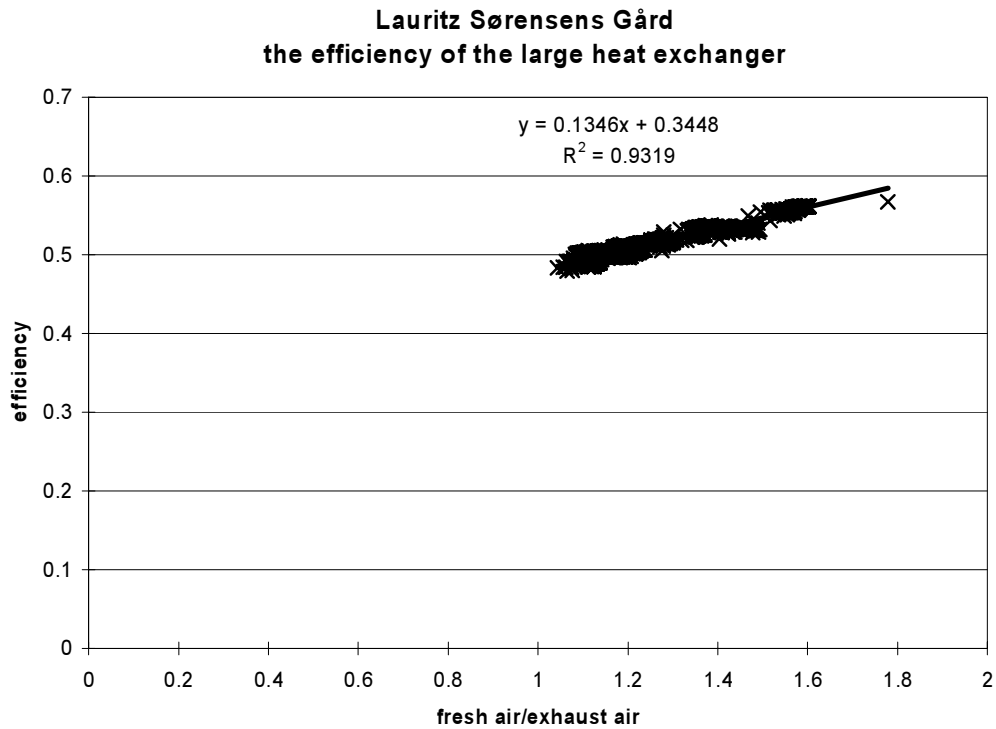


Figure 4.46. The temperature efficiency dependent on the mass flow rate of fresh air divided with the mass flow rate of exhaust air during week 2, 2003 (January 6-12).

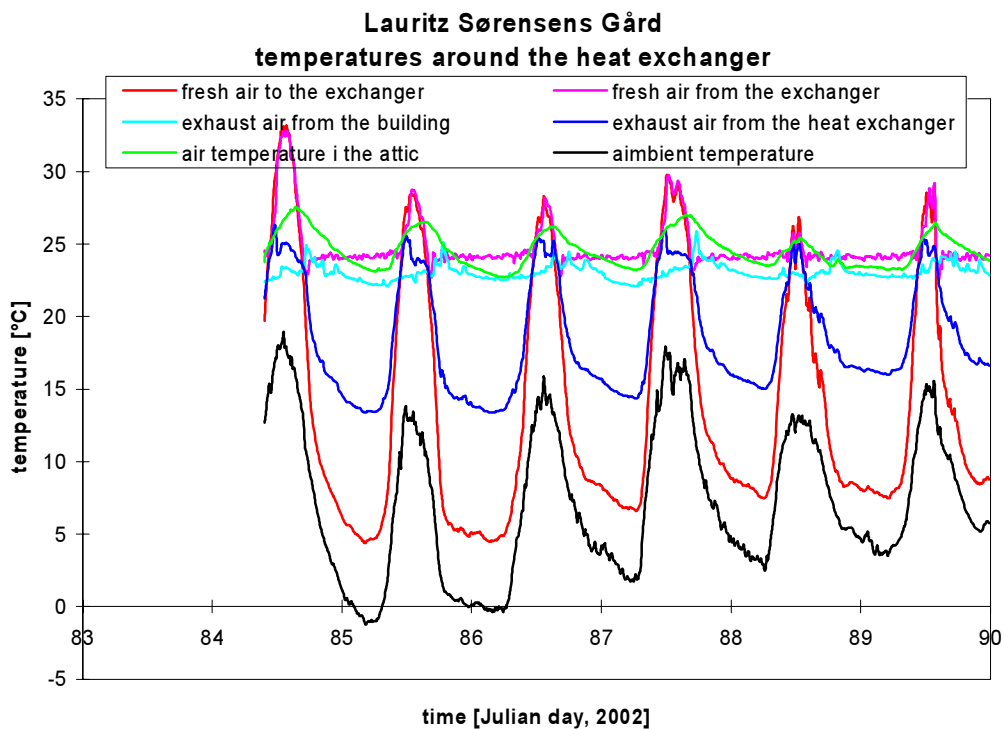


Figure 4.47. The air temperatures around the large heat exchanger during week 13, 2003 (March 24-30).

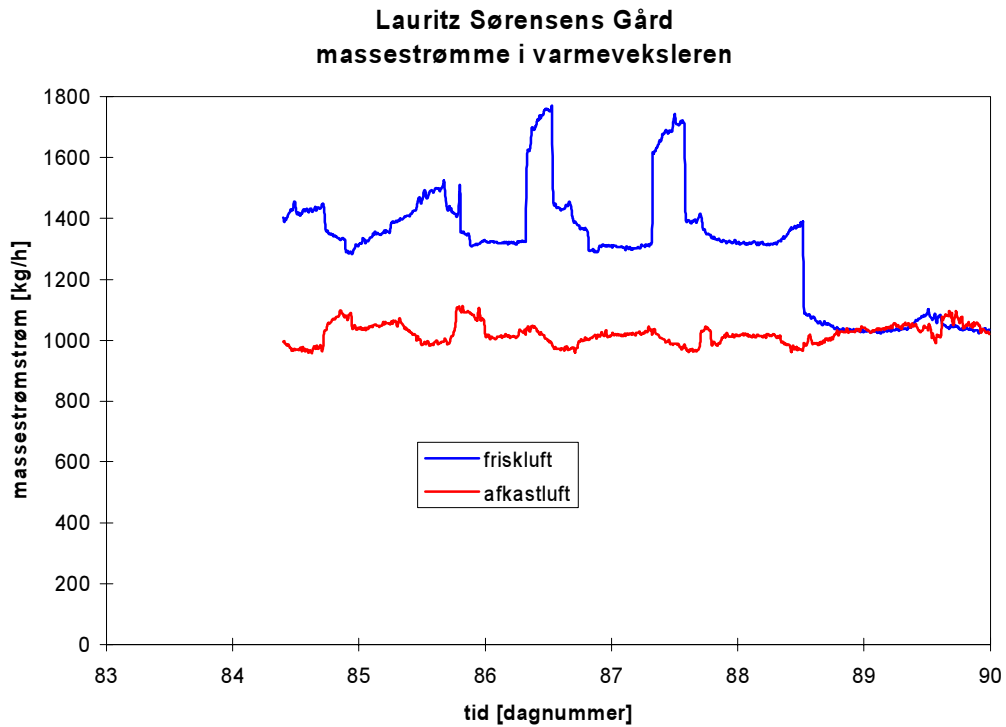


Figure 4.48. The mass flow rates of fresh air and exhaust air through the large heat exchanger during week 13, 2003 (March 24-30).

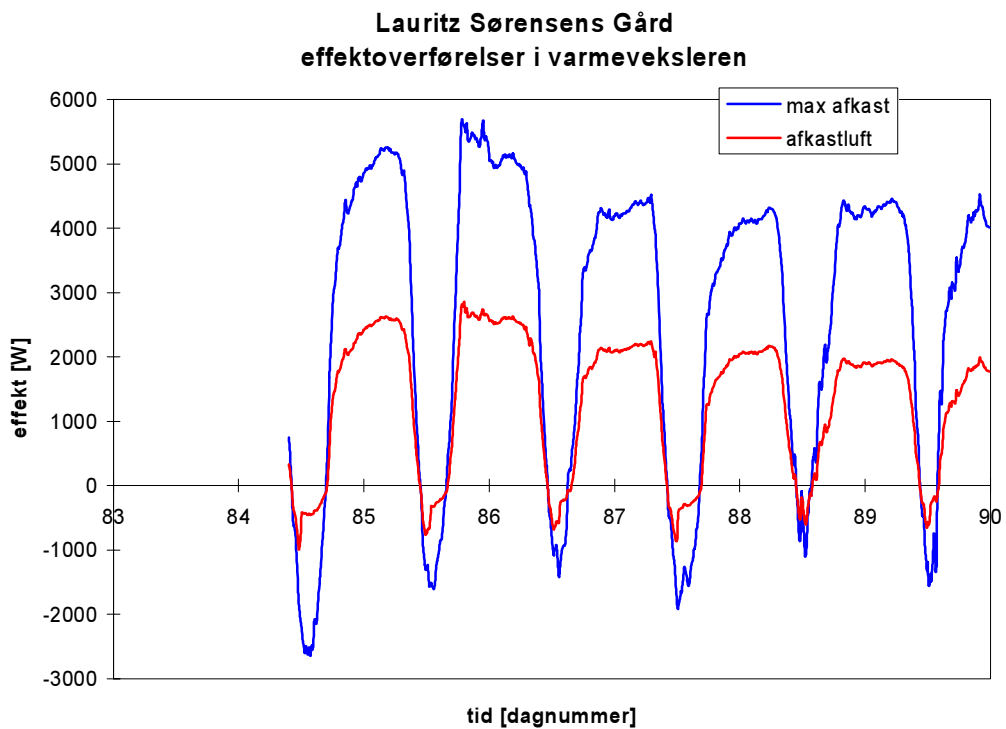


Figure 4.49. The actual and max power transfer in the heat exchanger during week 13, 2003 (March 24-30).

### 4.3. Conclusions

Based on the measurements the systems at Lauritz Søensensvej 24 has been evaluated and characterized.

The PV-array performs electrically as could be expected based on the actual conditions.

The air flow of fresh air to the building has no or minor influence on the temperature of the PV-panels. The air flow of fresh air seems not to increase the cooling of the PV-panels already present by the buoyancy driven air flow.

The part of the solar air collector covered with PV-panels does not contribute to the heating of the fresh air to the building. A poor distribution of the air over the solar air collector due to centrally located draw off from the solar air collector decreases the performance of the solar air collector at low mass flow rates.

The fresh air to the building is also heated during the night due to the heat loss from the building through the roof.

The efficiency of the large heat exchanger has been measured to be in the range of 0.48-0.59, which is lower than the efficiency given by the manufacture – 0.6-0.65.

The results from the evaluation and characterization of the systems will be used in the following chapter to calculate the annual performance of the systems.

## 5. Annual performance of the systems

Based on the evaluation and characterization of the system at Lauritz Sørensensvej 24 the annual performance of the system will in the following be calculated and evaluated.

### 5.1. Power from the solar air collector

The equations in figure 4.31 and figure 4.38 describe the heating of the air through the solar air collector during the day and night respectively. However, the values these equations are based on are rather scattered. It is, therefore, difficult to obtain good agreement when comparing measured and simulated values for each time step of the measurements. However, good agreement may be obtained for the sum over larger time span.

Figures 5.1-5.4 compares measured and simulated values for the power transfer to the air in the solar air collector. Poor agreement is often observed on a daily basis – but the agreement is not that bad after all. Over the total time span – January 1-April 20, 2003 the agreement is rather good as seen in table 5.1. The two equations, however, tend to be a bit conservative in the prediction of the power transferred to the air in the solar air collector.

Based on figures 5.1-4 and table 5.1 it is concluded that the equations from figure 4.31 and figure 4.38 describe the performance of the solar air collector sufficiently well to be used in a simulation model of the total system.

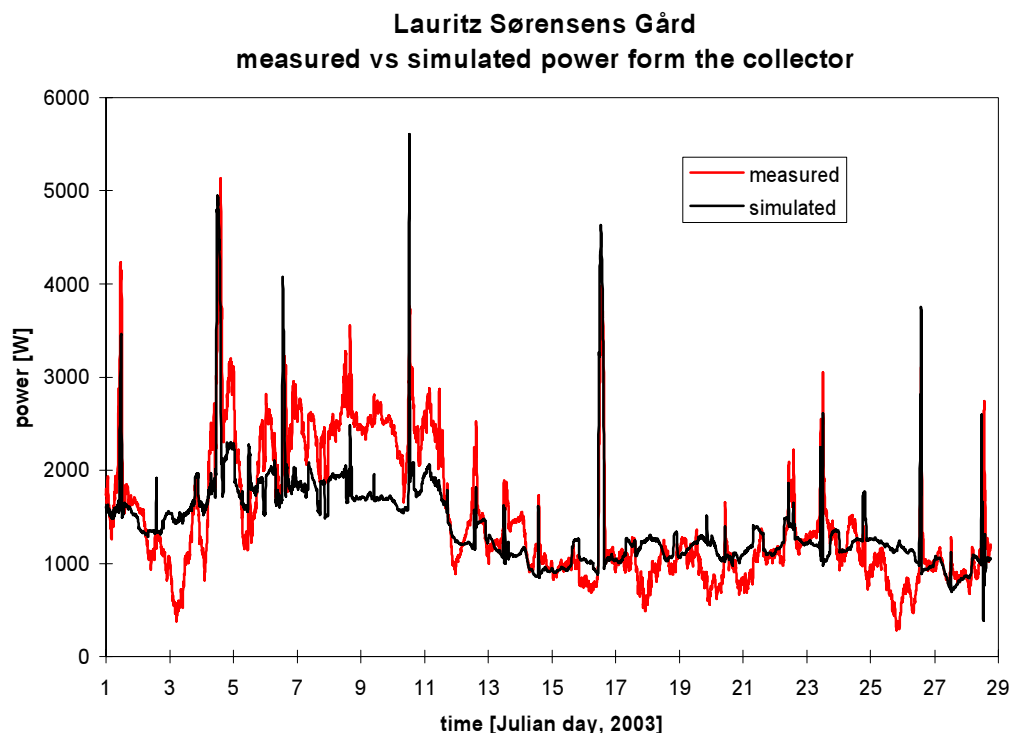


Figure 5.1. Measured and simulated power from the solar air collector.

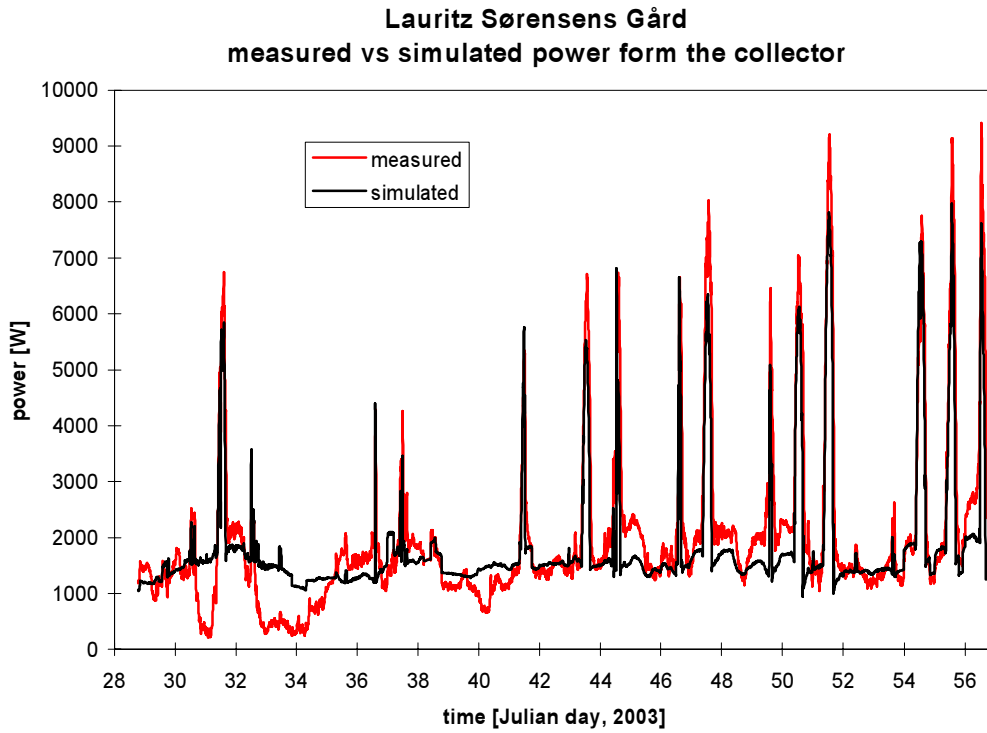


Figure 5.2. Measured and simulated power from the solar air collector.

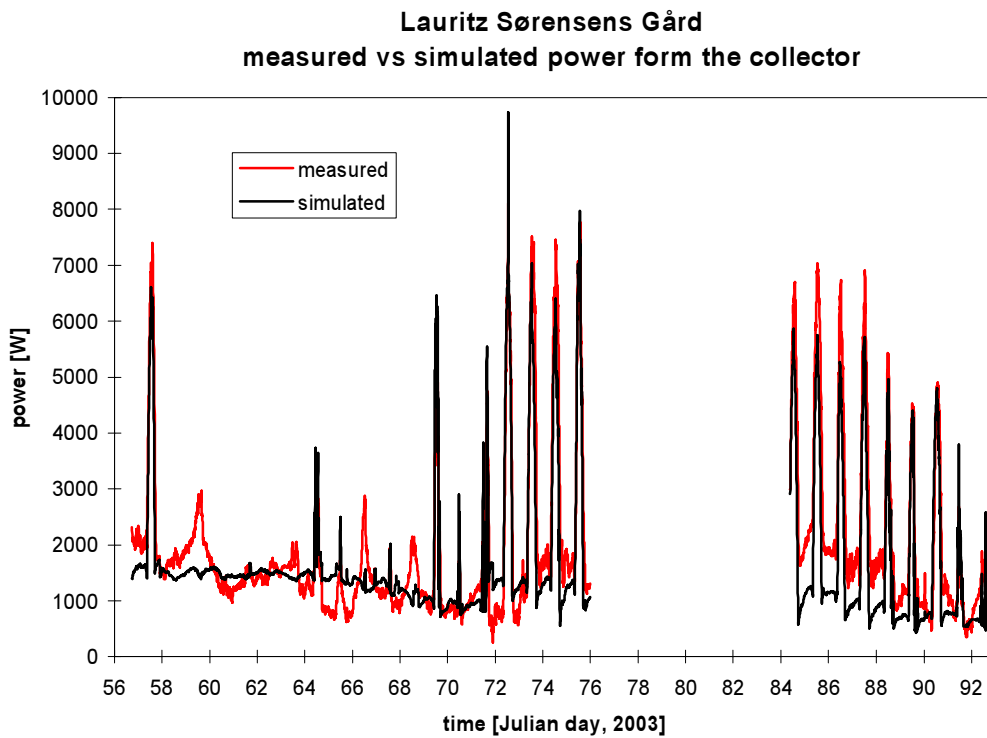


Figure 5.3. Measured and simulated power from the solar air collector.

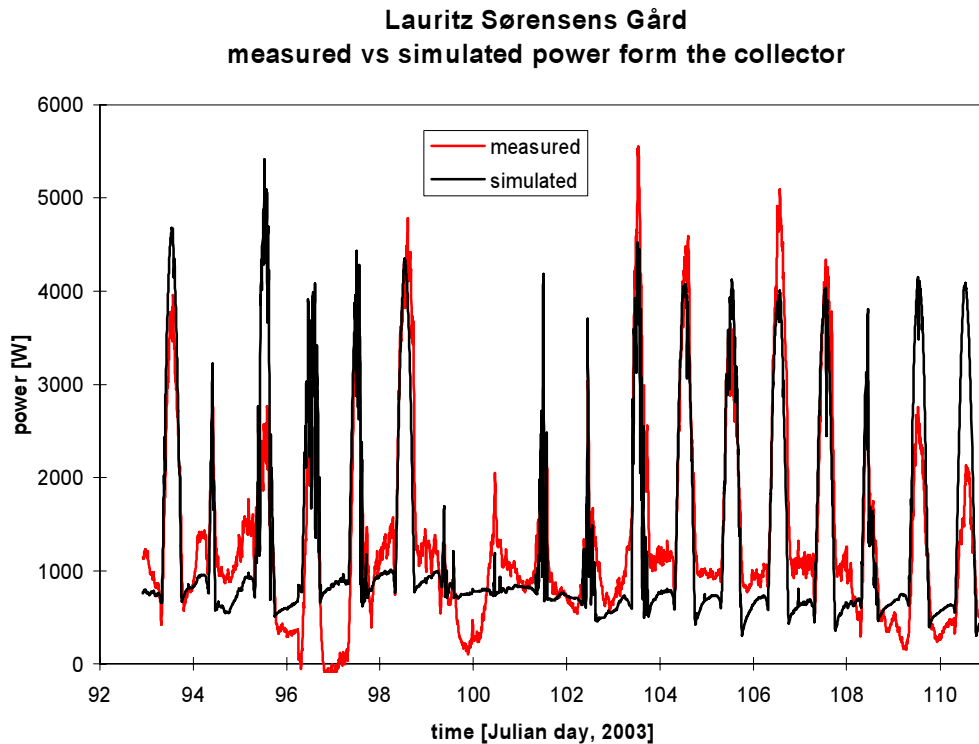


Figure 5.4. Measured and simulated power from the solar air collector.

	measured kWh	simulated kWh	difference %
Power from the sun solar radiation >200 W/m <sup>2</sup>	1,330	1,225	7.9
Power 24 hour a day	4,175	3,845	7.9

Table 5.1. Comparison between measured and calculated power to the air in the solar air collector.

## 5.2. Annual performance of the system

Based on the equations for the heating of the fresh air in the solar air collector tested in the previous section a simple simulation model for the total system has been developed. The model calculates hour by hour the temperatures and energy flows in the system. As weather input is used the Danish Test Reference Year (TRY) (SBI, 1982).

### 5.2.1. PV-panels

The yearly yield of the PV-panels is 6% of the total solar radiation hitting the PV-panels - found in section 4.2.1.1. For the considered orientation of the PV-panels the annual solar radiation is 1,158 kWh/m<sup>2</sup>. With an PV-array of 12.4 m<sup>2</sup> the annual performance of the PV-panels is 860 kWh.

### 5.2.2. Solar air collector

For the heating of the fresh air to the solar air collector the equations from figure 4.31 and figure 4.38 are as already mentioned used. The equation giving the highest outlet temperature at an actual time step is used for that time step.

The total area of the solar air collector is 35.3 m<sup>2</sup>.

It is assumed that the flow rate of fresh air to the 12 apartments is as specified in the Danish Building Code – i.e. exhaust 126 m<sup>3</sup>/h and fresh air 90% of the exhaust = 113.4 m<sup>3</sup>/h. The flow rate of fresh air through the solar air collector is thus 1360 m<sup>3</sup>/h.

### 5.2.3. Heat exchanger

In order to simplify the model it is assumed that the exhaust air from all apartments is let through the large heat exchanger. The air flow rate of exhaust air is thus 1510 m<sup>3</sup>/h. The ration between fresh air and exhaust air is, therefore, 0.9. The efficiency of the heat exchanger is using the equation in figure 4.46 found to 0.47.

Two cases are investigated: 1) the fresh air to the heat exchanger is preheated by the solar air collector and 2) the fresh air is not preheated by the solar air collector – i.e. the ambient temperature is here used as inlet to the heat exchanger. By doing this it is possible to determine the actual benefit of the preheating in the solar air collector as this preheating decrease the performance of the heat exchanger.

### 5.2.4. Demands

The model includes no thermal model of the building – i.e. no calculation of the actual heating demand of the building is included in the model. However, in order to exclude periods with no heating demand the model is only run for the Danish heating season: September 24-May 8. During the heating season periods with no heat demand may occur so the model is further switched of if the ambient air temperature is above 17°C.

The temperature of the exhaust air is assumed to be 22°C.

### 5.2.5. Annual performance

#### 5.2.5.1. The system above Lauritz Sørensenvej 24.

Electricity from the PV-panels:	860 kWh/year
Preheating during the night:	4,940 kWh/year
Preheating during the day:	2,710 kWh/year
<hr/>	
Total preheating:	7,620 kWh/year
Energy in the exhaust air:	49,480 kWh/year
Recovered energy without preheating:	23,255 kWh/year

Total energy gain incl. preheating: 27,140 kWh/year

Actual benefit of the preheating: 3,885 kWh/year (27,140-23,255)

65% of the preheating of the fresh air through the solar air collector is recovered heat loss through the roof while only 35% is solar heat.

The actual benefit of the preheating (day and night) in the solar air collector is 3,885 kWh/year while the heating of the fresh air in the solar air collector is 7,620 kWh/year. The yield is thus decreased by 49% due to the heat exchanger.

Without the preheating in the solar air collector 47% of the heat in the exhaust air is recovered. Due to the preheating this is increased to 55%. The preheating in the solar air collector increases thus the savings by 17%.

During the whole year the total solar radiation on the solar air collector is 1,158 kWh/m<sup>2</sup>. Of this solar radiation  $3,885 / (1,158 \cdot 35.3) = 9.5\%$  is utilized. During periods with heat demand the solar radiation is 485 kWh/m<sup>2</sup> - here 23% is utilized. If no heat exchanger was installed in the system up to 19 and 45% of the solar radiation would be utilized.

Although the yield from the solar air collector is reduced due to the heat recovery unit the thermal performance of the solar air collector is 3,5 times higher than the electrically performance of the PV-panels.

#### 5.2.5.2. The system above Lauritz Sørensenvej 28.

The area of the PV-panels is here 11.5 m<sup>2</sup>, while the total area of the solar air collector is 31.7 m<sup>2</sup>. The efficiency of the heat exchanger is here assumed to be 80%. The performance of this system is calculated to be

Electricity from the PV-panels: 800 kWh/year

Preheating during the night: 4,940 kWh/year

Preheating during the day: 2,710 kWh/year

---

Total preheating: 7,620 kWh/year

Energy in the exhaust air: 49,480 kWh/year

Recovered energy without preheating: 39,585 kWh/year

Total energy gain incl. preheating: 40,820 kWh/year

Actual benefit of the preheating: 1,235 kWh/year (40,820-39,585)

The preheating through the solar air collector is identical to the values for stair case 24. This is because the collector area is decreased by 11%. This leads to an increase in the air flow rate of also 11% which again lead to an increase of the efficiency of the collector of 11% – see the equation in figure 4.31. The preheating during the night is further not dependent on the air flow rate as seen in figures 4.39-40.

The actual benefit of the preheating (day and night) in the solar air collector is 1,235 kWh/year while the heating of the fresh air in the solar air collector is 7,620 kWh/year. The yield is thus decreased by 84% due to the heat exchanger.

Without the preheating in the solar air collector 80% of the heat in the exhaust air is recovered. Due to the preheating this is increased to 82.5%. The preheating in the solar air collector increases thus the savings by 3%.

During the whole year the total solar radiation on the solar air collector is 1,158 kWh/m<sup>2</sup>. Of this solar radiation  $1,235 / (1,158 \cdot 31.7) = 3.4\%$  is utilized. During periods with heat demand the solar radiation is 485 kWh/m<sup>2</sup> - here 8% is utilized.

The benefit of the solar air collector above Lauritz Sørensenvej 28 is thus rather small, which of course is due to the assumed high efficiency of the heat recovery unit. The higher efficiency of the heat recovery unit the lower the benefit of additional preheating of the fresh air in a solar air collector.

### **5.3. Conclusions**

The annual electrical performance of the two PV-arrays are around 800 and 860 kWh.

The simulations shows an annual preheating of the fresh air of 7,620 kWh for both systems of which 35% is due to the sun while 65% is due to recovered heat loss through the roof the solar air collector is mounted on.

Due to the heat recovery units in the ventilation systems the actual benefit of the above preheating of fresh air in the solar air collector is reduced to 3,885 and 1,235 kWh/year for Lauritz Sørensenvej 24 and 28 respectively. The preheating in the solar air collector increases the annual savings of the ventilation system by 17 and 3% for Lauritz Sørensenvej 24 and 28 respectively.

The total annual thermal savings due to the heat recovery unit and the solar air collector are 27,140 and 40,820 kWh for Lauritz Sørensenvej 24 and 28 respectively. 55 and 83% of the heat lost by the exhaust air is recovered or gained from the sun for Lauritz Sørensenvej 24 and 28 respectively.

## 6. Conclusion

The systems at Lauritz Sørensensvej 24 have from a measuring point of view been a nightmare. Nearly all possible error which can be imagined were present in the systems after the installation and they were corrected very late – almost an year after installation. The complexity of the systems and the very little space in the technician room further made it very difficult to obtain precise measurements.

However, in spite of all the experienced difficulties valuable information on this type of systems have been achieved.

The PV-array performs electrically as could be expected based on the actual conditions - the annual electrical performance of the two PV-arrays are around 800 and 860 kWh.

The air flow of fresh air to the building has no or minor influence on the temperature of the PV-panels. The air flow of fresh air seems not to increase the cooling of the PV-panels already present by the buoyancy driven air flow.

The part of the solar air collector covered with PV-panels does not contribute to the heating of the fresh air to the building. A poor distribution of the air over the solar air collector due to centrally located draw off from the solar air collector decreases the performance of the solar air collector at low mass flow rates.

The fresh air to the building is also heated during the night due to the heat loss from the building through the roof. 65% of the preheating of the fresh air is recovered heat loss through the roof while 35% is gained solar energy. The annual preheating of the fresh air in the solar air collector is for both systems calculated to be 7,620 kWh.

The efficiency of the large heat exchanger has been measured to be in the range of 0.48-0.59, which is lower than the efficiency given by the manufacture – 0.6-0.65.

Due to the heat recovery units in the ventilation systems the actual benefit of the preheating of fresh air in the solar air collector is reduced to 3,885 and 1,235 kWh/year for Lauritz Sørensensvej 24 and 28 respectively. The preheating in the solar air collector increases the annual savings of the ventilation system by 17 and 3% for Lauritz Sørensensvej 24 and 28 respectively.

The total annual thermal savings due to the heat recovery unit and the solar air collector are 27,140 and 40,820 kWh for Lauritz Sørensensvej 24 and 28 respectively. 55 and 83% of the heat lost by the exhaust air is recovered or gained from the sun for Lauritz Sørensensvej 24 and 28 respectively.

## 7. References

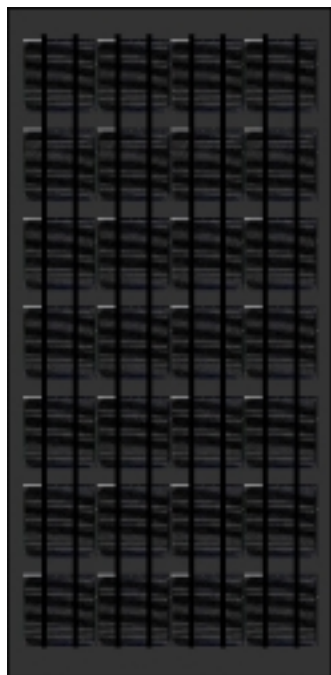
- Duffie, J.A. and Beckman, W.A., 1991. Solar Engineering of Thermal Processes. John Wiley & Sons, New York. ISBN 0-47-51056-4.
- Exhausto, 2003. VEX140 – Luftbehandlingsaggregat med kassettefilter. [www.exhausto.dk](http://www.exhausto.dk).
- Fechner, H., 1999. Investigations on Series Produced Solar Air Collectors. IEA Task 19 Solar Air Systems. Arsenal Research, Austria.
- Jensen, S.Ø., 1999. Solar Shutters – a movable solar panel (in Danish). Solar Energy Centre Denmark, Danish Technological Institute. ISBN 87-7756-549-5.
- Jensen, S.Ø., 2001. Results from measurements on the PV-VENT systems at Lundebjerg. Solar Energy Centre Denmark, Danish Technological Institute. SEC-R-14. ISBN 87-7756-611-0.
- Jensen, S.Ø. and Bosanac, M., 2002. Connectable solar air collectors. Solar Energy Centre Denmark, Danish Technological Institute. SEC-R-22. ISBN 87-7756-656-4.
- Nielsen, J.E., 1995. Dokumentation of KVIKSOL – a program for simulation of solar heating systems (in Danish). Version 5.0. Solar Energy Laboratory, Danish Technological Institute Energy.
- Olsen, H. et al. 2003. Development and optimization of an energy efficient straightner ventilation unit with build in chopper heat exchanger. Danish Technological Insitutte Energy. ISBN 87-7756-702-1.
- SBI, 1982. Weather Data for HVAC and Energy – Danish Test Reference Year (in Danish). Danish Building Research Establishment. SBI Report no. 135.

# **Appendiks A**

## **The PV-panels**

# Solcellepanel type

## GS37MIX / GS39MIX / GS40MIX / GS42MIX



GSxxMIX

### Produktegenskaber

- ☼ Produceres efter kundespecificerede ydelse

### Komponenter

- ☼ Serieforbundne monokrystallinske solceller
- ☼ Forside: Hærdet jernfattigt glas med høj transmissionsevne i 4 mm tykkelse
- ☼ Bagside: Sort/Hvid Tedlar plastmateriale
- ☼ Boks i IP 67 klasse

### Anvendelsesområder

- ☼ Nettilsluttede systemer.

### Tekniske specifikationer

Elektriske karakteristika <sup>(1)</sup>	GS37MIX	GS39MIX	GS40MIX	GS42MIX
Nominel effekt, $W_p$	37	39	40	42
Min. garanteret effekt, $W_p$	34	36	37	39
Spænding				
• Peakspænding, $U_p$ (V)	13,4	13,6	13,7	13,8
• Tomgangsspænding, $U_t$ (V)	16,6	16,6	16,7	16,7
Strømstyrke				
• Peakstrøm, $I_p$ (A)	2,80	2,89	2,96	3,03
• Kortslutningsstrøm, $I_k$ (A)	3,06	3,14	3,22	3,30
Temperatur koefficient på $W_t$ :	-0,45%/°C			
Dimensioner	960 × 460 × 20 mm			
Vægt:	10,0 kg			

1. Målt ved standard betingelser (STC), 1000 W/m<sup>2</sup>, AM 1.5 og 25 °C.

Gaia Solar fremstiller solcellepaneler i henhold til ESTI 503.

Gaia Solar garanterer at den nominelle effekt efter 10 år holder sig inden for +/- 10% afvigelse. Ligeledes giver Gaia Solar en garanti på 5 år for mekaniske defekter på solcellepanelet.

